Review

Postmortem changes in brain cell structure: a review

Margaret M. Krassner[1,2,3], Justin Kauffman[1,2,3], Allison Sowa[4], Katarzyna Cialowicz[4], Samantha Walsh[5], Kurt Farrell[1,2,3], John F. Crary[1,2,3], Andrew T. McKenzie[1,2,3,6]

[1] *Department of Neuroscience, Icahn School of Medicine at Mount Sinai, New York, New York, USA*

[2] *Friedman Brain Institute, Departments of Pathology, Neuroscience and Artificial Intelligence & Human Health, Icahn School of Medicine at Mount Sinai, New York, New York, USA*

[3] *Neuropathology Brain Bank & Research Core and Ronald M. Loeb Center for Alzheimer's Disease, Icahn School of Medicine at Mount Sinai, New York, New York, USA*

[4] *Microscopy and Advanced Bioimaging Core, Icahn School of Medicine at Mount Sinai, New York, New York, USA*

[5] *Hunter College Libraries, CUNY Hunter College, New York, NY*

[6] *Department of Psychiatry, Icahn School of Medicine at Mount Sinai, New York, New York, USA*

Corresponding author:
Andrew T. McKenzie · Icahn School of Medicine at Mount Sinai · Icahn Building 9th Floor, Room 20 · 1425 Madison Avenue · New York, NY 10029 · USA
andrew.mckenzie@icahn.mssm.edu

Additional resources and electronic supplementary material: supplementary material

Submitted: 14 April 2023 · Accepted: 15 May 2023 · Copyedited by: Georg Haase · Published: 31 May 2023

Abstract

Brain cell structure is a key determinant of neural function that is frequently altered in neurobiological disorders. Following the global loss of blood flow to the brain that initiates the postmortem interval (PMI), cells rapidly become depleted of energy and begin to decompose. To ensure that our methods for studying the brain using autopsy tissue are robust and reproducible, there is a critical need to delineate the expected changes in brain cell morphometry during the PMI. We searched multiple databases to identify studies measuring the effects of PMI on the morphometry (i.e. external dimensions) of brain cells. We screened 2119 abstracts, 361 full texts, and included 172 studies. Mechanistically, fluid shifts causing cell volume alterations and vacuolization are an early event in the PMI, while the loss of the ability to visualize cell membranes altogether is a later event. Decomposition rates are highly heterogenous and depend on the methods for visualization, the structural feature of interest, and modifying variables such as the storage temperature or the species. Geometrically, deformations of cell membranes are common early events that initiate within minutes. On the other hand, topological relationships between cellular features appear to remain intact for more extended periods. Taken together, there is an uncertain period of time, usually ranging from several hours to several days, over which cell membrane structure is progressively lost. This review may be helpful for investigators studying human postmortem brain tissue, wherein the PMI is an unavoidable aspect of the research.

Keywords: Postmortem changes, Oncotic necrosis, Autolysis, Staining methods, Species differences, Brain mapping

freeneuropathology.org

Copyright: © 2023 The author(s). This is an open access article distributed under the terms of the Creative Commons Attribution 4.0 International License (https://creativecommons.org/licenses/by/4.0/), which permits unrestricted use, distribution, and reproduction in any medium, provided the original author and source are credited, a link to the Creative Commons license is provided, and any changes are indicated. The Creative Commons Public Domain Dedication waiver (https://creativecommons.org/publicdomain/zero/1.0/) applies to the data made available in this article, unless otherwise stated.

Table of contents

Introduction

In studying the structure, function, and etiopathology of neurobiological disorders in the human brain, direct examination of postmortem autopsy human brain tissue has an unparalleled role (Buja et al., 2019). Compared to postmortem autopsy tissue, biopsy tissue is limited in size and obtainable only in a narrow set of conditions justifying neurosurgical intervention, neuroimaging studies have limited spatial and biomolecular resolution, and animal models have lower fidelity to human neurobiology. However, studying autopsy tissue presents significant confounds, crucial among them alterations occurring during the postmortem interval (PMI). The PMI is defined as the time elapsed between the subject's death and the autopsy and preservation of the brain tissue. In practical brain banking settings, the PMI generally lasts from a period of hours to several days until the autopsy is completed and the tissue is processed (Beach et al., 2015; Henstridge et al., 2015; Samarasekera et al., 2013; Vonsattel et al., 2008). Left unprocessed, postmortem brain tissue will eventually disintegrate and liquefy, which has the obvious potential to significantly confound neuropathologic investigation (Gonzalez-Riano et al., 2017; Hayman and Oxenham, 2017). Because of the value of studying donated autopsy human brain tissue, there is a critical need to understand and account for the changes that occur during the PMI.

A diverse set of assessments can be performed on autopsy brain tissue, which we can loosely bracket into three categories: functional, biomolecular, and morphological properties. Functional properties such as electrophysiological activity or cellular viability tend to be lost relatively rapidly during the PMI but can also be maintained for a surprising amount of time, on a timescale of minutes to hours (Bailey, 2019; Charpak and Audinat, 1998; Madea, 1994). Biomolecular properties vary widely regarding their maintenance during the PMI, depending on the biomolecule's class (e.g. RNA, protein, or lipid), individual type (e.g. particular RNA transcripts), and property (e.g. enzyme activity, conformation state, or subcellular location). Several studies and reviews have discussed the rate of postmortem decomposition of biomolecules (Beach et al., 2015; Kretzschmar, 2009; Nagy et al., 2015; Samarasekera et al., 2013; Stan et al., 2006). In contrast, morphological properties have received less attention. Morphological properties of the brain can be macroscopic (i.e., gross) or microscopic. Macroscopically, brains with the least decomposition have clear internal anatomy, no softening, and are able to be extracted from the calvaria without fragmentation (Hayman and Oxenham, 2017). As the brain begins to decompose, which generally occurs over a time course of days, it liquefies and eventually reaches a paste- or fluid-like consistency (Hayman and Oxenham, 2017).

Microscopically, a great deal of morphologic information can be measured in the postmortem brain. Here, we focus on the decomposition of cell membrane morphology, also known as cell “morphometry,” which refers to the external shape of a cell. Specifically, we focus on general morphometric properties such as the presence of visible dendritic spines, rather than on detailed properties such as cell membrane width. This focus is because numerous neurobiological disorders have been associated with morphometric alterations, including those in dendrites, synapses, or myelin (Kulkarni and Firestein, 2012; Stadelmann et al., 2019). For example, in Alzheimer’s disease, evidence suggests that disruptions in the actin cytoskeleton of dendritic spines is a key mediator of disease pathogenesis (Pelucchi et al., 2020). As another example, dendritic spine density has been found to be lower in the cortical tissue of brain donors with a diagnosis of schizophrenia (Berdenis van Berlekom et al., 2020). Thus, understanding how cell morphometry degrades in the PMI is a crucial consideration.

Cell membranes are made up of a multiple classes of biomolecules; by mass, about equal amounts of proteins and lipids with much more diversity in the types of proteins (Lodish and Rothman, 1979). Because cell morphometry is dependent on a multitude of biomolecules, morphometric alterations may proceed at either a slower or faster rate than the decay of any one type of the constituent biomolecules. To keep the review tractable, we do not focus on intracellular morphologic features, such as nuclear shape, the presence of rough endoplasmic reticulum, or other aspects of organelles, except in-

sofar as they affect cellular morphometry. To integrate diverse empirical findings of postmortem changes into a unified understanding, it is essential to have a model of how cell membranes decompose after death. Brain cell membrane shape is largely maintained through the cytoskeleton, a gel-like network of proteins that exhibits both passive elastic and active viscous behavior (Ananthakrishnan et al., 2006; Eberhardt et al., 2022; Mogilner and Manhart, 2018). In particular, cell membrane biomolecules are tethered to the underlying actin cortex through interacting proteins (Chugh and Paluch, 2018; Svitkina, 2020). During the postmortem interval, the cytoskeleton and other gel-like networks in the cell break down. This is initially due to fragmentation and diffusion associated with autolysis, and later putrefaction if microorganisms are present (Hau et al., 2014). After an extended postmortem period, the cytoskeleton and other gel-like structures will ultimately liquefy. It is essential to distinguish the chronological PMI from the amount of biological decomposition that occurs during that time. Several modifying factors may affect the rate of postmortem decomposition, such as the storage temperature, which need to be accounted for as well.

There are three complementary approaches to address the confound of the PMI in the study of neurobiological disorders. The first is to match cohorts by the duration of the PMI; for example, to ensure that the cases and controls each have the same average PMI (Swaab and Bao, 2021). The second is to adjust any quantitative traits under investigation by the measured PMI prior to or alongside statistical inference. The third is to restrict the PMI to a relatively short amount of time. For example, one recent study on the size of the synaptic surface in Alzheimer's disease limited the sample to autopsy brains with PMIs of less than 4.5 hours, yielding very high quality ultrastructure of the samples (Montero-Crespo et al., 2021). Another study also reported that restricting the PMI to four hours or less provided higher quality ultrastructural data (Roberts et al., 1996). All these approaches may benefit from an improved understanding of changes in the PMI, which otherwise has the potential to confound inference about group differences due to disease (Schwab et al., 1994). An accurate estimate of how long it is expected for a particular morphologic feature to degrade in the postmortem period can help in designing a study with the highest possible statistical power. A better understanding of postmortem changes may also help in addressing the possibility that postmortem changes interact with disease states or agonal factors, i.e. the terminal state before death or the manner of death. Indeed, agonal factors are often thought to contribute more to donated brain tissue quality than relatively short PMIs (Vonsattel et al., 2008; Williams et al., 1978).

While there have been many empirical studies measuring the degree of histologic degradation after different PMIs, to the best of our knowledge there has been no recent, large-scale review that attempts to summarize these studies and to construct a model of how cell membranes decompose during the postmortem period. Here, we perform a comprehensive literature search to build a database of studies addressing this topic. We enumerate the mechanisms by which brain cells have been proposed to decompose and we build a database of the timescales over which cell morphometry has been found to degrade in different contexts. We discuss how variation in decomposition outcomes can be explained by different visualization methods, the aspect of cell membrane morphology under study, and modifying variables affecting the state of the brain tissue. Our overarching goal is to review progress towards building a coherent model of how brain cell morphometry decomposes during the PMI, which investigators who are banking or studying autopsy brain tissue can use to guide their approaches.

Review methods

Review framework

We adopted a “realist synthesis” approach which incorporates aspects of a systematic review but focuses on theoretical understanding and pragmatism (Wong et al., 2013). We chose this review style because of the wide-ranging and variably defined nature of the topic. We report on our adherence to the associated RAMESES criteria (**Supplementary File 1**) (Wong et al., 2013). Prior to the formal search method development as described be-

low, scoping of the literature was performed primarily via searches on PubMed and Google Scholar, alongside discussions among the authors. Additional methods, including the search query, can be found in Supplementary File 2.

Eligibility criteria

Any scholarly publication such as a journal article that describes the effect of the PMI on cell membrane morphology in the brain was included. The PMI was defined as the amount of time that elapses between when (a) death is declared, which generally means that blood flow to the brain ceases, and (b) the brain tissue is preserved or otherwise processed. A wide range of durations of PMI, from minutes to weeks or months, were considered. Cell morphometry could be evaluated with any form of histology. To be included, studies had to contain a measurement of shape rather than solely a quantification of biomolecules. Additionally, the study needed to measure cell membranes, not solely intracellular features such as nuclear or other organellar morphology. Studies on humans or non-human animals of any age were included. To exclude the archaeological literature, PMI lengths of a year or more were not considered (Morton-Hayward et al., 2020). Review articles, studies on the retina, and non-English studies were also excluded.

Qualitative data analysis

We performed an assessment of the degree to which cell membrane structural features tend to degrade. For qualitative synthesis, decomposition timelines were considered both as a whole and, where possible, grouped by structural features (e.g. dendrites, somata, and axons), visualization methods (e.g. morphological staining, immunohistochemistry, or electron microscopy), or modifying variables (e.g. storage temperature during the PMI). We also reviewed the decomposition mechanisms posited by the different included studies. Building upon these, we attempted to describe a model of how cells in the brain degrade after death and how this affects the ability to visualize cell morphometry in autopsy brain tissue.

Characteristics of included studies

Screening identified 172 studies that met our inclusion criteria, including 22 outside of the formal search (**Figure 1;** Supplementary File 3**;** Supplementary File 4). These studies were classified as correlational studies (n = 90), time series studies (n = 84), and case reports (n = 6). Of the 172 included studies, 133 (77%) used only light microscopy, 33 (19%) used only electron microscopy, and 6 (3%) used a combination of the two. There was substantial heterogeneity in the methods. Among the 84 time series studies, there was a diversity of species studied, with 31 (37%) studying rat brains, 11 (13%) human brains, 9 (11%) mouse brains, and the rest studying brains from other or multiple species. All but one of the correlational and case report studies were on human brains.

Mechanisms and associated microscopic outcomes

Cell death by oncotic necrosis

A cell death pathway describes a stereotyped sequence of events by which the functions and structure of a cell are lost. Delineating cell death is complex, as there are usually not exact boundaries for when a cell has undergone an irreversible cessation of its functions and is therefore considered dead (Galluzzi et al., 2018). It is a widely replicated finding that brain cells do not necessarily “die” immediately after somatic death. Neurons can retain electrophysiological functions for hours after somatic death (Abbas et al., 2022; Charpak and Audinat, 1998). According to a consensus definition, cell death is mediated by the loss of cell membrane integrity (Galluzzi et al., 2018). However, cell morphometry can potentially be visualized – or partially visualized – for a window of time even after the loss of cell membrane integrity. Therefore, even if a cell is dead, it may still be possible to extract useful data from visualizing it.

The major cell death pathway associated with global cerebral ischemia, a *sine qua non* of the postmortem brain, is oncotic cell death, also known as

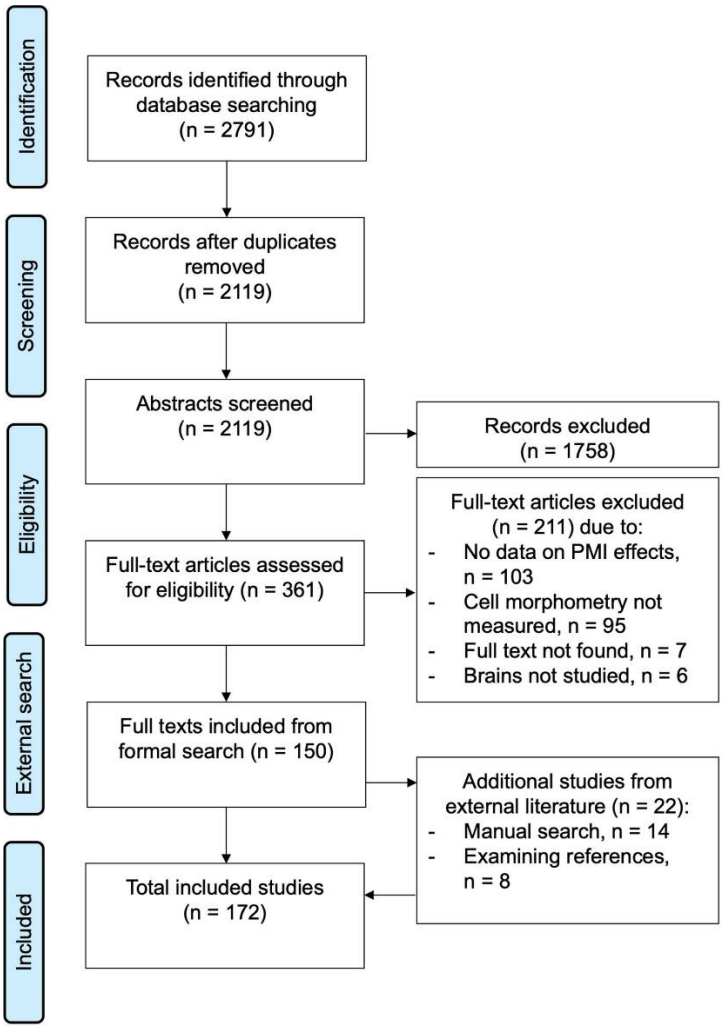

Figure 1. Study selection flow diagram.

Studies were screened and selected using the web-based software Covidence (available at https://www.covidence.org/). An export of the Covidence database for this review containing the individual study screening decisions is available (**Supplementary File 3**).

oncosis (Fricker et al., 2018; Loh et al., 2019; Majno and Joris, 1995; Weerasinghe and Buja, 2012). Oncosis was coined by von Recklinghausen in 1910 to describe cell death with swelling, from the Greek root *onkos*, which refers to "mass" or "bulk" (Majno and Joris, 1995). Subsequently oncosis fell out of favor as a concept, but in recent years has become more commonly used as cell death pathways are precisely dissected (Fricker et al., 2018; Majno and Joris, 1995). The driver of oncotic cell death, which can also be triggered by causes other than ischemia, is the loss of cellular ATP (Fricker et al., 2018). Global cerebral ischemia causes the depletion of ATP because oxygen is no longer delivered to cells through the blood, thus halting oxidative phosphorylation, after which energy stores such as glycogen are rapidly consumed (Pélissier-Alicot et al., 2003). Global cerebral ischemia also stops the process of metabolic waste product removal that is normally ensured by the blood flow (Jenkins et al., 1979). Oncosis is a non-regulated form of cell death, thus distinguishing it from the many different types of regulated cell death (Galluzzi et al., 2018; Lossi, 2022). In causes of death that directly affect the brain, such as death due to a toxin or traumatic brain injury, the postmortem cell death pathway may be much different.

There are three stages of oncotic cell death (D'Arcy, 2019; Majno and Joris, 1995; Pélissier-Alicot et al., 2003; Weerasinghe and Buja, 2012). In the first stage, loss of ATP causes inactivation of the sod-

ium–potassium ATPase, resulting in increased intracellular sodium and chloride concentrations, a net gain in solute, and usually an associated osmotic influx of water leading to cell swelling (Kramer and Myers, 2013). There is a concomitant increase in intracellular calcium, leading to activation of catabolic enzymes (Majno and Joris, 1995; Trump et al., 1997). In the second stage, there is a non-selective increase in membrane permeabilization, leading to vacuolization and cell membrane blebbing. In the third stage, there is physical disruption of the cell membrane, leading to a loss of membrane integrity. At this point, the cell is generally considered dead, initiating the necrosis phase. During the process of necrosis, cellular contents fragment, condense, convert from a gel-like phase to a liquid phase, and ultimately progress towards equilibrium with the environment (Majno and Joris, 1995; Weerasinghe and Buja, 2012). Alternatively, some investigators use the term necrosis to describe the morphological alterations at this stage of cell death (Fink and Cookson, 2005; Fricker et al., 2018). We describe this entire sequence of decomposition as cell death by oncotic necrosis. This cell death pathway has also been described as coagulative or ischemic necrosis (Levin et al., 1999).

Among the articles included in our review, several mention cell death pathways. Shepherd and colleagues, in their study of postmortem rat brains, provide the only article that specifically describes oncotic cell death (Shepherd et al., 2009). They found a substantial increase in calpain-specific spectrin hydrolysis products at 1 and 4 h postmortem, which they attributed to catabolic molecular changes consistent with oncosis (Shepherd et al., 2009). Another frequently used term to describe postmortem cell death is autolysis, which is used to describe the self-destruction of a cell due to its own enzymes (Nakabayashi et al., 2021; Tafrali, 2019). For example, Wenzlow and colleagues describe the postmortem cell death pathway observed in horse brains as cell autolysis (Wenzlow et al., 2021). They note that the observed morphological changes are similar to *in vivo* necrosis, with the exception of inflammatory cell infiltrates in the latter. Most of the early decomposition in the postmortem brain is due to autolysis as opposed to putrefaction, which is decomposition driven by microbial agents (Ith et al., 2011). However, we prefer the term oncotic necrosis to describe the postmortem cell death pathway, in part because the term autolysis assumes an aseptic mechanism that is usually not directly tested. Moreover, autolytic cell death can also occur *in vivo* and is not always associated with ATP depletion, making it a less specific term than oncotic necrosis (Fricker et al., 2018).

Intracellular structures

Several studies we identified note that cell membranes are generally more resistant to postmortem decomposition than intracellular organelles (Karlsson and Schultz, 1966; Van Nimwegen and Sheldon, 1966). For example, Schulz 1980 reported that after 22 h of PMI, there were significant intracellular changes including cytoplasm lysis, but there were no associated significant changes in the size and form of cells at this time point (Schulz et al., 1980). The loss of cytoplasmic components can lead to cells becoming hypereosinophilic on H&E, which are sometimes then referred to as “red neurons” (Garman, 2011; Finnie et al., 2022). Most authors refer to red neurons as distinct from postmortem changes, because the preferential breakdown of cell content leading to hypereosinophilia may be an active, ATP-requiring process. Because intracellular content can theoretically be lost without significant alterations of cell shape, we do not focus on red neurons or this distinction here. However, red neurons can also be associated with cell shrinkage, which would be a change in cell morphometry (Finnie et al., 2022).

Temporary versus permanent ischemia

A common area of confusion, which raises concern about the value of studying brain tissue after extended PMIs, is the finding that just a few minutes of *temporary* cerebral ischemia can cause severe structural and functional damage to the brain. However, this brain damage is a delayed phenomenon that occurs hours to days following reperfusion, due to the triggering of ATP-dependent cell death pathways (Lipton, 1999; Lee et al., 2019). This process diverges from the cell death mechanisms in the postmortem brain, in part because it is an active process requiring ATP. On the other hand, after *permanent*

ischemia of one or more (but not all) cerebral blood vessels, the resulting histologic changes are similar to those observed in the postmortem period (Tao-Cheng et al., 2007). For example, Solenski and colleagues found that in the ischemic core of the cortex exposed to permanent ischemia due to occlusion of the middle cerebral artery, neuronal swelling was present by 3 h, became more severe by 5 h, and by 24 h neurons had shrunken with edema of the neuropil, broadly consistent with the expectations of the pathway of cell death by oncotic necrosis (Solenski et al., 2002). This study also corroborated that cell death was more advanced in tissue that had been reperfused (Solenski et al., 2002). As another example of permanent focal ischemia, Garcia and colleagues permanently occluded the right middle cerebral artery in rats and found that acute shrinkage and swelling were prominent within 6 h, followed by delayed necrotic changes occurring onwards from 6 to 12 h (Garcia et al., 1995). Using a similar methodology, this same group reported that leukocyte invasion into the ischemic parenchyma was present by 12 h and peaked at 24 h after occlusion (Garcia et al., 1994b). Leukocyte invasion is one mechanism through which the rate of tissue decomposition after occlusion of an isolated cerebral blood vessel can be faster than during the global cerebral ischemia that occurs postmortem (Lipton, 1999).

Compacted or "dark" neurons

Another form of postmortem histological damage that has been investigated is the formation of compacted neurons. Also known as "dark neurons" or basophilic neurons, these are a common artifact in preserved brain tissue described by several studies (Bywater et al., 1962; Cammermeyer, 1978). Compacted neurons have a shrunken cell body, shrunken dendrites, intact membranes, and a hyperbasophilic staining pattern on H&E (Cammermeyer, 1978; Kovács et al., 2007). They occur following of a diverse set of stressors including mechanical trauma of unfixed tissue. The compaction phenomenon is considered haphazard, as it does not affect all neurons but tends to occur in clusters. Biophysically, there is strong evidence that compaction involves rapid loss of water and gel-gel phase transition (Kovács et al., 2007). Following this striking change in cell morphology, compacted neurons are not expected to follow the typical changes in oncotic necrosis, although they still will eventually undergo necrosis (Cammermeyer, 1979).

The preponderance of studies report that compacted neurons do not become more common during the PMI, and in fact, that they may become less frequent (Garcia et al., 1995; Kherani and Auer, 2008). This may be because intracellular gel-like networks are weakened during the PMI, making a gel-gel phase transition less likely. However, one study noted that solitary compacted neurons could be stimulated due to a perfusion fixation delay of five to ten min (Cammermeyer, 1978). Additionally, another study postulated that one of two types of compacted neurons they studied was associated with 3 h of PMI, because these cells also had other morphological signs of postmortem decomposition, such as vacuoles and nuclear damage (Badonic et al., 1992). Thus, shorter but not longer periods of postmortem decomposition may be associated with the formation of compacted neurons following fixation (Garman, 2011).

Apoptosis

Apoptosis, a form of programmed cell death, is a tightly regulated and controlled process by which cells undergo self-destruction, often in response to cellular damage (Galluzzi et al., 2018). This cell death pathway is characterized by distinct morphological findings, such as chromatin condensation, cell shrinkage, and the formation of apoptotic bodies. Apoptosis is not prominent in postmortem tissue, because it is an active, ATP-dependent process, and cellular ATP stores are rapidly depleted postmortem. Caspase inhibitors, which prevent apoptosis, have been found to protect against cell death in focal but not global cerebral ischemia (Fricker et al., 2018).

The preponderance of studies report that apoptosis markers are not associated with the PMI (Brück et al., 1996; Del Bigio et al., 2000; Geiger et al., 2006; Hausmann et al., 2007; Lucassen et al., 1995; Müller et al., 2001). For example, one study found that apoptotic morphology was not present in any of the postmortem human brains studied (Lucassen et al., 1997). These authors also noted that necrotic cell death takes longer to complete than

apoptotic cell death, the latter of which would be expected to take only a few hours to be completed. As another example, one study found that that positive neuronal ssDNA immunostaining, a marker of apoptosis, was not correlated with the PMI in a large (*n* = 335) study of postmortem brains with a PMI range of 2.8 to 48 h (Michiue et al., 2009). However, apoptotic markers were associated with certain causes of death such as drowning and drug intoxication. This finding is consistent with the notion that markers of apoptotic cell death beginning prior to death can be identified in postmortem brains but these markers are not expected to progress postmortem.

In contrast to most studies, a few studies have reported increases in certain markers of apoptosis in the PMI. For example, in postmortem rat brains, one study noted an increase in immunostaining for the apoptosis marker caspase-3 that peaked at 9 h of PMI (Sheleg et al., 2008). At that time, 2.5% of cortical neurons were found to stain strongly positive for caspase-3. As another example, Schallock and colleagues reported that one marker of apoptosis, i.e. clusters of cells labeled with the *in situ* end-labeling technique, appeared after 48 h of PMI in mouse brains stored at room temperature (Schallock et al., 1997). Labeled cells were generally found in isolation, not in clusters, and moreover the cells did not consistently show morphological changes of apoptosis. As a result, the authors reasoned that this marker was more likely due to DNA fragmentation associated with postmortem degeneration. Because of the potential for certain antigens to be unmasked during the PMI, some markers of apoptosis could also be seen due to decomposition during oncotic necrosis.

Postmortem fluid shifts

At the time of death, the brain is largely composed of gel-like networks of different strengths, organized at a range of scales from the extracellular matrix to sub-cellular structures as well as localized compartments of liquids. After death, oncotic necrosis begins wherein catabolic enzymes break down tissue macromolecules. As gel-like networks break down, their components solubilize, increasing the fluid content of the brain. At the same time there is a disruption of the blood brain barrier and other tissue barriers allowing fluid that is typically cordoned off to diffuse into the parenchyma, further increasing the free fluid content of the brain. This fluid is made up of water, lipids, and other soluble molecules. The end result is that the brain is transformed to the liquid state (Miller and Zachary, 2017).

Consistent with these theoretical expectations, the fluid content of the brain has been found to increase after death. One study of rat brains found that the fluid content increased from an average of 77.8% at the time of death to 79.4% at 3 h PMI, 79.6% at 6 h PMI, and 80% at 24 h PMI (Leonard et al., 2016). Notably, in this study, a head-down position was not associated with increased brain fluid content, suggesting that postmortem fluid increases are primarily due to processes within the brain rather than migration from other areas of the body. Another study reported an increase in the water content of the brain by around 10% in the PMI (Ansari et al., 1976b).

Macroscopically, in neuroimaging studies, a decline in grey-white matter differentiation occurs at PMIs longer than 24 h, which also occurs in cerebral edema and has been attributed to autolysis and fluid shifts (Wagensveld et al., 2017; Martin et al., 2022). Large-scale fluid shifts can also manifest across the postmortem brain. For example, as a result of gravity, blood has been reported to migrate to dependent parts of the calvarium during the PMI in a phenomenon known as hypostasis (Takahashi et al., 2010). Microscopically, postmortem fluid shifts also lead to many of the defining cellular changes that occur in the PMI, including circumscribed rarefaction and vacuolization, discussed below.

Perivascular rarefaction

Several studies using light microscopy have reported that perivascular rarefactions appear and increase in frequency and size during the PMI (Bywater et al., 1962; Garcia et al., 1978; Liu and Windle, 1950; Schwarzmaier et al., 2022). Morphologically, these non-staining areas generally appear as ellipsoid shapes around blood vessels (**Figure 2a**). They have been described as “a rose-branch beset with thorns” because intertwining glial fibers frequently remain between the non-staining areas (Bruce and Dawson, 1911).

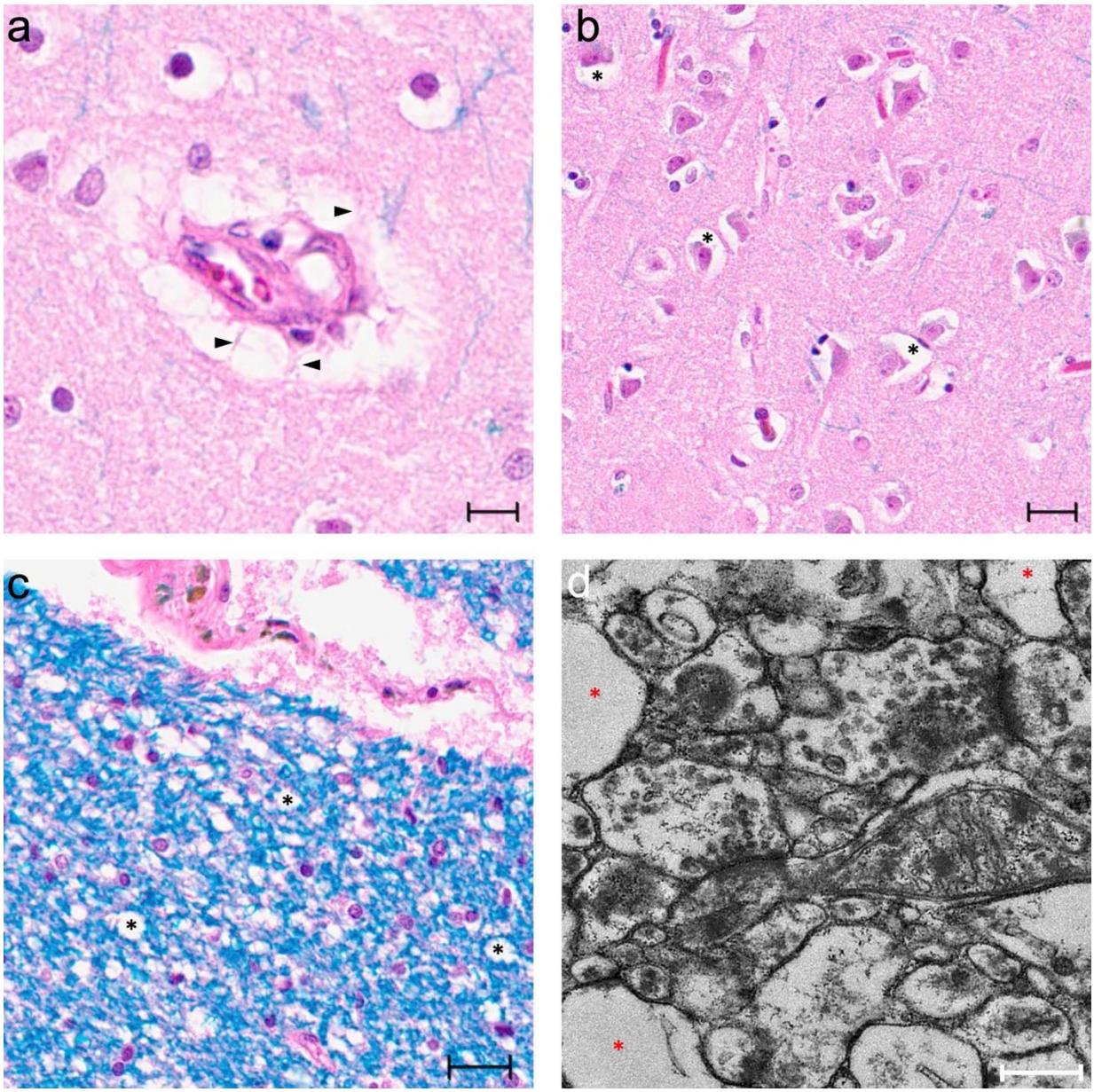

Figure 2. Representative micrographs demonstrating rarefaction and vacuolization in the postmortem brain.

Tissue from the frontal cortex tissue of an 87-year-old man with a PMI of 28 hours. A: H&E/LFB (Luxol fast blue)-stained image demonstrating a perivascular rarefaction in the grey matter. Arrowheads denote examples of intertwining fibers. Scale bar = 10 µm. B: H&E/LFB-stained image showing variable degrees of asymmetric pericellular rarefactions (asterisks). Scale bar = 20 µm. C: H&E/LFB-stained image of white matter vacuoles (asterisks) and pericellular rarefactions. White matter vacuoles are found haphazard in distribution, but appear more common near blood vessels, likely because of postmortem fluid extravasation. Scale bar = 20 µm. D: Electron photomicrograph in grey matter demonstrates prominent electron lucent areas that appear to be swollen cellular processes (asterisks). Scale bar = 500 nm.

The underlying nature of perivascular rarefactions seen on light microscopy has caused controversy for generations of neuroanatomists (Bruce and Dawson, 1911; Maynard et al., 1957; Weller et al., 2018). Frequently described as a “space” or “cleft”, we do not favor these terms because they imply an underlying mechanism. Similarly, the term “retraction artifact” implies a physical separation of the blood vessel from the parenchyma occurring during the tissue processing procedure. Instead, we prefer the more agnostic term “rarefaction” to describe the non-staining areas. Another potential point of confusion is that the perivascular rarefactions that develop in the PMI can be distinct from

the dilated perivascular spaces seen on neuroimaging *in vivo* (Kwee and Kwee, 2007; Weller et al., 2018). For example, in one correlative postmortem study, these were found to stain positive for collagen (Haider et al., 2022).

Sometimes, these perivascular rarefactions are described as resulting from a fixation artifact, although this is considered less likely, as they also occur in postmortem brain tissue preserved via freezing in liquid nitrogen (De Groot et al., 1995). Instead, electron microscopy data from ischemic or postmortem states and detailed analysis of light microscopy data suggest that perivascular rarefactions are actually due to swollen astrocyte processes (Maynard et al., 1957; Arsénio-Nunes et al., 1973; Garcia et al., 1994a; Garman, 2011; Weller et al., 2018; Dehghani et al., 2018). Other than postulating that perivascular rarefactions on light microscopy are swollen astrocyte processes, or other swollen tissue elements, perhaps the only other explanation for the divergence between light and electron microscopy data would be differences in tissue processing between the two techniques, which is less consistent with the available data. These swollen areas of astrocytes have been described as vacuoles and contain predominantly fluid, so it makes sense that they are electron lucent and do not stain positive on light microscopy for astrocyte markers such as GFAP (Schultz et al., 1957; Gibson and Tomlinson, 1979; Lafrenaye and Simard, 2019). Consistent with this, GFAP staining decreases in brain tissue following a hypoxic/ischemic period (Sullivan et al., 2010). Protoplasmic astrocyte processes can have irregular geometries, allowing them to fit into narrow spaces (Schultz et al., 1957).

Pericellular rarefaction

As with perivascular rarefactions, pericellular rarefactions have also been found to develop in the PMI (**Figure 2b**) (Bywater et al., 1962; De Groot et al., 1995; Dehghani et al., 2018; Liu and Windle, 1950; Shepherd et al., 2009). Similarly to perivascular areas, electron microscopy data in grey matter shows that astrocyte processes, including end feet, swell in the perineuronal area in postmortem and ischemic conditions, thereby accounting for the change observed on light microscopy (**Figure 2d**) (Kuroiwa et al., 1998; Suzuki, 1987). These non-staining areas are heterogenous, as they do not occur in all cells to the same degree and are more pronounced in some brain regions than others (Snyder et al., 2021). In white matter, oligodendrocyte cell bodies have also been found to swell (Kuroiwa et al., 1998). This accounts for the frequently described pericellular “halos” of oligodendrocytes, leading to an overall “fried egg” appearance on light microscopy (Snyder et al., 2021).

It is generally supported that the major mechanism of perivascular and pericellular swelling of tissue elements in the postmortem period is fluid shifts. For example, pericellular and perivascular swelling is a microscopic finding seen in brain edema (Dreier et al., 2013). It is well-described that astrocyte processes become dramatically enlarged in ischemia, mediated via passive aquaporin-4 channels, which is thought to be a protective response to minimize brain damage (Nahirney and Tremblay, 2021). The observed astrocyte process swelling at 30 min of complete global cerebral ischemia has been found to be reversible with recirculation, consistent with the idea that this is a homeostatic process (Arsénio-Nunes et al., 1973).

It is still undetermined why astrocyte processes are more liable to swell around cells and around blood vessels than in other areas of brain tissue. In breast cancer, where the presence of pericellular areas on histology correlates with an unfavorable prognosis, similar areas have been attributed to functional pre-lymphatic spaces (Acs et al., 2012). The predilection for swelling in these areas in the postmortem brain may reflect aspects of the *in vivo* functioning of the glymphatic system, which operates by shuttling water via aquaporin-4 channels on astrocytes (Silva et al., 2021). Regardless, the extent to which fluid shifts into astrocytes or other cells will depend on the local anatomic and biochemical context.

Intracellular vacuolization

The formation of vacuoles is a common finding in oncotic cell death and is also associated with fluid shifts in the postmortem brain (Shubin et al., 2016; Weerasinghe and Buja, 2012). Vacuoles are homogenous, spherical areas visualized under the microscope. Vacuolization is a common endpoint of a het-

erogeneous set of physiologic or pathologic processes, such as water accumulation, lipid droplet formation, dilatation of organelles, fusion of small vesicles, invagination of the plasma membrane, degradation of cytoplasmic components, or artifact formation during slide preparation (Henics and Wheatley, 1999; Ilse et al., 1979; Wohlsein et al., 2013). As with perivascular and pericellular rarefactions, the precise underlying nature of vacuolization is often unknown.

Many studies describe vacuoles as a characteristic morphologic finding in postmortem brain cells (Haines and Jenkins, 1968; Hilbig et al., 2004; Koenig and Koenig, 1952). For example, Lindenberg 1956 found that in cat brains stored at 37° C, small vacuole-like transparencies were first seen at 30 min PMI, while at 6 h PMI larger vacuoles could be seen in some cells (Lindenberg, 1956). In this study, the rate of development of the vacuoles was slower at lower temperatures: when the brains were stored at 18 °C, it took until 12 h PMI for vacuoles to appear. Albrechtsen 1977 noted that small vacuoles were commonly seen in cerebellar granule cells, preceding necrotic changes as one of the first signs of decomposition, and that only minimal vacuole formation was seen in cerebella without necrosis of the granule layer (Albrechtsen, 1977a). In an early paper about postmortem degeneration, Koenig 1952 reported that cytoplasmic vacuoles appeared at 3 h of PMI, increase in size and frequency throughout the PMI, and stated that their nature was not known (Koenig and Koenig, 1952). Subsequent electron microscopy studies have attributed the vacuoles in brain cells that accumulate postmortem or in ischemia to swollen mitochondria and dilatations of the endoplasmic reticulum or Golgi apparatus (Badonic et al., 1992; Shibayama and Kitoh, 1976; Suzuki, 1987). It is not clear if all the vacuoles are due to the swelling of these organelles, or if some vacuoles could be due to other factors. Also using electron microscopy, Sele and colleagues found that the number of vacuoles increased during the PMI and speculated that they resulted from degraded cellular compartments (Sele et al., 2019).

Intracellular vacuoles have the clear potential to affect cell morphometry by causing asymmetric cell membrane distortions. Neuronal somata have also been found to have lateral expansions, or blisters, during the PMI (Williams et al., 1978). The presence of organelle-free membrane blisters or blebs is also a commonly described finding in oncotic cell death that may be associated with vacuolization (Weerasinghe and Buja, 2012). Gibson and colleagues report that there is an increase in electron translucent vacuoles in human cortical tissue during the PMI (Gibson and Tomlinson, 1979). They associate vacuolization with the swelling of cell processes, especially astrocytic processes, and found a highly significant correlation between the PMI and the degree of vacuolization up to 33 h, followed by no significant change up to 69 h PMI. While they did not detect any obvious structural degeneration of membranes during the PMI range studied, this vacuolization led to a severe compression of the tissue. For example, there was a significant decrease in the number of recognizable synapses during the PMI, even though there was no structural disintegration of synapses observed, indicating that the presence of large vacuoles could prevent the visualization of other cellular structures.

Neuropil and white matter vacuolization

Vacuolization can also occur during the PMI in parts of brain tissue that are not as clearly associated with a single cell, including the white matter (**Figure 2c**) (Hilbig et al., 2004). White matter vacuoles often look like randomly distributed holes and have been reported to occur in densely myelinated areas such as the corpus callosum or the internal capsule (Snyder et al., 2021). In ischemia, electron microscopy shows that white matter vacuoles can result from swollen astrocyte processes, swollen axons, or the separation of the myelin sheath from the axon, with fluid filling the resulting potential space (Pantoni et al., 1996).

Vacuoles can also be seen in the neuropil during the PMI. In their study of horse brains stored at 22 °C, Wenzlow and colleagues found a non-linear trend for neuropil vacuolization: it increased up to 24 h PMI and then decreased until 72 h PMI (Wenzlow et al., 2021). However, they did not find a significant change in cytoplasmic vacuolization over the PMI range studied. Garcia 1978 reported that the sponginess seen in the neuropil on light microscopy in regional ischemia was due to extensive swelling of astrocytic processes and presynaptic ter-

minals seen on electron microscopy (Garcia et al., 1978). Consistent with the idea that neuropil vacuoles result from fluid shifts, incubating brains in saline prior to fixation has also been found to lead to vacuolization of the neuropil (Garman, 1990).

Biomolecule degradation

The primary macromolecules making up brain cells are proteins and lipids while nucleic acids and carbohydrates account for only a small percentage (Susaki et al., 2020). Therefore, understanding how proteins and lipids disintegrate in the PMI is critical for charting how cell structure changes postmortem. In the postmortem brain, proteins are thought to be primarily broken down by enzyme-mediated proteolysis. This is consistent with findings that the uncatalyzed hydrolysis of peptide bonds at neutral pH is extremely slow, with reaction half-lives on the order of hundreds of years (Mahesh et al., 2018; Radzicka and Wolfenden, 1996).

Calpains and cathepsins are two of the major enzyme families that contribute to autolytic proteolysis. Calpain activation is not dependent upon ATP, but thought to be triggered by the postmortem increase in intracellular calcium concentration (Sorimachi et al., 1996; Zissler et al., 2020). Empirical results have indicated that calpain enzymes are indeed active in the postmortem brain (Geddes et al., 1995; Harada et al., 1997; Sorimachi et al., 1996). Cathepsin family enzymes, which are activated by acidic pH, also have activity in the postmortem brain (Compaine et al., 1995). Cathepsin family enzymes are usually cordoned in lysosomes, but lysosomal membrane integrity is lost during the PMI, which is thought to allow cathepsin-catalyzed proteolysis to catabolize cytoplasmic proteins (Compaine et al., 1995).

If lysosomes rupture or are permeabilized during the PMI, the release of catabolic enzymes would accelerate the breakdown of cell structure. Indeed, one study defines lysosomal cell death, i.e. cell death resulting from lysosomal membrane permeabilization and the resulting activity of cathepsins and other proteases, as a synonym for autolysis (Fricker et al., 2018). Multiple studies have reported that lysosomal enzymes contribute substantially to decomposition in the postmortem brain (Albrechtsen, 1977a; Shibayama and Kitoh, 1976). While some studies report that the number or size of lysosomes increase during the PMI, the evidence for this is mixed, the effect size is not strong, and lysosomal expansion is not required for lysosomal enzymes to contribute to decomposition (Sheleg et al., 2008; Tafrali, 2019; Van Nimwegen and Sheldon, 1966).

Different protein substrates can have differential sensitivity to enzyme-mediated proteolysis. For example, Geddes and colleagues report that MAP2, NF-M, and NF-L are relatively more sensitive to calpain-mediated proteolysis, while tau and NF-H are more resistant (Geddes et al., 1995). As another example, Sarnat and colleagues report that NeuN immunoreactivity tends to degrade within 6 or 12 h of PMI, while synaptophysin is much more resistant to postmortem autolysis and can be detected even in brains with PMIs of more than 96 h (Sarnat et al., 2010). Different regions of the same protein can also have different rates of postmortem proteolysis. For example, Li and colleagues studied the postmortem degradation of different epitopes of glutamate transporters in rat brains after 0-72 h PMI (Li et al., 2012). They found that the termini of GLT-1 degrade much faster than the central parts of the protein. They also found that the proportions of immunolabeling signal observed for different epitopes varies by the PMI. If the region of a protein recognized by an antibody is proteolyzed first, then the protein could appear to be totally absent when immunolabeled with that antibody, even though other parts of the protein could still be present. Even if a biomolecule does not disintegrate into component parts during the early PMI, it could still undergo a change in conformation, which could also lead to a false negative result when attempting to measure the protein's distribution with a particular label.

Postmortem proteolysis does not always decrease antigenicity, but instead is often found to increase the immunolabeling signal for certain proteins. For example, multiple studies reported that postmortem proteolysis leads to more accessible epitopes of the astrocyte marker GFAP (De Groot et al., 1995; Hilbig et al., 2004). Similarly, immunoreactivity for the vascular basement membrane marker laminin increased during the PMI, which has been attributed to unmasking by proteolytic processes (Mori et al., 1992; Szöllősi et al., 2018). Hayes and

colleagues found that during the PMI, staining for somatostatin 28 decreased, while staining for its breakdown products somatostatin 14 and somatostatin 28_{1-12} increased, suggesting post-mortem proteolytic processing of somatostatin 28 (Hayes et al., 1991). Monroy-Gomez and colleagues found that immunostaining for rabies antigens increased substantially in the postmortem period, which they attributed to autolytic disintegration of the intracytoplasmic viral inclusions and subsequent dispersion of the viral antigen (Monroy-Gómez et al., 2020)

As with protein processing, lipid breakdown is also thought to be enzyme-mediated, via the activity of lipases such as phospholipase A2 (Jernerén et al., 2015). Lipids can be divided into metabolic and structural classes. Metabolic lipids such as endocannabinoids are often rapidly degraded in the PMI (Palkovits et al., 2008). However, the levels of structural lipids are liable to be stable for longer periods. For example, one study in rat brains found that the composition of glycerophospholipid, a major structural lipid component of cell membranes, did not change significantly up to a PMI of 18 h (Pearce and Komoroski, 2000).

Many studies have been performed on the biomolecular composition of the brain in the early PMI. While a full analysis is outside of the scope of this review, a general trend is that the levels of proteins in the brain, including synaptic proteins, tend to be surprisingly well maintained for many hours and often up to one or two days of PMI (Fountoulakis et al., 2001; Halim et al., 2003; Knudsen and Pallesen, 1986; Siew et al., 2004; Stan et al., 2006). It is worth noting, however, that the effect of the PMI on protein breakdown is highly variable depending upon the protein considered (Ferrer et al., 2007). Another source of variability in postmortem proteolysis is across cell types. Li and colleagues reported that there was a significant heterogeneity of postmortem proteolysis rates across cells, resulting in patchy immunolabeling patterns (Li et al., 2012). In the cerebellum, postmortem proteolysis has been suggested to occur earlier in the granule cells than in the Purkinje cells (Albrechtsen, 1977a).

Alterations of biomolecule distribution

For this review, we are interested in the extent to which the postmortem spatial distribution of populations of biomolecules matches their *in vivo* distribution. We are not focused on the precise location of individual biomolecules, which are thought to be exchangeable in their functions and are often diffusing within a given cellular region *in vivo* regardless. We define two spatial scales when discussing altered location of biomolecules: the *structural feature* level, which considers alterations in the location of objects made of many biomolecules seen under the microscope, and the *biomolecule* level, which considers alteration of locations of individual types of biomolecules. Cells themselves can be thought of as structural features and can also move in the PMI, although many non-blood cells are tethered to one another and to the extracellular matrix by connections that are relatively resistant to postmortem decomposition.

Although the structure of individual biomolecules is often stable in the early PMI, if the biomolecules that comprise cell membranes move sufficiently far from their original locations, then cell morphometry can still be lost. Indeed, cell membrane morphology is often reported to break down prior to the breakdown of its biomolecular constituents. For example, Hukkanen 1987 reported that myelin ultrastructure in surgical specimens had degenerated after 24 h of PMI at 25 °C, even though the levels of the major myelin glycoprotein were unaltered (Hukkanen and Röyttä, 1987).

Subcellular structural features such as organelles are frequently reported to move in the PMI. This can occur due to mechanical forces that arise by swelling, shrinkage, or other fluid shifts, leading to an increase in local pressure and thereby causing the intermolecular bonds stabilizing structural features to break. It can also occur due to catabolism of the biomolecules that typically maintain the structure in place. For example, several studies have found that myelin lamellae tend to split during the PMI, which is likely due to a combination of mechanical forces and the breakdown of the biomolecules typically connecting the lamellae (Ansari et al., 1976a; Hukkanen and Röyttä, 1987; Rees, 1976; Shibayama and Kitoh, 1976). As another example, one study found

that cilia on ependymal cells had fused together and sunk down onto the ependymal surface after 1 h of PMI (Hetzel, 1980). This may be due to a postmortem fluid shift within ventricular spaces.

At the level of individual biomolecules, the situation can be more complex, requiring us first to understand how biomolecules are organized during life before we can understand how this organization is lost postmortem. There are three types of biomolecular organization patterns that we will consider, which are not mutually exclusive: *confinement* in compartments, *inclusion* in gel-like networks, and *maintenance* by active transport mechanisms.

The most obvious form of biomolecular organization results from containment within cell compartments, such as within a cell or organelle membrane. In living cells, diffusion is often constrained to a local area, such as by an organelle membrane or cytoskeletal structure. The nature of the confinement depends on the size and properties of the molecule as well as the properties of the confining material. After death, membranes will eventually become permeable and therefore there will be a loss of confinement.

The next form of biomolecular organization is the gel-like network. Structural features seen under the microscope are often composed of densely aggregated, gel-like networks (Douglas, 2018). For example, the nucleolus is made up in part by a concentrated gel of enmeshed rRNA (Lafontaine et al., 2021; Riback et al., 2022). Gel-like networks can be formed by covalent and non-covalent interactions that lead to the aggregation of biomolecules. During the PMI, intra- and inter-molecular bonds will degrade due to hydrolysis and loss of active maintenance, causing these gel-like networks to break down. However, many of the constituent biomolecules may still be present in the local area, just no longer densely aggregated enough to be seen under the microscope. As a result, changes in the PMI can cause gel-like structures such as the nucleolus to no longer be visualized under the microscope, even though the local levels of their constituent biomolecules, such as rRNA, may be relatively stable. Notably, the ability to visualize gel-like networks under the microscope can also depend on the strength of crosslinking fixation, which stabilizes them (Wang and Minassian, 1987).

Another major form of *in vivo* biomolecular organization is active transport. In active transport, ATP is expended to move biomolecules and ions against a concentration gradient. After death, ATP will be depleted, so active transport will cease, causing a potential loss of the spatial distribution of biomolecules maintained *in vivo*. An example of this is the loss of sodium–potassium ATPase activity very early in the PMI.

We can next consider what happens to individual biomolecules once these organizing structures and functions are lost in the PMI. Molecular diffusion is the primary driving force of individual biomolecule movement in the PMI, due to thermal fluctuations of molecules in the liquid, which causes constituent biomolecules to be displaced in random directions (Schavemaker et al., 2018). Each biomolecule has its own diffusion coefficient, resulting from its size, lipophilicity, the temperature, how it interacts with the solvent, and the extent to which it is bound to other molecules (Schavemaker et al., 2018). If a population of biomolecules is localized to a particular location or "point" *in vivo* and the organizing factors maintaining the localization are lost postmortem, then its distribution is expected to increasingly spread out during the PMI as a result of diffusion (Schavemaker et al., 2018; Ślęzak and Burov, 2021). In the absence of barriers, postmortem diffusion would be expected to cause the spread of biomolecules to follow a Gaussian displacement distribution, with the degree of displacement depending on the PMI (Manzo and Garcia-Parajo, 2015). However, in biological systems, barriers to diffusion, such as the actin cytoskeleton and extracellular matrix, are ubiquitous, meaning that non-Gaussian spread of biomolecules is commonplace (Manzo and Garcia-Parajo, 2015; Ślęzak and Burov, 2021). Diffusion speeds are substantially decreased in the crowded cytoplasm compared to pure solution, often to an order of magnitude less (Kekenes-Huskey et al., 2016). As the cytoplasm becomes less crowded and structures break down during the PMI, effective diffusion coefficients will accelerate. Because of the complex factors that affect the rate and spread of postmortem diffusion, the outcome of biomolecular diffusion after a given PMI is largely an empirical question about which it is difficult to make precise predictions *a priori*.

Many studies describe the phenomenon in which biomolecules redistribute from a localized to diffuse distribution in the PMI. Sex steroid receptors in brain cells have been found to diffuse from a nuclear to a perinuclear distribution after 24 h of PMI (Fodor et al., 2002). Oehmichen reported that enzymes redistribute from localized to diffuse distributions at different postmortem time courses, beginning for several enzymes at 32 h PMI (Oehmichen, 1980). Hilbig and colleagues found that during the PMI, localized synaptophysin immunoreactivity was lost after 4 h when brain tissue was stored at 22 °C and after 12 h when it was stored at 4 °C (Hilbig et al., 2004). It is also a well-known phenomenon that biomolecules eventually leak into the extracellular space as autolysis progresses (Pélissier-Alicot et al., 2003). As a result, cell membrane visualization will become less distinct when the tissue is labeled by a biomolecule that has undergone postmortem diffusion.

Another complicating factor for predicting the outcome of biomolecular diffusion is that population level movement patterns can be non-random due to sinks that capture biomolecules. As a possible example of this, Mori 1991 studied changes in the distribution of immunostained immunoglobulin during the PMI (Mori et al., 1991). They noted that immunoglobulin leaked out of blood vessels, evolving from a focal to diffuse pattern as the PMI increased, as expected based on random diffusion. Additionally, they found that immunoglobulin underwent a selective neuronal uptake phenomenon where it was incorporated into shrunken, hyperchromatic neurons that had been damaged by trauma. Because such compacted neurons result from a gel-gel phase transition, the uptake may occur as a result of the gel matrix in these neurons capturing diffusing immunoglobulins (Kovács et al., 2007). While this is a plausible mechanism for the postmortem localization patterns of immunoglobulin, it requires further study.

It is also critical to distinguish between the population level biomolecule distribution that is observed under the microscope and the changes in the tissue that led to that observation. As discussed in the previous section, postmortem metabolism can also cause dramatic changes to the composition and/or conformation of individual biomolecules. If postmortem metabolism is not uniform during the PMI, this can affect the observed localization of populations of biomolecules in the PMI. We can call this phenomenon *differential metabolism*. For example, there could be different concentrations of proteases, phospholipases, or endonucleases in different parts of the cell or across cells. Alternatively, there could be a differential change in epitope accessibility between compartments during the PMI, for example due to a decrease in cytoplasmic crowding. As a term agnostic to mechanisms, we will use the term *redistribution* to describe an observed change in the spatial distribution of a type of biomolecule measured at a particular postmortem timepoint.

Several articles described redistribution of certain labeled biomolecules from neurites to cell bodies (i.e. the perikarya) (D'Andrea et al., 2017; Gärtner et al., 1998; Geddes et al., 1995; Irving et al., 1997; Kitamura et al., 2005; Schwab et al., 1994). Among these, Geddes and colleagues reported the redistribution of several different neurofilament proteins, including NF-H, NH-M, MAP2, and tau, from neurites to cell bodies in the PMI, which they call perikaryal accumulation (Geddes et al., 1995). In their discussion, they posed the question of whether this redistribution was due to (a) a shift in the cellular localization of the proteins themselves or (b) a change in the antigenicity of neurofilament epitopes in different compartments, for example due to calpain activation, which we would consider a type of differential metabolism.

Gärtner and colleagues studied the spatial distribution of tau at baseline and after 30 min of PMI in rat brains using seven different tau-specific antibodies, which label for different epitopes of the protein (Gärtner et al., 1998). They found that labeling with two of the antibodies, Tau-1 and 12E8, led to a perikaryal accumulation of staining intensity following the PMI. On the other hand, labeling with three of the antibodies for tau led to no change in the distribution of tau immunostaining in the PMI. They reasoned that their results could be explained by differential dephosphorylation of tau in different compartments of neurons, as opposed to movement of the tau protein itself. Irving and colleagues also reported that the postmortem redistribution of tau was dependent upon the antibody used (Irving et al.,

1997). Taking these studies together, the observed perikaryal redistribution of many neurofilament proteins is more likely due to differential metabolism in different neuronal compartments, rather than a shift in the location of the individual protein molecules.

A special type of postmortem differential metabolism is postmortem synthesis. During the PMI, new biomolecules can be synthesized, leading to population-level shifts in the distribution of the synthesized biomolecule. For example, certain RNA transcripts have been suggested to be transcribed postmortem in the mouse brain (Pozhitkov et al., 2017). While some of these findings could also be attributed to complex differential metabolism, the possibility of postmortem synthesis remains valid and has the potential to alter the spatial distribution of biomolecules (Schwab et al., 1994).

As an insight from an adjacent field, the postmortem redistribution of small molecule drugs across body compartments is a commonly studied phenomenon in forensic pathology (Pélissier-Alicot et al., 2003). Mechanistically, drug redistribution can result from diffusion away from drug reservoirs, cell death, putrefaction, and postmortem metabolism (Yarema and Becker, 2005). More basic and more lipophilic drugs are more likely to move in the postmortem interval. One source notes that the brain is not clearly affected by the postmortem redistribution of drugs (Pélissier-Alicot et al., 2003).

While many biomolecules are observed to have postmortem redistribution, these are not omnipresent findings. Many of the included studies that measured the spatial distribution of biomolecules postmortem did not find a significant degree of postmortem redistribution (Blair et al., 2016; Quartu et al., 2005; Serra et al., 2005). For example, Blair and colleagues found that the expected neuronal localization of NeuN immunostaining localization in isolated human brain tissue did not change during the PMI time points analyzed, up to 53 h of PMI (Blair et al., 2016). As another example, Serra and colleagues found that immunostaining patterns for GFRalpha-1, GFRalpha-2, GFRalpha-3 and Ret receptor molecules were not substantially altered up to 72 h of PMI in rat brains (Serra et al., 2005).

Summary

There are numerous distinct mechanisms that lead to changes in observed cell morphometry during the PMI (**Table 1**). These include the initiation of cell death by oncotic necrosis, fluid shifts causing swelling of tissue elements and vacuolization, biomolecular breakdown by catabolic enzymes, and biomolecular redistribution. By characterizing the mechanisms of postmortem decomposition, our goal is to allow predictions to be made about how cell membrane morphometry will degrade during the PMI. These mechanisms have the potential to differ substantially from biological processes occurring *in vivo*. They also have implications for which methodologies are likely to be most robust for use in postmortem brains. For example, individual biomolecules may have artifactual disintegration or redistribution during the PMI. As a result, using individual biomolecular labeling as a proxy for cell membrane morphology is not expected to be as robust of a method as staining nonspecifically for classes of biomolecules, unless the labeled biomolecule is highly stable in the PMI.

Rates of postmortem decomposition

Time series

Describing the mechanisms of postmortem decomposition does not tell us about the kinetics over which the decomposition occurs. There are three types of empirical studies that we will review next to address this question: time series studies, correlational studies, and case reports.

In a time series study, the PMI is experimentally controlled, thus allowing an estimate of the effect of a given PMI on cell membrane morphology. Because the time series study design is less susceptible to confounding biases, it allows for the most reliable estimates of the three study types. As an example of a time series study, we highlight the study by Haines and Jenkins (Haines and Jenkins, 1968). In this study, the authors measured the effect of PMI on cell structures in the habenulopeduncular tract and nucleus of adult dogs. After death, the brains were kept inside of the head (i.e., *in situ*) and stored at around

Mechanism or associated outcome	Role in postmortem brain decomposition
Cell death by oncotic necrosis	The main cell death pathway in the postmortem brain, wherein the loss of ATP leads to a sequence of morphological changes and eventual necrosis
Autolysis	Primary role in the early postmortem decomposition of brain cells
Apoptosis	Not a substantial contributor to postmortem decomposition, because this cell death pathway requires ATP
Compacted neurons (a.k.a. dark neurons)	May become more common after short periods of PMI, but less common with longer periods of PMI; is not thought to contribute to postmortem decomposition
Temporary ischemia	Temporary cerebral ischemia followed by reperfusion has much different mechanisms of decomposition (e.g. requiring ATP) than the permanent global cerebral ischemia that occurs postmortem
Postmortem fluid shifts	Biomolecular breakdown and blood extravasation leads to dramatic fluid shifts in the early postmortem brain; eventually, the brain is transformed to a paste- or fluid-like consistency
Perivascular and pericellular rarefactions	These areas expand and become more frequent in the PMI, which appears to be due to the swelling of astrocyte processes and other cells, causing those areas to not stain on light microscopy
Vacuolization	Common finding in postmortem brain cells and tissue spaces such as the neuropil that evolves throughout the PMI and can cause alteration of cell morphometry or compression of other structures
Biomolecule degradation	Largely driven by enzymes, biomolecule breakdown is a key driving force of postmortem decomposition, varying in rate based on many factors, such as the substrate and the temperature
Biomolecule redistribution	The breakdown of the factors stabilizing biomolecules in place *in vivo* leads them to eventually diffuse away from their original locations, with degrees of both Gaussian and non-Gaussian spread

Table 1. Summary of the role of postmortem brain cell decomposition mechanisms.

25°C. At multiple PMI time points – 0, 6, 12, 18, 24, 38, and 48 h – they extracted the brain, isolated the habenula, and fixed it via immersion in 10% buffered formalin. The tissue was morphologically stained with a method designed to distinguish myelin, axons, and general cell architecture. They reported that general cell architecture began to become indistinct by 18 h of PMI, while myelin and axons were relatively well preserved over the course of the study up until 48 h of PMI. This is an example of how one study can make multiple descriptions about the degree of decomposition of cell morphometry at different time points or for different structural features, which we call "observations".

To build a database and draw comparisons across studies, we extracted the observations from the text of each included time series study (**Supplementary File 5**). For each observation, multiple raters independently graded the severity of decomposition on a subjective 0-3 scale. Note that we are using the term "grade" in the sense of severity rating, as opposed to the use of the term in neoplastic grading. We next calculated inter-rater reliability

scores based on these decomposition grades, using the intraclass correlation (ICC) statistic. The ICC value was calculated as 0.721, with a 95% confidence interval of 0.657 to 0.775 (F-test p-value = 7.9 * 10^{-43}). This score is considered to be of moderate reliability, which likely reflects limitations in both the clarity of the categories we defined as well as the precision by which the observations were described in the included studies (Koo and Li, 2016).

To elucidate the variability in outcomes between studies, we plotted these decomposition grades at different PMIs (**Figure 3**). We found a wide range of PMIs after which histology reaches different decomposition severities across studies, experimental designs, and structural features of focus. Because the studies were very heterogeneous, it was not possible to perform a detailed quantitative meta-analysis of decomposition kinetics across studies. However, as expected, we did identify a significant positive rank correlation between the PMI and the decomposition severity grade when pooling all observations ($\rho = 0.29$, p-value = 4.0 x 10^{-7}).

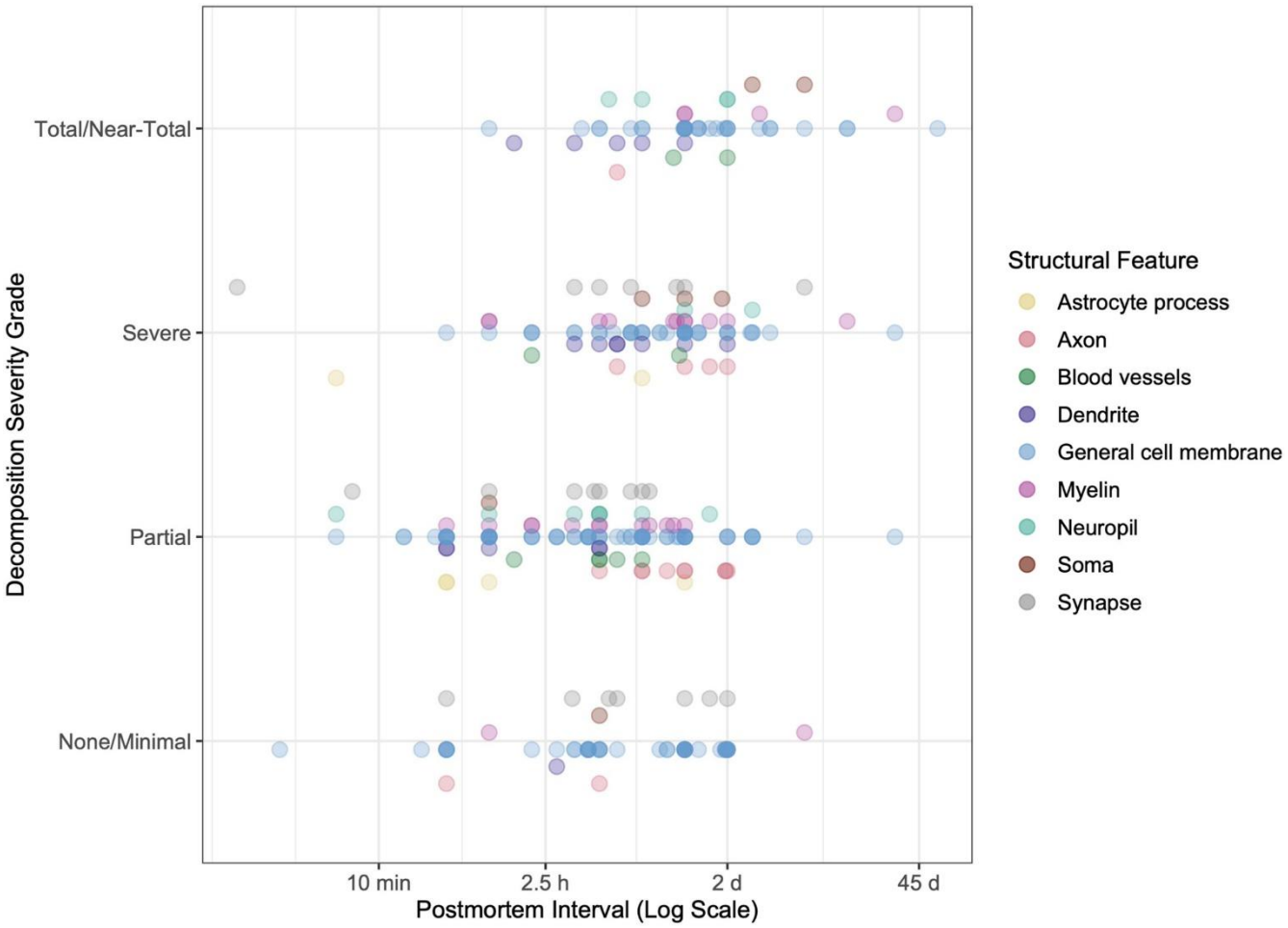

Figure 3. Temporal progression of structural decomposition in time series studies.

Consensus decomposition severity grades (y-axis) plotted with the postmortem interval (x-axis, log scale). Each data point is a single observation made by a study. Each study can have one or more observations. To avoid overplotting, the opacity of each data point is lowered so that overlapping points can be distinguished as darker. Data points are colored by the structural feature. Each structural feature needs to have at least six observations to be in its own category. Otherwise, it is categorized as a type of "general cell membrane".

Correlational studies

Rather than making observations at defined time points, correlational studies make observations about how the appearance of a structural feature varies over a range of PMIs. Because these studies are correlative, before discussing them further, it is important to consider the limitations when using correlational studies to estimate the effect of PMI on cell membrane degradation (Lewis, 2002; Palmer et al., 1988). These are not limitations of the original studies, which often do not have this task as the primary goal, but rather limitations of using this data for our purposes in this review.

The first limitation is the potential for confounding variables, such as agonal state and tissue pH (Glausier et al., 2019). A second limitation is that many studies correlate multiple structural features with the PMI but do not perform an adjustment for multiple hypothesis testing, raising the probability of a spurious correlation. A third limitation are statistical floor or ceiling effects, based on the range of PMIs. If the shortest PMI is several hours after death, or the longest PMI is relatively short, this restricts our ability to infer what occurs in brain tissue outside of the PMI range sampled. A fourth limitation in the many included studies that treat the PMI as a nuisance variable that must be considered is the possibility of publication bias. Finally, a fifth limitation is selection bias if tissue requires a quality standard for inclusion in a study. This would clearly affect any naïve correlations measured with the PMI. As an example of quality selection bias, one study included 16 brains with PMI < 24 h (Jacobs and Scheibel, 1993). This study also included 4 brains with PMI of longer than 24 h because those brains had been refrigerated and the tissue appeared to be in good condition. While the study found no correlation between PMI and total dendritic length as measured by Golgi-Cox staining, this result is more difficult to interpret in terms of PMI effects given that brains with longer PMIs were included because of relatively better markers of tissue quality.

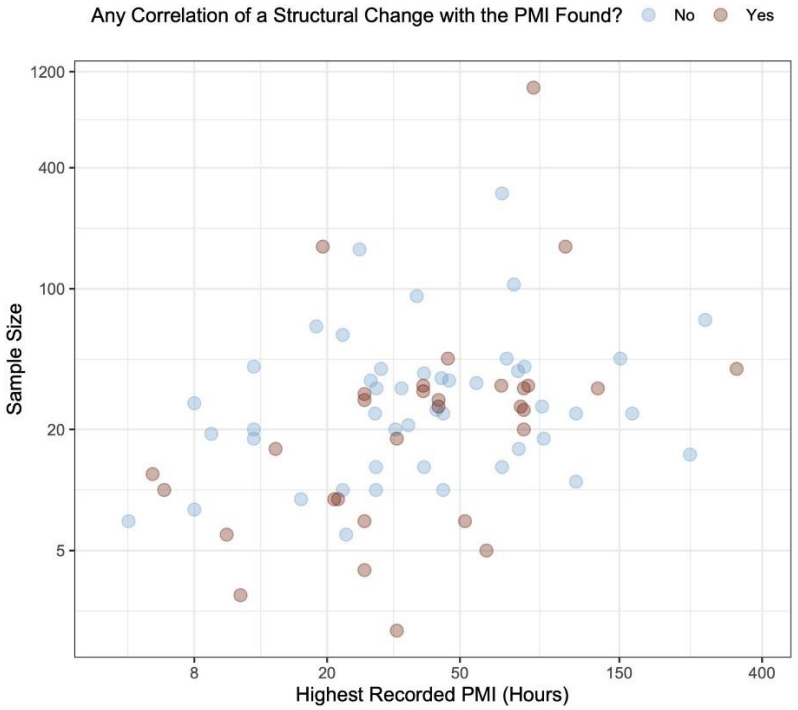

Figure 4. Cell morphometry changes associated with the postmortem interval in the included correlational studies.

In this plot, each correlational study is a data point. If the study describes an association between the postmortem interval (PMI) and a change in any type of cell morphometry, based either on statistical significance or the qualitative impression of the authors, then that data point is considered positive or "yes", and vice versa for "no". If it is unclear whether there was an association reported in the study, then the data for that study is not included in the plot. If there are multiple structural changes tested and at least one of them has an association with the PMI, then that is considered positive for the purposes of this visualization. Both the sample size of the study (i.e., the number of brains considered, y-axis) and the highest recorded PMI (x-axis) are plotted on log scales.

Despite the potential limitations of correlational studies, they are still helpful, especially for exploring large effect sizes over the PMI range studied. Correlational studies can aid in bounding the range of plausible postmortem effects over the time ranges studied. Evaluating this literature is helpful for investigators studying tissue stored in brain banks, because it is most representative of the brain tissue that is available for study.

We found as an overall trend from correlational studies that the PMI often does not have a substantial effect on cell morphometry (**Figure 4**; Supplementary File 6). Some studies even find this with PMIs of several days. For example, Garey and colleagues used rapid Golgi impregnation to study cell morphometry in 24 brains with a PMI range of 4 to 120 h, finding that there was no significant effect of this time range on the observed dendritic spine density of pyramidal neurons (Garey et al., 1998). However, other studies have found that even relatively shorter PMIs can have a substantial effect. For example, Booze and colleagues found that there was a loss of staining for fine varicose axons over a PMI range from 1 to 6 h (Booze et al., 1993). The effect of PMI likely depends on characteristics of the cohort studied, such as whether the bodies were refrigerated, as well as the visualization methods and structural feature investigated.

Case reports

Case report studies, of which six were identified, describe the degree of preservation of cell morphometry in relation to the PMI of a single brain (Supplementary File 7). For example, MacKenzie reported a case of a body that was immersed in water in late autumn and winter for 10 weeks prior to autopsy (MacKenzie, 2014). The histology quality of this brain was reportedly "good", with morphological changes of anoxic neuronal injury and axonal spheroids still able to be identified. As another example, Gelpi and colleagues described a case of where a body was stored in a mortuary cooling chamber for 2 months after death prior to autopsy (Gelpi et al., 2007). Histomorphology was described as "well preserved", with all cell types, neuropil, and axons appropriately visualized, although they did note moderate vacuolization of brain parenchyma. On the other hand, Suárez-Pinilla and Fernández-Vega described a case with severe autolysis of granule and Purkinje cells in the cerebellum after only 6 h of PMI, which was associated with a metabolic insult (Suárez-Pinilla and Fernández-Vega, 2015). Notably, the rest of the brain was found to have essentially normal microscopic findings.

Case reports demonstrate exceptions from the typical way that practitioners in the field are perceived to think about the problem, thereby making these findings especially interesting for publication. In this sense, the case reports collectively show that it is considered surprising when cell membrane structure is maintained after a PMI of several weeks, or when it is lost in one brain region after a PMI of only 6 h.

Summary

The studies we identified had a wide range of PMIs, over which cell morphometry was altered to different degrees. Time series studies offer experimental control but create artificial contexts divergent from naturalistic studies relevant in brain banking. Correlational studies have several confounds limiting their interpretation, but they represent the practical contexts that investigators encounter. Finally, the few case reports identified may illustrate the limits of our understanding and they may challenge paradigms. As an attempt to explain the high heterogeneity between studies, we next turn our attention to potentially modifying variables.

Differences in decomposition rates across assessment methods

Changes identified due to the PMI depend in complex ways on the methods used to visualize them. For example, there might be selective degradation or inaccessibility of the label measured in the visualization procedure, rather than the structure itself. Intracellular regions could also become more difficult or easier to stain if the cell membranes are partially degraded, for example due to changes in membrane permeability.

Immunohistochemistry

Immunohistochemistry (IHC) is a method commonly used as a proxy of cell membrane morphology. IHC involves the use of specific antibodies that

can bind to target antigens of biomolecules, which are then labeled with a detectable marker, allowing for the visualization of the antigen under the microscope. In IHC, an abnormal staining pattern could result if the labeled biomolecule (a) is totally lost from the tissue, (b) has been fragmented, (c) has undergone a conformation change, (d) has bound to another biomolecule that blocks the epitope, or (e) the antibody is not able to diffuse closely enough to the biomolecule due to accessibility issues. For example, Gärtner and colleagues used different anti-tau antibodies to study how tau immunostaining is affected by 30 min of *ex situ* postmortem storage at 37° C (Gärtner et al., 1998). They found that three antibodies were not affected by the PMI, two others revealed alterations in the labeling patterns identified, and two others showed complete loss of immunoreactivity. This is an example of how different epitopes of the same protein can be variably affected by the PMI.

While caution is warranted in the interpretation of IHC signals for antigens that are unstable in the PMI used as a proxy for the structure of cell membranes more broadly, IHC staining for certain biomolecules that do not undergo changes postmortem can be useful. For example, one study found that immunostaining for Calbindin-D28K was more sensitive in postmortem brain tissue than Nissl staining for detecting Purkinje cells, although neither of these methods were found to vary with the PMI range studied of 3 to 48 h (Whitney et al., 2008). Another study found that neuronal morphology was lost with toluidine blue staining at 30 h PMI, but that immunostaining for rabies antigen was still able to delimit the profile of the soma of infected cells at this time point (Monroy-Gómez et al., 2020).

Morphological staining

The most common morphological stain is H&E. Hematoxylin stains basophilic regions of tissue such as the nucleus and rough endoplasmic reticulum, while eosin stains acidophilic regions such as the cell membrane, extracellular matrix, proteins, and most organelles (Chan, 2014). Nissl staining is also common, wherein basic dyes such as cresyl violet or thionine bind to nucleic acids in the cell including RNA in the rough endoplasmic reticulum or in free ribosomes (Kádár et al., 2009). Because certain neurons have high concentrations of rough endoplasmic reticulum, Nissl staining can highlight neuronal cytoplasm, but morphology is poorly visualized, although basic structural aspects of somata may be discerned.

While H&E and Nissl stains are not effective at visualizing neuronal processes, other specialized chromogenic dyes can be helpful. For example, Das and colleagues used staining with the lipophilic dye DiI and found that dendritic spines can be visualized for up to 28 h of PMI in cases of sudden death (Das et al., 2019). They conclude that this is a longer period of dendritic spine stability during the PMI than previously thought, and that they were able to detect dendritic spines at extended time points because of their novel method.

The Golgi impregnation is a different technique that completely stains a subset of cells including their entire dendritic tree (Kang et al., 2017). There are differences in the sensitivity of different Golgi stains to the PMI. Specifically, rapid Golgi stains are more sensitive to changes in the PMI than Golgi-Cox. One study found that a PMI of more than 4 h leads to a reduction in visualized dendrite length in rapid Golgi stained tissue (de Ruiter and Uylings, 1987). Another study suggested that Golgi-Cox impregnation had robust visualization of dendritic spines with longer PMIs (up to 28 h tested), while rapid Golgi staining only had similarly good visualization for one case with a shorter PMI of 6 h (Buell, 1982).

In contrast to Golgi methods, the Bielschowsky method uses silver to stain essentially all types of cells and neural processes in the brain (Switzer, 2000). It is most often used to visualize axons and has been reported to be robust to changes in the PMI. For example, one study found that there was no change with Bielschowsky staining after 24 h of PMI (as cited in (Haines and Jenkins, 1968)). In a case report of a brain with a PMI of 2 months, another study reported that Bielschowsky silver impregnation was more robust for the visualization of axons than staining with anti-neurofilament antibodies (Gelpi et al., 2007). However, as the likelihood of putrefaction increases with extended PMIs, Bielschowsky stained tissue needs to be examined with more caution, because colonies of microorganisms can also stain positive and mimic neuritic plaques (MacKenzie, 2014).

Taken together, as opposed to IHC for potentially unreliable antigens, morphological stains are reported to be more robust to changes in the PMI, because they label classes of biomolecules rather than specific ones.

Electron microscopy

The electron microscopy (EM) studies included in this review generally stain tissue with osmium tetroxide, which primarily labels unsaturated lipids in membranes, and uranyl acetate, which has binding affinity towards proteins and provides contrast (Hua et al., 2015; Moscardini et al., 2020). However, staining protocols for EM are fastidious and require precise optimization (Tapia et al., 2012). Because the properties of brain tissue might be substantially altered during the PMI, additional optimization of the staining protocol for postmortem conditions might be required, which is not necessarily always performed. As a result, as with all stains, it is possible that with increasing PMI, what is lost when visualizing tissue with EM is not the structural components of cell membranes themselves, but rather the ability to identify them with the particular methods employed.

For example, as previously discussed, Gibson and Tomlinson claim that the decrease in visualized synapses on EM over the first day or two of the PMI is largely due to cell process swelling which compresses synapses and makes them more difficult to visualize in 2D sections (Gibson and Tomlinson, 1979). If this is the case, then the compressed synaptic membranes could still potentially be visualized by an alternative approach such as a high-resolution volumetric EM method or an immuno-EM method that labeled for a particular synaptic protein that is relatively resistant to postmortem decomposition. Consistent with the sensitivity of EM to changes in the PMI, Sarnat and colleagues claim that EM is more sensitive to PMI artifacts than their light microscopy method of visualizing synapses by immunostaining with synaptophysin (Sarnat et al., 2010). Other authors have also claimed that light microscopy is more robust than EM to changes in the PMI in the visualization of synapses (Peroski et al., 2016).

Summary

Taken together, various methods of visualizing brain cell membranes differ in their robustness to changes in the PMI (**Table 2**). As a result, investigators need to be aware of the potential for bias when using methods that are not as robust to postmortem changes.

Selective vulnerability to decomposition

During the PMI, some aspects of cell membranes decompose faster than others. These structural features include various aspects of cell membranes, such as dendrites or synapses. Each instance

Method	Reported robustness to postmortem decomposition
Immunohistochemistry	Often sensitive to postmortem changes, but highly dependent on the antigen labeled
H&E and Nissl	Relatively robust to postmortem changes, but unable to visualize cell processes
Specialized chromogenic dye	Some methods are relatively more robust to postmortem decomposition (e.g., DiI staining)
Golgi	Golgi-Cox is more reliable than rapid Golgi
Bielschowsky	Reported to be generally robust to changes in the PMI, but can show false positive staining for microorganisms
Electron microscopy	May be more sensitive than light microscopy to postmortem changes. Structures may be not visualized on two-dimensional images due to compression

Table 2. Summary of the relative robustness of different visualization methods to postmortem decomposition in the brain.

of a feature is generally composed of millions or billions of individual biomolecules, which make up the underlying biochemical material. Our attempt to summarize these collections of biomolecules by describing them with a single name is meant to be a useful abstraction, although there is a significant heterogeneity of biomolecular content within features of the same type.

Models of selective vulnerability

As an initial way to think about how quickly different features might degrade, we can consider a naïve model in which: (a) the density or composition of biomolecules does not vary significantly between features and (b) the decomposition rate of each biomolecule is independent of its local context. Under this model, features will degrade at a rate proportional to their size. Of course, both assumptions of this model are false. Different features are clearly composed of different types of biomolecules; for example, the cytoskeleton of axons tends to be made of more longitudinal neurofilaments, whereas the cytoskeleton of dendrites tends to be made of microtubules, which may degrade at different rates postmortem (Schwab et al., 1994). Similarly, the decomposition rate of each biomolecule will clearly depend on its local context, such as the density of catabolic enzymes. A size-proportional decomposition model, under which structural features decompose at a rate proportional to their size, may still be a helpful first approximation. Smaller features will have fewer biomolecules, a lower probability of a label binding to that biomolecule, and therefore a lower probability of being visualized as its constituent biomolecules begin to degrade and it eventually disintegrates during the PMI.

Brain region and cell type heterogeneity

Before discussing sub-cellular features, it is important to consider how rates of decomposition vary across brain regions and cell types. Certain brain regions, such as the hippocampus, are well-known to be more susceptible to degeneration due to temporary cerebral ischemia followed by reperfusion injury. However, damage following temporary ischemia is an active process and therefore caused by a different decomposition mechanism than what occurs postmortem. Multiple studies reported that postmortem decomposition generally progresses at equal rates in the different brain regions studied, instead of progressing faster in brain regions more susceptible to temporary ischemia (Garcia et al., 1978; Spector, 1963).

The main brain region that has been associated with a faster rate of postmortem decomposition is the cerebellum (Averback, 1980; Furukawa et al., 2015; Finnie et al., 2016). Bywater and colleagues reported that the cerebellum is the most sensitive region to postmortem autolysis, with significant changes occurring within 20 min, which they attribute to the high enzyme content of the granular layer (Bywater et al., 1962). Ikuta and colleagues also reported that there is a selective disintegration of the granular layer of the cerebellum in the PMI, without a change in glia or adjacent Purkinje cells, due to similar enzyme-mediated autolysis in granular cells (Ikuta et al., 1963). Albrechtsen noted that there is a significant correlation between the pH of the brain tissue and the degree of decomposition of the granule cell layer of the cerebellum, consistent with a role of enzyme-mediated autolysis (Albrechtsen, 1977a).

Aside from the cerebellum, some sources described the relative vulnerability of other brain regions, although not as consistently. Multiple sources reported that white matter tends to be better preserved than other regions of the brain (Furukawa et al., 2015; MacKenzie, 2014). One source noted that the cortex tends to be better preserved than the basal ganglia and thalamus (MacKenzie, 2014). Oehmichen noted that the pons and certain thalamic nuclei are the first to show damage in the PMI (Oehmichen, 1980). Yeung and colleagues, studying an extended PMI of 30 d, found that outer layers of the cortex (I-III) were less well preserved than the inner layers of the cortex (IV-VI) (Yeung et al., 2010). Notably, there can also be a patchy heterogeneity of decomposition within a local area of the brain (Lesnikova et al., 2018). Some regional differences may also be confounded by immersion-based preservation methods, which is discussed below.

In terms of cell types, one source noted that ventral thalamic nucleus neurons and small cells of the striatum are the most vulnerable to postmortem decomposition, while large pyramidal cells in the parietal cortex are the least vulnerable (as cited in

(Choe et al., 1995)). Several other sources also report that larger neurons are better preserved and/or that smaller neurons have more rapid postmortem changes (Irving et al., 1997; Lindenberg, 1956; Williams et al., 1978). It has been reported that there is a large heterogeneity in the decomposition rate within a cell class (as cited in (Choe et al., 1995)). In the anterior pituitary, significant variability of decomposition rate has also been reported within cell type classes, attributed to the functional state of the cell at the time of death (Ilse et al., 1979). Overall, decompensation kinetics are highly variable even within a cell type class, but certain types of smaller cells may be relatively more vulnerable.

Alterations in cellular and subcellular volumes

In cell death by oncotic necrosis, cells are expected to initially swell in the first stage, and eventually shrink as necrosis progresses. However, the presence or absence of cell swelling depends on the local environment, including any fluid take-up by other nearby cells. Indeed, cells may even shrink initially if nearby cells take up relatively more fluid. Moreover, swelling may also be transient and not captured by the histological techniques at any given timepoint (Majno and Joris, 1995). Therefore, the potential effects of PMI on cell volume are challenging to predict.

Cell swelling is one of the most common morphometric findings early in the PMI. Schulz and colleagues reported cell swelling after 30 seconds of PMI that disappeared with continued postmortem time (Schulz et al., 1980). They explain the mechanism as due to an increase in intracellular cations, leading to a rise in intracellular oncotic pressure. Shibayama and Kitoh noted swelling of pyramidal cells at 1 h PMI, which they reported was more pronounced near the white matter (Shibayama and Kitoh, 1976). In their study of isolated biopsy brain tissue, Dachet and colleagues found that neuronal swelling first appeared by 2 h of PMI and that by 4-8 h, a majority of neurons were swollen (Dachet et al., 2021).

Cell volume changes can have complex evolution patterns over the PMI. Hayes and colleagues found that average neuron size in the white matter of monkey brains increased only slightly following a 2 h PMI, then increased substantially at a 12 h PMI, and then there was no additional increase at 24 or 48 h (Hayes et al., 1991). They note that the inclusion of brains with relatively longer PMIs in human cohorts may be helpful to factor out the effect of PMI on neuron size. In their study of horse brains, Wenzlow and colleagues noted a linear decrease in the size of the cytoplasm up to 3 d of PMI when brains were stored at stored at 8 °C, although no volume changes were detected when brains were stored at 22 °C (Wenzlow et al., 2021). Tafrali found that neurons shrank at 12 h PMI, while astrocytes and to a lesser extent oligodendrocytes increased in size (Tafrali, 2019). As opposed to swelling of many cell types, capillaries have been found to have decreased volume at 22 h PMI (Hunziker and Schweizer, 1977).

Consistent with the previously described mechanism of fluid shifts, many studies describe swelling of astrocytes and astrocyte processes (Dachet et al., 2021; Gibson and Tomlinson, 1979; Shibayama and Kitoh, 1976; Tafrali, 2019; Williams et al., 1978). Jenkins 1979 noted that astrocytic cell bodies and processes were more dramatically swollen than neurons or oligodendrocytes, starting at 5 min of PMI and continuing until 25 min of PMI (Jenkins et al., 1979). Arsénio-Nunes and colleagues described pronounced astrocyte process swelling in the molecular layer and at the level of vascular end feet at 30 min PMI (Arsénio-Nunes et al., 1973). Finnie and colleagues reported that Bergmann glia had cytoplasmic swelling much earlier than Purkinje cells in the PMI (Finnie et al., 2016). Del Bigio and colleagues described pronounced swelling of astrocytes and oligodendrocytes during the PMI that could be spatially associated with a hemorrhagic lesion prior to death (Del Bigio et al., 2000). They attributed the postmortem etiology of this swelling as due to the uptake of leaked plasma proteins from the extracellular space by these cell types during the PMI. Rees found that astrocyte processes were “markedly swollen” at 2 h of PMI and that this was especially evident in astrocytes around blood vessels (Rees, 1976).

In summary, postmortem cell volume changes very frequently occur in the PMI. Swelling can occur very early in the PMI and may either persist, revert, or convert to shrinkage. Generally, the volume of a

given cell or cell sub-region assessed after a given period of PMI cannot be assumed to be the same as it was *in vivo*. Cell volume changes are also heterogenous across cell type, between brain regions, and dependent on local events such as hemorrhage.

Dendrites

Dendrites play a critical role in information processing in the brain and have a wide variety of shapes and configurations. They can be very narrow, with diameters of less than 500 nm in certain areas (Harris and Spacek, 2016). Dendritic spines have especially narrow necks connecting them to dendritic shafts, with diameters of 50-400 nm (Adrian et al., 2014). Based on the size-proportional decomposition model, dendrites are expected to be among the most vulnerable features to postmortem decomposition.

Several studies using immunohistochemical approaches have noted that immunoreactivity is lost from dendrites relatively early in the PMI. Boekhoorn and colleagues found that doublecortin immunoreactivity was greatly diminished in dendrites after a PMI of only 1 h in rodent brains and was effectively lost by 8 h PMI, while soma immunoreactivity was retained for a longer time (Boekhoorn et al., 2006). Using calretinin staining in the monkey hippocampus, Lavenex and colleagues found that dendrite staining became coarser over a PMI of 2 to 48 h (Lavenex et al., 2009). Specifically, while dendrites could still be visualized in the later PMI brains, they appeared as a string of discontinuous agglomerates as opposed to a series of ovals connected by a continuous fiber. Multiple studies used the antibody SMI-32, which binds to neurofilament H and can be used to visualize neuronal processes including dendrites. Gonzalez-Riano and colleagues did not find any changes in the distribution of staining for SMI-32 in mouse brains at a PMI of 5 h (Gonzalez-Riano et al., 2017). Hilbig 2004 noted that details of the dendritic tree in large pyramidal cells were visible up to a PMI of 12 h with immunostaining for SMI-32. With increasing PMI after 12 h, a granular-like immunostaining of disintegrated dendritic neurofilaments was found instead.

There is a substantial literature on postmortem MAP2 immunostaining, which has also been generally found to degrade relatively rapidly during the PMI, thus reducing visualization of dendrites in MAP2-stained sections (Irving et al., 1997; Kitamura et al., 2005; Lingwood et al., 2008; Schwab et al., 1994). For example, Nakabayashi 2021 performed immunostaining for MAP2 in rat brains, reporting a fragmentation of secondary dendrites at 6 h PMI and a disappearance of primary dendrites at 1 d PMI (Nakabayashi et al., 2021). MAP2 postmortem redistribution has been speculated to be due to the sensitivity of the MAP2 protein to postmortem proteolysis, although the precise mechanism is unclear (D'Andrea et al., 2017).

Some studies using morphological staining have also found that dendrite structure is altered relatively early in the PMI. For example, in a study using the Golgi rapid method to visualize pyramidal neurons in mouse brains, Williams and colleagues noted that dendrites degenerated in a "moniliform" fashion, i.e. with alternating varicosities and constrictions, which was first noticed at 6 h PMI (Williams et al., 1978). At 6 h of PMI, there were also patchy areas of dendrites that had a decreased density of spines. They also reported a centripetal loss of dendrite visualization with increasing PMI, wherein distal segments were lost first followed by more proximal areas. Using an alternative visualization method of differential interference contrast optics, they found that this loss was at least partially attributable to a failure of silver impregnation of distal dendritic segments with increasing PMI. As another example of early dendritic changes in the PMI, Bywater and colleagues used a silver impregnation method and reported that dendrites began to "curl up in a corkscrew manner" by 4.5 h of PMI in monkey brains (Bywater et al., 1962). In their EM study, Rees 1976 found that dendrites were swollen after 30 min of PMI (Rees, 1976). Roberts and colleagues, also using EM, noted that dendrites, along with axon terminals, spines, and mitochondria, became "bloated and/or irregular in contour" at PMIs of greater than several hours, and therefore they restricted their PMI range to less than 4 h (Roberts et al., 1996).

Other studies using morphological staining methodologies found that dendrite morphology is stable for longer PMIs. For example, as previously discussed in the visualization section, Das and colleagues found that dendritic spines can be visualized

via staining with the dye DiI for up to a PMI of 28 h (Das et al., 2019). Within their sample, they found that the PMI was not associated with spine density, spine head diameter, or spine length. Jacobs and Scheibel reported that dendrite morphology was well-preserved in their cohort of human brains, with PMIs up to 32 h (Jacobs and Scheibel, 1993). They used the Golgi-Cox staining method because it had been reported to be less sensitive to postmortem autolysis. They did not find the markers of autolysis (e.g., irregular varicose enlargements and loss of spines) that had been previously reported with the rapid Golgi method by Williams and colleagues (Williams et al., 1978). Yeung 2010 found that dendritic branching patterns could be visualized with Bielschowsky silver staining in a subset of pyramidal cells from human brains after even 30 d of PMI with storage at 4 °C (Yeung et al., 2010).

Much of the correlational literature in human brain cohorts suggests a relative stability of dendritic structures in the PMI, including studies with a PMI range up to 9 h using EM (Kolomeets et al., 2005), up to 28 h or 78 h using Golgi-Cox staining (Boros et al., 2017; Buell, 1982), up to 74 h using immunostaining for glutamate receptor subunits (Benes et al., 2001), or up to 120 h using the rapid Golgi method (Garey et al., 1998). An exception is the study of Tóth and colleagues that used IHC and found that dendrites on calretinin-immunoreactive cells appeared to be shorter, varicose, and degenerating with increasing PMI over a range of 2 to 10 h (Tóth et al., 2010).

It is challenging to reconcile differences in the decomposition rate of dendrites observed across these studies. However, problems with dendrite visualization in studies finding that dendrites degrade relatively faster could help to explain this divergence, whereas it is more difficult to imagine how the literature suggesting dendrites are stable for longer periods of time could be systematically flawed.

In summary, dendritic swelling can occur early in the PMI (Rees, 1976; Roberts et al., 1996). Additionally, there is evidence for clumping or beading of dendritic components (Lavenex et al., 2009; Williams et al., 1978). However, total loss of dendritic cell membranes is not a commonly reported early phenomenon in the PMI. As a result, dendrite tracing in volumetric microscopy data may be possible even in brains with relatively longer PMIs if robust visualization methods are used. Certain morphological staining methods, such as the Golgi-Cox impregnation method, are more resistant to PMI artifacts than others. Experiments labeling for particular biomolecules, such as MAP2 or SMI32, should not be considered dispositive of the state of dendrite morphology more generally.

Axons

Like dendrites, axons are narrow, and have been found to have similar sized or lower average diameters compared to dendrites (Faitg et al., 2021). This makes axons similarly vulnerable to postmortem changes under a size-dependent model. In studies using morphological stains, axons tend to be relatively well preserved, albeit with volume changes at early PMIs. Using rapid Golgi staining, Williams and colleagues found that axons tend to exhibit bead-like changes and become more lightly impregnated after a PMI of more than 6 h, which was a slower change than they reported for dendrites (Williams et al., 1978). In the EM studies by Rees and Roberts and colleagues, it was reported that axons were swollen at the same early time periods as dendrites (Rees, 1976; Roberts et al., 1996).

In their study using light microscopy to visualize the habenular nuclei of dog brains, Haines and Jenkins found that a few large axons started to show areas of slight dilation and constriction at 12 h PMI (Haines and Jenkins, 1968). At 36 h PMI, these areas of constriction and dilation were found in most axons, and almost every axon started to have areas with short loops. Generally, they found that axons retained their integrity up to 48 h PMI and were relatively stable postmortem, which corroborated the previous reports they cited. Segmental axon swelling has also been reported as a consequence of focal ischemia in ultrastructural studies (Pantoni et al., 1996). Notably, this postmortem artifact is distinct from axonal spheroids, which are marked by accumulation of amyloid precursor protein (APP) and can occur in the context of blockage of fast axonal transport (Coleman, 2005).

In immunostaining studies, axon definition can be lost after an extended PMI (Sarnat et al., 2010). For example, Blair and colleagues found that immunostaining for α-tubulin was lost at 48 h PMI in 3/6 of the human brains profiled (Blair et al., 2016). On the other hand, in this study, neurofilament proteins were still detectable at these extended PMIs and axons were still able to be thereby visualized. Eggan and Lewis studied the immunoreactivity of cannabinoid receptor 1 in axons of monkey brain tissue sections with light microscopy (Eggan and Lewis, 2007). They found that after a 24 h PMI, axons became less distinct, and axon terminals became swollen. Booze and colleagues found that immunostaining for fine varicose axons with tyrosine hydrolase was lost between 1 and 6 h of PMI (Booze et al., 1993).

Taken together, axons have similar postmortem decomposition patterns as dendrites, with early swelling and patches of alternating constrictions and varicosities that become more common in the PMI. Some evidence suggests that axons may degrade slightly slower than dendrites postmortem, although this is highly uncertain and may relate to visualization methodology.

Synapses

Time series studies using EM and short PMIs have found that aspects of synaptic morphometry can be altered very rapidly in the PMI, within minutes. Routtenberg and Tarrant found that after 1 min of PMI, there was a substantially diminished concavity of the synapse and a thickening of the postsynaptic membrane (Routtenberg and Tarrant, 1974). Tao-Cheng and colleagues also found that after 6.5 min of PMI, there was a change in curvature and an increased thickness of the postsynaptic density (Tao-Cheng et al., 2007). Karlsson and Schultz found that after 60 min of PMI there were fewer and flattened synaptic vesicles, as well as occasional plasma membrane separation and an increase in extracellular space (Karlsson and Schultz, 1966). Roberts and colleagues noted that as the PMI extends beyond several hours in human brains, the postsynaptic density becomes thicker, thus obscuring whether the synapse is asymmetric or symmetric (Roberts et al., 1996). Huttenlocher noted that in human postmortem brains, presynaptic and postsynaptic markers are less sharply demarcated, and intracleft areas cannot always be seen (Huttenlocher, 1979).

While morphometric properties of synapses are rapidly altered, they are usually found to be demonstrable with EM following a more extended PMI. Rees found that synapses had not disintegrated by 4 h of PMI in cats or 5.5 h of PMI in monkeys (Rees, 1976). Vrselja and colleagues found that postsynaptic densities were preserved at 10 h of PMI, although the presynaptic vesicle pool was not maintained (Vrselja et al., 2019). Tang and colleagues found that there was no significant decrease in visualized synaptic density at 2 d of PMI in mammalian brains (Tang et al., 2001). Shibayama and Kitoh found that synaptic contacts were preserved for PMI of up to 10 h although vesicles decreased in number (Shibayama and Kitoh, 1976). In isolated rat brains stored at 37 °C, de Wolf and colleagues found that synapses were able to be visualized at a PMI of 13.5 h, but the ability to visualize them was lost by a PMI of 24 h (de Wolf et al., 2020). When stored at 0 °C, this study found that synapses could be visualized at 48 h of PMI but were lost at the next time point studied of 168 h of PMI.

One clear exception to the trend of postmortem synapse maintenance is the study of Petit and LeBoutillier which analyzed rat brain tissue with two EM staining methods, measuring both synaptic density and morphometry (Petit and LeBoutillier, 1990). The study required the presence of synaptic vesicles to identify a synapse and only counted synapses had a clear pre- and postsynaptic density. With an osmium-based staining method, it was found that synapse density dropped markedly from 0 to 1 h of PMI, and then markedly once again from 10 to 15 h of PMI. With an ethanol phosphotungstic acid method of staining, synapse density dropped more slowly from 1 h to 15 h of PMI, with a total of 60-70% of synapses lost by the latest PMI time point tested. Notably, synaptic structure within identified synapses was found to be “remarkably stable” up to the longest PMI they studied of 15 h, suggestive that synapses in an intermediate disintegrating state were not frequently found. In the osmium-stained tissue, the decline in the number of synapses from 1 h to 15 h of PMI mirrored an increase in the number

of contacts without synaptic vesicles. The authors suggest that the observed decline in synaptic density in the PMI may be due to a loss of synaptic vesicles and therefore the ability to identify a connection as a synapse, although they noted that other explanations were also possible.

Correlational studies using EM in human brain cohorts have had mixed results regarding synapse preservation. Glausier and colleagues found that there was a significant decrease in the number of postsynaptic densities identified as the PMI increased up to 24 h (Glausier et al., 2019). However, Glausier and colleagues did not find a significant correlation between the PMI and the postsynaptic density length or with the total number of neuronal profiles identified. Roberts and colleagues found that pre- and postsynaptic membrane structures were lost or distorted with PMI of greater than 7 h (Roberts et al., 1996). On the other hand, Roberts and colleagues reported that synapse classification and morphology was equivalent in cases with PMI of up to 7 h (Roberts et al., 2005). Scheff and colleagues found that there was no association between PMI up to 13 h and the synaptic features they studied (Scheff et al., 1990; Scheff and Price, 1993). Kolomeets and colleagues found that there was no correlation between the PMIs of their cohort, which had an average of 6-7 h, and the number of synaptic contacts identified per mossy fiber terminal (Kolomeets et al., 2007). Gibson and Tomlinson found that the numbers of recognizable synapses decreased by 77% at 33 h of PMI, at which point it stabilized until up to 69 h of PMI (Gibson and Tomlinson, 1979). As previously discussed, these authors suggested that the loss of recognizable synapses could be accounted for by the compression of synapses due to astrocyte vacuolization.

It is not clear how to reconcile the differences between studies regarding the postmortem decomposition of synapses. Several studies suggest that synapse visualization can be lost within the first hours of the PMI, while other studies suggest that the delay is longer and that the apparent loss of synapses is due to technical problems rather than synaptic disintegration. The latter prospect is consistent with the finding that partially disintegrated synapses are rarely reported, whereas one would expect to see these if synapses were disintegrating in the early PMI as opposed to becoming not recognizable with the techniques used.

In summary, certain synaptic morphometric changes, such as thickening of the postsynaptic membrane and changes in curvature, can begin in the earliest minutes of the PMI. However, the preponderance of evidence suggests that synapses can remain generally intact for an extended period, up to many hours or even multiple days of PMI. Certain methods of visualizing synapses are more robust in the postmortem period, suggesting that technical approaches are crucial to consider carefully when designing these experiments.

Myelin

One of the major myelin artifacts that is consistently noted in the PMI is myelin lamellae separation. Shibayama and Kitoh noted that myelin lamellae are partially distorted at 30 mins of PMI (Shibayama and Kitoh, 1976). Choe and colleagues described concentric unraveling of myelin at 1 h of PMI (Choe et al., 1995). Karlsson and Schultz noted that there are infrequent myelin membrane separation defects after 1 h of PMI (Karlsson and Schultz, 1966). Rees noted marked separation of lamellae in some myelin sheaths in monkey brains at 4 h of PMI (Rees, 1976). Hukkanen noted the formation of network-like structures in myelin lamellae at 24 h (Hukkanen and Röyttä, 1987). de Wolf and colleagues noted unravelling of myelin sheaths at 9 h PMI with storage at 37 °C (de Wolf et al., 2020). Ansari and colleagues noted that myelin lamellae splitting can also occur in cerebral edema and that its occurrence may be associated with the postmortem increase in the water content of the brain (Ansari et al., 1976b). Another phenomenon, which may be related to lamellae splitting, is volume changes in myelin sheaths. Haines and Jenkins noted a slight swelling of myelin in some areas, first noticed at 18 h of PMI (Haines and Jenkins, 1968). On the other hand, de Wolf and colleagues described myelin thinning, first noticed at 3.86 h of PMI with storage at 37 °C (de Wolf et al., 2020). Aside from these artifacts, myelin is generally reported to be stable in the PMI. Myelin lamellae splitting is not associated with a break in the continuity of the separated lamellae (Ansari et al., 1976a). Several studies note that myelin is a rela-

Feature	Key points of decomposition patterns
Brain region differences	The cerebellum can have faster decomposition than other regions
Cell type differences	Smaller cells may decompose faster than larger cells
Cell volume	Cell volumes changes are rapid and occur within minutes. Ongoing swelling, shrinkage, and compression processes evolve throughout the PMI
Dendrite	Segmental swelling within hours. Highly sensitive to visualization method, and appear to be more stable with more robust methods of visualization
Axon	Segmental swelling and volume changes, similar to dendrites
Synapse	Morphometric changes, including postsynaptic membrane thickening and changes in curvature, occur within minutes. Variability based on visualization method, but their overall presence is relatively stable in the early PMI
Myelin	Lamellar separation without a break in continuity of the separated lamellae. Relatively slow decomposition overall

Table 3. Summary of relative postmortem decomposition rates of different structural features of cell membranes in the brain.

tively robust structure to postmortem decomposition (Haines and Jenkins, 1968; Karlsson and Schultz, 1966; Sele et al., 2019; Vrselja et al., 2019).

Summary

Among brain cell-specific membrane structures, volume and geometry changes are a frequent occurrence early in the PMI, and there are several types of common postmortem artifacts in these structures (**Table 3**; **Figure 5**). However, studies using robust visualization methods tend to find that approximate cell membrane location information is still able to be delineated in the early postmortem period. This suggests that the basic connectivity scheme of brain cells can likely be mapped even after postmortem decomposition has begun.

Variables modifying decomposition rates

Temperature

The temperature at which the brain is stored during the PMI has a very well-replicated role in mediating the rate of postmortem decomposition. Mechanistically, cold storage temperature slows down diffusion, decreases enzymatic activity, and inhibits microbial growth, all of which delay decomposition (Schavemaker et al., 2018). Low temperature storage refers to temperatures down to 0 °C, as below causes ice crystal formation and accompanying tissue damage. Storage temperature has been reported to have the strongest effect on the rate of brain protein breakdown of any modifying variable (Ferrer et al., 2007). One study in sheep brains shows that decreasing the storage temperature dramatically delays the average onset time of a sudden concentration change in several metabolites, attributed to the initiation of putrefaction, from 30 h PMI at 26 °C to 700 h PMI at 4 °C (Ith et al., 2011).

Many studies find that the storage temperature plays a substantial role in the retention of cell membrane structure during the PMI. In their study of synapses in human brains, Kay and colleagues report that they can perform effective ultrastructural analyses on tissue with PMIs of up to 100 h (Kay et al., 2013). They note that a key factor for ultrastructure tissue preservation is whether the cadaver is stored at cold temperature of 4-6 °C to reduce structural degradation. de Wolf and colleagues found that advanced necrosis developed in isolated rat brain tissue at 36 h PMI when stored at 37 °C, compared to 2 months PMI when stored at 0 °C (de Wolf et al., 2020). Hukkanen and Röyttä found that the white matter of isolated human surgical specimens

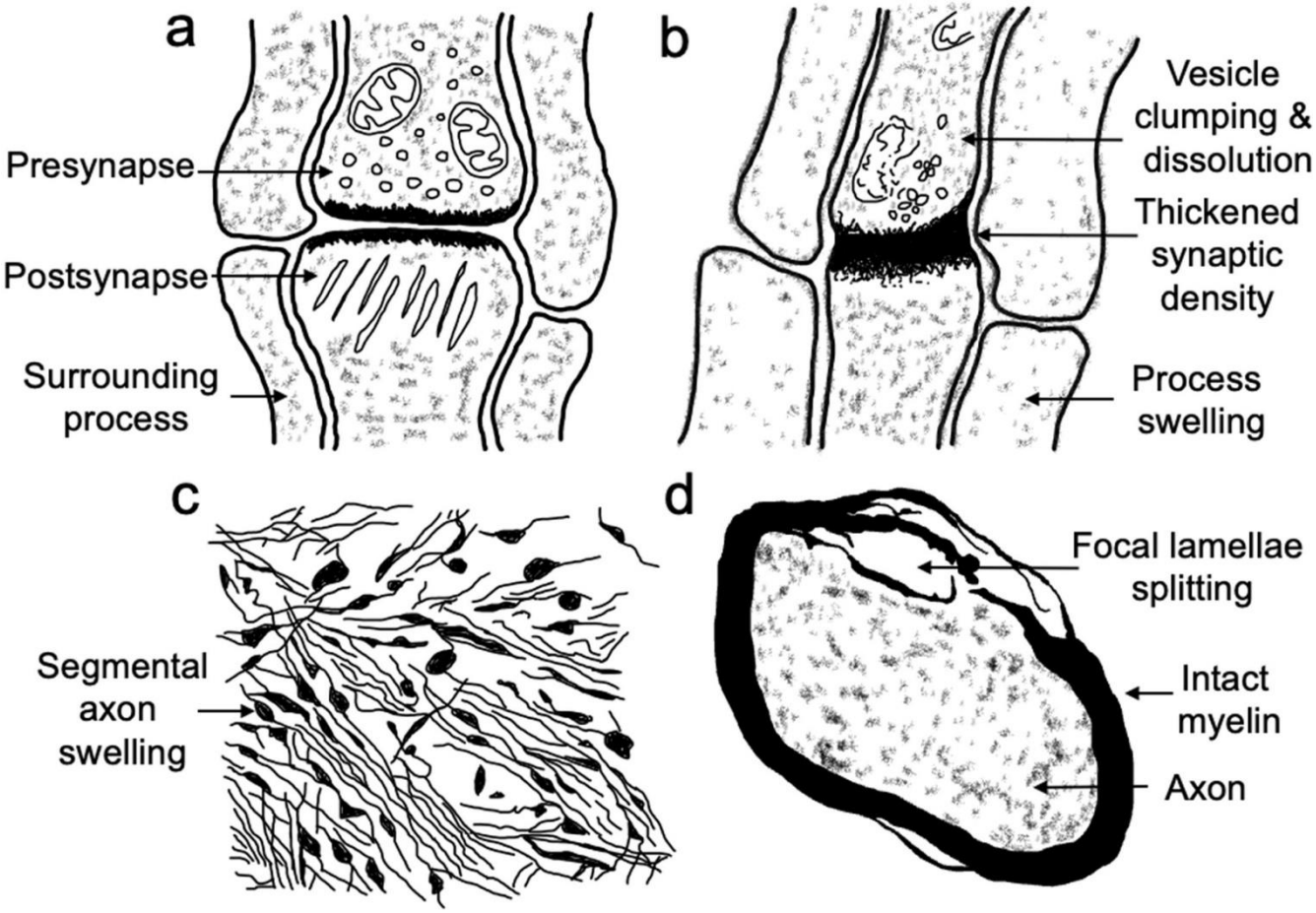

Figure 5. Possible morphometric changes of structural features in the postmortem brain.

A-B: Ultrastructural diagram of a human synapse at an earlier PMI (1 hour; A) with insignificant postmortem changes. Compared to a later PMI (12 hours; B), at which point there are several changes, including vesicle clumping and loss, increased synaptic density with possible difficulty identifying the cleft, swelling of surrounding processes, and mitochondrial damage. These diagrams were adapted from (Anders, 1977) (Figure 2). C: Segmental swelling of axons, adapted from an image of Bielschowsky silver-stained ischemic rat brain tissue from (Pantoni et al., 1996) (Figure 6). D: Myelin lamellae splitting, adapted from an electron microscopy image of postmortem human brain tissue from (Glausier et al., 2019) (Figure 1).

showed degradation patterns at 6 h of PMI when stored at 25 °C, resembling those seen at 24 h of PMI when stored at 4 °C (Hukkanen and Röyttä, 1987).

The environmental temperature at the time of death can also be relevant which has practical implications. For example, more rapid postmortem changes in the brain have been associated with death in summer months, while hypothermia at death is associated with slower postmortem decomposition (Albrechtsen, 1977b; Kitamura et al., 2005). Some brain bankers record the refrigeration delay in addition to the PMI, which is the interval of time between death and when the body was stored at 4 °C (Torres-Platas et al., 2014; Vonsattel et al., 2008). A formula that predicts the amount of brain decomposition based on storage temperature could allow for more accurate estimation of the impact of PMI. For example, the Q10 rule suggests that the speed of chemical reactions in biological systems increases two-fold or slightly more with each 10 °C rise in temperature (Vass, 2011). In the forensic literature, there is a related metric of "accumulated degree days" (Vass, 2011). If the Q10 rule holds, then reducing the storage temperature from a typical room temperature of 20-24 °C to 0-4 °C would be expected to decrease the decomposition rate by ap-

proximately 4-fold. A challenge is that brain temperature does not immediately equilibrate with the environment. Even when the brain is stored at refrigerator temperatures of 8 °C, it can take 20-30 h for the tissue itself to actually reach that temperature, because of the slow rate of heat conduction (Perry et al., 1977). As a result, the effects of refrigerator storage are nonlinear. Consistent with this, studies investigating postmortem effects at earlier PMI time points, such as 4-12 h of PMI, tend to report smaller effects of refrigeration (Hilbig et al., 2004). For the same reason of the low thermal conductivity of brain tissue, refrigerator storage is also expected to have a larger effect on the surface of the brain tissue, in smaller brains, and in isolated brain tissue.

Acidity and agonal damage

Across tissues, high acidity is strongly associated with faster decomposition rates in the PMI. For example, in a study on fish, postmortem decomposition was the fastest in the gastrointestinal tract and slowest in muscle tissue, with the brain somewhere in the middle, as expected based on their relative pHs (George et al., 2016). Across donated brains, those with relatively lower pH values have been found to have more postmortem structural breakdown following a given PMI (Albrechtsen, 1977a; Glausier et al., 2019). A major reason that lower pH is associated with faster postmortem decomposition is that acidic conditions activate certain autolytic enzymes, such as those in capthesin family (Kies and Schwimmer, 1942; Albrechtsen, 1977a; Compaine et al., 1995).

Postmortem acidic conditions in the brain are usually attributed to an increase in the production of lactic acid as a result of anaerobic glycolysis in the absence of oxygen delivery (Powers, 2005). Anaerobic glycolysis, in turn, has been reported to occur predominantly in two time periods: (a) the agonal phase and (b) the first few hours of the PMI.

The agonal phase is the period during which a person is gravely ill and under profound physiologic stress, usually associated with cerebral hypoxia (Lewis, 2002). For some brain donors, the agonal phase can last for only minutes or less prior to death, while for others, it can last for hours or days (Li et al., 2004). Numerous studies have found that a lower brain tissue pH is strongly correlated with a longer agonal phase (Hardy et al., 1985; Johnston et al., 1997; Li et al., 2004). The agonal phase can contribute to damage measured postmortem in two ways. First, brain tissue can decompose during the agonal phase itself, leading to a higher total amount of decomposition after any given amount of PMI. Damage associated with prolonged agonal states can be immense, which is why it is considered extremely important in mediating the degree of tissue decomposition in brain banking (Ohm and Diekmann, 1994; Waldvogel et al., 2006; McCullumsmith et al., 2014; Glausier et al., 2019). Second, because brain cells are hypoxic during the agonal phase, they will produce excess lactic acid during this period, leading to lower pH levels and a faster rate of autolysis once the PMI commences.

In addition to the agonal phase, pH has also been found to decrease over the first several hours of the PMI. For example, one study found that there was a significant inverse relationship of PMIs between 1.5 and 4.5 h and brain tissue pH (Beach et al., 2008). This is likely because some brain cells still have intact metabolic function in this early time range and therefore are still able to perform anaerobic glycolysis. On the other hand, it has been reported that brain pH does not continue to decrease in the PMI after the initial several hours (Albrechtsen, 1977a; Lewis, 2002).

Taken together, because of the complex associations of low pH with postmortem decomposition, tissue acidity is a critical variable to be cognizant of when evaluating the literature on postmortem decomposition. For example, pH has been proposed to be the most decisive determinant of postmortem necrosis in the granule cell layer of the cerebellum (Albrechtsen, 1977a).

Hydration

The water content of the brain has implications for postmortem decomposition rates. Mechanistically, an increased water content can increase biochemical reaction rates (Vass, 2011). Across tissues, atmospheric humidity rates of greater than 85% are associated with an increase in decomposition rates (Vass, 2011). Because the brain is encased in the cal-

varia, atmospheric humidity likely does not substantially affect decomposition speed in the relatively early PMI ranges most relevant to brain banking. However, when the brain is taken out of the calvaria, either as a part of the preservation procedure or for *ex situ* storage in a time series study, investigators need to choose how to store the tissue. The brain is typically moist in its *in situ* location, bathed in cerebrospinal fluid (CSF). One option for storage is to submerse tissue in a solution that matches the composition of the CSF, although this risks worsening fluid shifts and associated artifacts such as vacuolization (Fix and Garman, 2000). Alternatively, the brain can be stored in the dry air, although this is likely to lead to severe tissue damage due to dehydration (Budday et al., 2015). Additionally, the brain's relatively high water content, which has been found to increase in the postmortem period, may play a role in its relatively faster rate of postmortem autolysis compared to some other tissues (Ansari et al., 1976b; Zhou and Byard, 2011). As a result, premortem conditions in brain donors that promote water accumulation, such as cerebral edema, may predispose to a faster decomposition rate during the PMI.

Oxygen content

The atmospheric oxygen content also affects the rate of postmortem decomposition across tissues (Cockle and Bell, 2015; Vass, 2011). Mechanistically, high oxygen content leads to oxidative damage to biomolecules as well as increased bacterial growth, thus promoting putrefaction (Cockle and Bell, 2015). The brain is relatively insensitive to changes in atmospheric oxygen content in the early stages of the PMI, due to its protection in the calvaria and the relative isolation of the brain from bacteria in the gastrointestinal tract. However, the brain is likely much more susceptible to changes in atmospheric oxygen content in the later postmortem period when bacteria have had time to proliferate in the brain tissue. This may help to explain the relatively good long-term preservation of brains stored in environments with low oxygen content, such as the body described in a case study that was immersed underwater for 10 weeks prior to autopsy (MacKenzie, 2014). Additionally, when the brain is taken out of the calvaria without protection from oxygen, it is likely to be more susceptible to oxidative damage and putrefaction due to the increased exposure to atmospheric oxygen.

Putrefaction

To what extent there are microbes present in the brain under normal conditions remains an open question (Link, 2021). Regardless, there is evidence that proliferation of putrefactive bacteria is not a typical occurrence in the early PMI. Instead, autolysis is thought to be the main contributor to early decomposition within at least the first day of the PMI (Ith et al., 2011). Various factors could modify the rate at which putrefaction initiates, such as isolation from the gastrointestinal tract, the presence of premortem fever, sepsis, or bacterial encephalitis, and environmental storage conditions (Zhou and Byard, 2011). At later PMIs, the potential for putrefaction is a critical variable to consider. For example, Finnie and colleagues noted that there was no confounding bacterial invasion for the full 4 weeks of postmortem decomposition that they studied (Finnie et al., 2016).

In situ versus ex situ brain storage

One of the key distinctions in the methodologies of the studies we identified is whether the brain is stored *in situ* or excised to be stored *ex situ* during the PMI. Although the decomposition rates between these two conditions were not directly compared among the included studies, this has been found to affect the rate of liver decomposition. Specifically, removal of liver fragments from its original location has been found to substantially accelerate the postmortem decomposition kinetics of the liver compared to leaving it *in situ* (Nunley et al., 1972). In studies of neuronal ischemia, morphological damage and disruption of the cytoskeleton have also been found to occur more quickly and intensely in slices than cells *in situ* (Lipton, 1999). In addition to differences in the other modifying variables between the *in situ* and *ex situ* conditions, other factors will also affect the rate of decomposition in these two much different environmental contexts. One possible mechanism is that removal of the brain could significantly affect the tissue's mechanical

state, such as its hydraulic permeability, which may affect decomposition rates (Jamal et al., 2021).

Variation across species in metabolic rate

Several studies noted differences in the decomposition rates between species (Lucassen et al., 1995; Martin et al., 2003). One notes that postmortem decomposition is likely to be faster in the smaller brain of a rodent and slower in the larger brain of a human (Roberts et al., 2014). Others suggest that human or bovine brain tissue appear to degrade relatively more slowly postmortem than rodent brain tissue (Ansari et al., 1975; Schwab et al., 1994). The most likely reason for species differences is that the metabolic rate varies, for example being much faster in rodents, which means that there may be a higher density of catabolic enzymes present in the postmortem period (Demetrius, 2005). Consistent with this, lesion evolution following cerebral infarction also appears to be markedly faster in rats than humans (Mena et al., 2004). The infarct process in general has been reported to occur faster in animals that are smaller with higher metabolic rates (Kloner et al., 2018). Across tissues, autolysis has been suggested to be faster in malignant tissues with higher metabolic rates (Lesnikova et al., 2018). As a result, studies using rodent models of human decomposition may overestimate the rate. This may account for the generally faster rates of decomposition reported in time series studies, which are primarily on rodents, compared with correlational studies, which are predominantly on human brains.

Premortem metabolic state

Lindenberg suggest that premortem metabolic state plays an important role in mediating postmortem decomposition rates (Lindenberg, 1956). They report that if antemortem hypoxia lasted for more than 60 min, then brain cells retained their microscopic structure for at least 18 h PMI, even if kept at the relatively high temperature of 37 °C. On the other hand, if there was no antemortem hypoxia, then brain cells lost their structure much more quickly. Their explanation is that cells exposed to antemortem hypoxia have already depleted and eliminated metabolic products that might otherwise contribute to structural damage. This hypothesis is inconsistent with many other studies finding that more severe agonal damage is associated with worse brain cell morphology (Williams et al., 1978; Glausier et al., 2019). However, because the underlying biology is complex and poorly understood, it remains true that certain antemortem metabolic states could be protective against postmortem decomposition, requiring further investigation. For example, premortem administration of metformin, a chemical that alters metabolism, has also been shown to decrease the rate of postmortem nuclear swelling (Dehghani et al., 2018).

Age

The evidence for the interaction of age with PMI effects is mixed and may depend on the structural feature considered. Williams and colleagues found that in general, the effects of the PMI were the same on neuronal morphology in juvenile (14 d old) and adult (60 d old) mice (Williams et al., 1978). Buell also reported that neuronal morphology in human brains with substantial PMIs was not dependent on age (Buell, 1982). However, Itoyama and colleagues, comparing young (7 d old) and adult rats, found that young rats had more perikaryal swelling of oligodendrocytes, more fragmentation of oligodendrocyte processes, and more myelin vacuolization at the same PMI (Itoyama et al., 1980). Additionally, Mori and colleagues found that blood vessels from older (32-month-old) rats were found to leak proteins at shorter PMIs than younger (3-month-old) rats (Mori et al., 1991). Myelin is known to have delayed development, while blood vessels are known to accumulate damage with age, which may make these features more vulnerable to differential decomposition in the PMI based on age.

Premortem pathology

The presence of premortem brain pathology may affect the rate of postmortem decomposition. This could occur due to factors affecting the cohesiveness or catabolic rate in the brain. In one case study, severe autolysis of granule cells and Purkinje cells in the cerebellum occurred after only 6 h of PMI, enormously faster than typical, which was attributed to severe diabetic ketoacidosis (Suárez-Pinilla and Fernández-Vega, 2015). Death due to un-

Modifying variable	Reported effect on the rate of postmortem changes
Storage temperature	Lower temperatures (above 0°C) are clearly associated with slower decomposition
Tissue acidity	Lower pH values are associated with faster decomposition and may be partially a marker for more damage in the agonal state
Tissue hydration	Atypically high or low hydration levels may be associated with faster decomposition rates
Oxygen content	Higher oxygen content is associated with oxidative damage to biomolecules and more rapid putrefaction
Putrefaction	Generally thought to make minimal contributions in the early days of the PMI, but can be more rapid in certain circumstances
Storage location	There is evidence that brains stored outside of the calvaria (*ex situ*) have more rapid decomposition compared to being stored inside the calvaria (*in situ*)
Species	There is evidence that smaller animals with faster metabolic rates, such as rodents, have faster decomposition rates
Premortem metabolic state	Complex effects of premortem metabolic state on decomposition rate that require further study before conclusions can be drawn
Age	Mixed evidence depending on the structural feature studied, with some showing no age dependency, and others, such as myelin and blood vessels, having some indication for an interaction
Premortem pathology	Certain pathologies, such as uncontrolled diabetes, are associated with faster postmortem decomposition rates

Table 4. Summary of variables potentially modifying the postmortem decomposition rate.

controlled diabetes has been associated with higher rates of necrosis of the granule cell layer of the cerebellum in other studies as well (Albrechtsen, 1977b). More generally, obesity, hyperglycemia, and ingestion of certain substances have been reported to promote the rate of postmortem decomposition of cadavers and may also therefore influence the rate of brain decomposition (Zhou and Byard, 2011). On the other hand, some conditions have been found to *not* increase the rate of postmortem decomposition, such as rabies infection (Monroy-Gómez et al., 2020).

Some types of premortem pathology could even predispose for stability in the PMI. Certain pathologic proteins in the brain, such as abnormal prion protein and amyloid beta, can be detected via IHC for months after death (Scudamore et al., 2011). In the paleoanthropology literature, tissue from a 2600-year-old brain was found to be partially intact, likely due to an aggregate of intermediate filaments, which may have been related to premortem brain pathology (Petzold et al., 2020).

The possibility of brain pathology affecting postmortem decomposition rates is especially important if investigators adjust for the effects of PMI on cell morphometry with a linear model. In this setting, if there is an interaction effect that is not considered, the investigator might conclude that brain pathology is associated with a particular aspect of cell morphometry, when the difference between groups could instead be due to an artifact of the PMI.

Summary

There are many ways that modifying variables can interact with PMI to affect the visualization of cell morphometry (**Table 4**). Well-controlled studies

will account for this possibility. These factors also can help to explain heterogeneity between studies.

Interactions between postmortem changes and preservation methods

Many studies have noted that the quality of perfusion as compared to immersion fixation could vary based on the PMI. Indeed, there is good reason to think that perfusion quality can be limited in the PMI, for example due to a loss of vascular patency, the perivascular accumulation of water, and/or postmortem clot formation (Cammermeyer, 1960; de la Torre et al., 1992; Garcia et al., 1978; Hansma et al., 2015; Kloner et al., 2018). Vascular abnormalities are thought to be the key limitation preventing the brain from tolerating ischemic episodes, thus being a primary cause of death, which makes the difficulty of postmortem perfusion-based preservation unsurprising (Jenkins et al., 1979). One study that performed postmortem perfusion, Routtenberg and Tarrant acknowledged that theoretically perfusion fixation may be lower quality in postmortem cases, and therefore delays in time prior to perfusion fixation may lead to changes in fixation quality rather than pure decomposition effects (Routtenberg and Tarrant, 1974). In their case, perfusing brains at up to 10 min PMI, they reported that perfusion quality was unlikely to have affected their results, because markers of high-quality perfusion, namely tissue hardness and clearing of blood vessels, were still observed. Koenig and Koenig used perfusion fixation on guinea pig brains at up to 23.5 h PMI and did not note decreased perfusion quality as an issue that affected their results (Koenig and Koenig, 1952).

Consistent with the known benefits of perfusion fixation on tissue quality, several studies note that this method yields substantially fewer postmortem artifacts than immersion fixation (McFadden et al., 2019). Bywater and colleagues, in a study of monkey brains, performed both perfusion and immersion fixation at the different time points studied (Bywater et al., 1962). They noted that brains with a PMI of 1 h preserved via perfusion fixation had similar postmortem artifacts as brains immersion fixed immediately after death. Liu 1950 noted that immersion fixed brains demonstrate widespread artifacts similar to postmortem artifacts found in brains with extended PMIs, which they attribute to inadequate fixation by immersion (Liu and Windle, 1950). Lavenex and colleagues reported that the difference between immunostaining patterns for SMI-32 was striking between perfusion fixed brains at 0 h PMI and immersion fixed brains at 2 h of PMI, but that there was no substantial difference between immersion fixed brains preserved at 2 h and 48 h of PMI, with postmortem storage at 4 °C (Lavenex et al., 2009). As a result, studies of PMI effects that do not account for the possibility of worse preservation with immersion as compared to perfusion fixation, for example using perfusion fixation as the baseline timepoint of zero PMI and immersion fixation at subsequent PMI timepoints, are susceptible to bias (Airaksinen et al., 1991; Garcia et al., 1978; Geddes et al., 1995; Terstege et al., 2022).

Another important distinction is the differences in fixation as compared to freezing, with several studies noting relative advantages of each. For example, Schulz and colleagues noted that dark neurons, a well-known fixation artifact, are seen in small tissue blocks that were fixed but not ones that were frozen, while frozen tissue blocks had freezing artifacts such as cytoplasmic vacuolization (Schulz et al., 1980). Itoyama and colleagues found a differential effect of a postmortem delay of 20 h when immunostaining for myelin basic protein in frozen as compared to immersion fixed tissue (Itoyama et al., 1980). They reported that myelin sheaths were slightly distorted following the PMI in immersion fixed tissue but had substantially worse quality in frozen tissue following the same PMI compared to the baseline state. Freezing artifacts could theoretically be worse in cases of longer PMI because more free water and weaker cellular structures may predispose to more mechanical ice damage, which warrants further investigation.

Finally, the fixative used can also influence observed PMI artifacts. One study found differential effects of a 24 h PMI on immunostaining properties for several antigens in blocks of human brain tissue based on the fixative used for preservation (Sillevis Smitt et al., 1993). When the tissue was preserved using Bouin and B5 fixatives, they found no effect of a 24 h PMI on the quality of immunostaining with SMI-32 and BF-10, which are two antibodies that recognize neurofilament. On the other hand, the

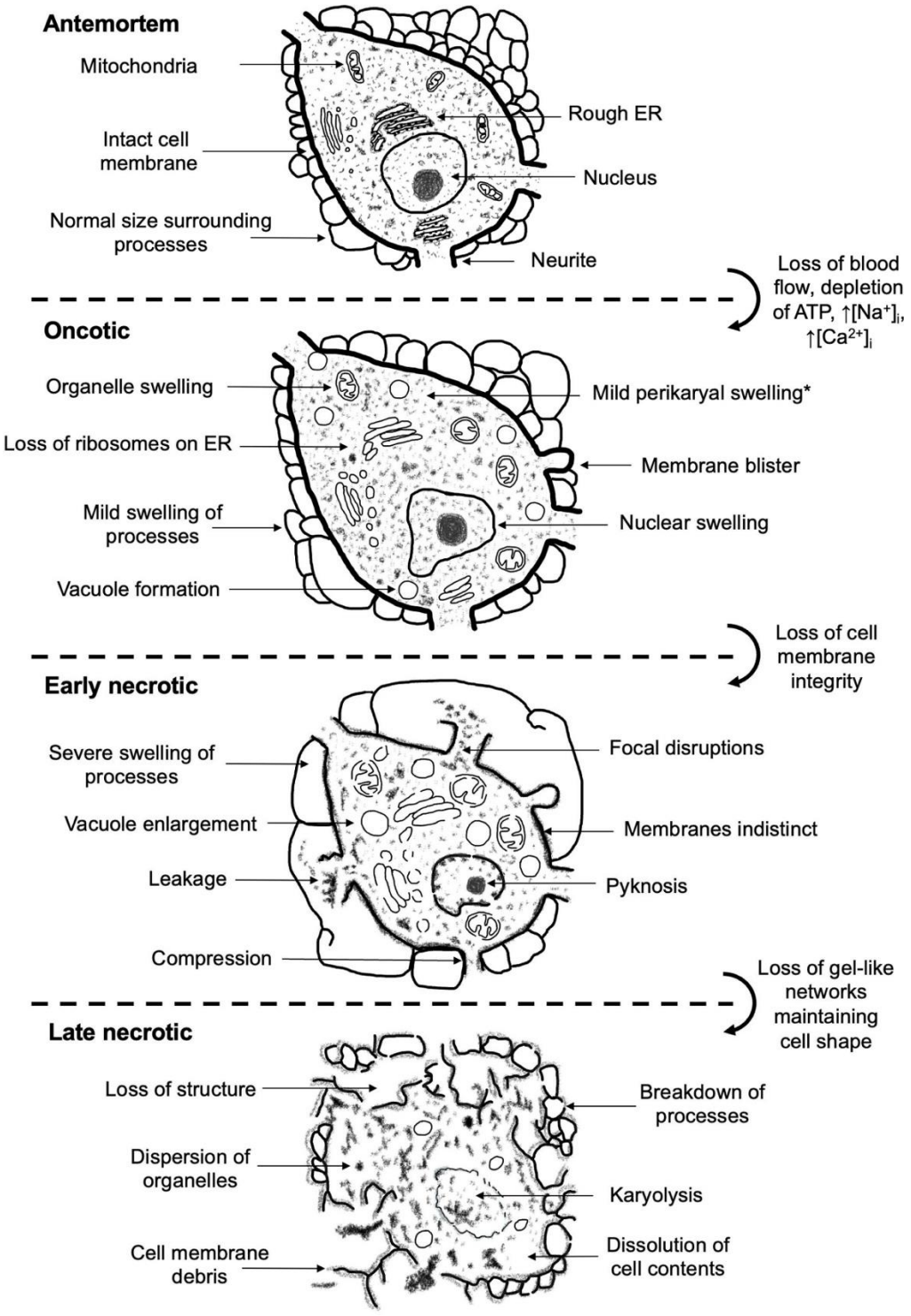

Figure 6. Model of the oncotic necrosis pathway of cell membrane deterioration in the brain.

Stage zero is the antemortem cell, which shows intact cell membrane and normal sized structures. Stage one is oncosis, wherein ischemia leads to loss of ATP, loss of ion pump activity, breakdown of biomolecules, bleb formatting, vacuolization, and other changes. The asterisk (*) indicates that while cell volume increases are possible, no change or shrinkage is also possible. Stage two is early necrosis, wherein the physical disruption of the cell membrane causes focal loss in cell membrane shape and leakage of intracellular contents. There is also severe swelling of surrounding processes, potentially compressing cellular structures such as neurites and synapses. From this point on, the cell has necrotic morphology. Stage three is late necrosis, wherein gel-like networks break down, eventually leading to a complete cellular dissolution, and only cell fragments or debris may remain. The main figures used for adaptation in building this model were: (Majno and Joris, 1995) (Figure 9), (Suzuki, 1987) (Figure 2.7), (Fricker et al., 2018) (Figure 3), and (Trump et al., 1984) (Figure 8).

immunostaining with these antibodies was diminished by a 24 h PMI when the tissue was preserved with a different fixative, Sensofix. It may be that fixation needs to be stronger in the presence of a longer PMI to prevent damage during dehydration and embedding.

Morphological staging of decomposition

We present a model of how cell morphometry changes during different stages of the oncotic necrosis pathway in the postmortem brain (**Figure 6**). Of note, the timeline of cellular events depicted here likely varies between cells, as these are rough guidelines, not absolute. Additionally, the intracellular changes shown, which are not a focus on this review, are primarily based on other sources (Choe et al., 1995; Majno and Joris, 1995; Suzuki, 1987).

In this model, oncosis is initiated by a lack of blood flow, leading to ATP depletion, a rise in the intracellular concentrations of Na^+ and Ca^{2+}, fluid shifts, and the initiation of biomolecular breakdown and redistribution. While cell swelling is a classical finding in oncosis, it may not occur, or shrinkage can occur instead, depending upon the cell and surrounding milieu. Cell volume can also evolve over the course of the PMI. Processes surrounding cells also tend to swell, which is an early event in the PMI. Finally, cell membranes can form blebs as well.

Early necrosis is initiated by focal disruptions of the cell membrane, leading to leakage of intracellular contents. The remaining cell membranes tend to become indistinct, although still visible. Processes around cells can become extremely swollen, in some cases larger than many cells themselves. Note that while these swollen cell processes are usually astrocyte processes, other studies also describe swelling of dendrites, axons, and oligodendrocyte processes (Rees, 1977; Gibson and Tomlinson, 1979). As a result, we describe these agnostically as cell processes.

Early necrosis is followed by late necrosis, which is characterized by further disruption of gel-like networks leading to the loss of the original cell shape. The ultimate speed of dissolution of cell structures likely depends upon the initial strength of the gel-like networks. For example, the strong compaction of myelin may help to explain why this structure tends to be highly stable in the postmortem period. The structures that last the longest are also the ones that are the most slowly catabolized in the postmortem period. The ultimate outcome of late necrosis is cellular liquefaction and coming to an equilibrium with the environment.

An implication of this model is that the transition which leads to loss of cell morphometry information – making the postmortem tissue no longer useful for studying cell morphometric alterations in neurobiological disorders – is most likely the transition from early necrotic to late necrotic, when the gel-like networks maintaining cell shapes are degraded. The transitions between these stages are not discrete but continuous, which may be a useful model for investigators studying postmortem brain tissue. We also present the histologic findings expected regarding cell morphometry at each of the stages (**Table 5**).

Stage of decomposition	Cell shape	Cell size	Cell membrane findings	Common artifacts
Antemortem	Intact	No change	Not applicable	Not applicable
Oncotic	Largely intact	Mild to moderate swelling or shrinkage is likely	May have blebbing or compression	Pericellular and perivascular rarefactions; vacuolization
Early necrotic	Largely intact	Some cells, especially astrocytes, are excessively enlarged, while others begin to shrink	Cell membranes may be indistinct, blurry, or partially damaged	Above artifacts, but more widespread and severe; intracellular contents may be seen in extracellular space
Late necrotic	Altered	Cells shrink as they dissolve	Cells are dissolved	Washed out tissue areas devoid of cells

Table 5. Typical cell morphometric findings at different stages of postmortem decomposition.

Implications for human brain mapping

To map the brain across large areas of brain tissue, surgically extracted tissue will not be sufficient. This draws attention to the inevitable PMI in autopsy brain samples which are of particular interest for designing brain mapping studies.

One relevant lesson is that postmortem brain mapping will have higher fidelity to *in vivo* states for some structural features compared to others. Cell volumes and feature morphometry such as synapse size are likely to be altered rapidly in the PMI. Cell membrane topography can also be altered relatively early due to the heterogeneous formation of vacuoles, blisters, and compression. On the other hand, cell membrane topological relationships are likely to be maintained across longer PMIs. As a result, it may be possible to map connectivity and circuitry, as well as circuit properties such as the rough degree of axon myelination, even after a relatively longer degree of postmortem decomposition. However, there is considerable uncertainty about how broadly this applies across brain regions and cell types. It is unknown what degree of postmortem decomposition can be tolerated before topological cell membrane relationships are also lost, requiring further research.

Another lesson for postmortem brain mapping is that, compared with animal brains preserved at the time of death, some visualization procedures will be substantially more robust than others. As previously discussed, IHC studies can be sensitive to the PMI, because certain antigens can be lost relatively early in the PMI. If IHC is to be used in postmortem tissue, then labeling antigens that are robust to postmortem decomposition is essential. Based on the studies we reviewed, synaptophysin (Liu and Brun, 1995; Sarnat et al., 2010), GFAP (Blair et al., 2016), and neurofilaments (Lavenex et al., 2009; Blair et al., 2016) are relatively stable in the postmortem period in visualizing cell morphometry, although this certainly warrants further investigation. Some morphological stains have also been shown to be resistant to postmortem decomposition, although there remain questions of how widely they can be used and the degree to which their neuronal mapping is unbiased. For example, Golgi-Cox staining only visualizes a small subset of neurons, although its resistance to postmortem decomposition makes it a valuable staining method.

While some antigens are sensitive to postmortem decomposition, others may be particularly stable in ways that could prove valuable. For example, ischemic fluid shifts such as severe dendrite swelling have been found to be partially reversible if there is a physiological correction within 20-60 minutes, which has been attributed to the resilience of the cytoskeleton (Zhang et al., 2005). This suggests that staining and mapping cytoskeletal biomolecules may be a way to infer cellular morphometry even in the setting of volume changes that might affect morphological stains.

Studies using electron microscopy to map the postmortem brain require particular attention to sample preparation. For example, some studies have found that synapses decrease in number during extended PMIs, although this is certainly not a universal finding (Huttenlocher, 1979; Petit and LeBoutillier, 1990; Roberts et al., 1996). As discussed, several lines of evidence suggest the loss of synapse visualization may be due to compression or loss of synaptic markers, rather than frank synaptic fragmentation or dissolution (Gibson and Tomlinson, 1979; Petit and LeBoutillier, 1990). As a result, the identification of synapses would likely be less affected by postmortem decomposition if they were visualized with a robust staining procedure and/or volumetric imaging. Multiple authors reported optimizing the standard electron microscopy procedures for using on postmortem human brains (Sele et al., 2019; Tang et al., 2001).

In addition to optimizing tissue processing, data analysis methods can also aid in reconstructing the original state of structures affected by postmortem artifacts. In reconstructive brain mapping, common artifacts could be computationally reversed – with some degree of fidelity to the original state – via deterministic or stochastic algorithms. For example, if myelin lamellae have split, it may be possible to infer the shape in which they were originally compacted. As an early example in this field, one study performed a 3D reconstruction of brain tissue based on EM images while using a set of models to correct the extracellular space volume fraction for shrinkage

attributed to hypoxia, fixation, and dehydration (Kinney et al., 2013).

It may also be possible to map the decomposed biomolecules that originally comprised a structural feature if the structure itself has fragmented. This could never be done perfectly but could potentially infer the original structure to a sufficient degree of accuracy in many cases. However, because of the ubiquity of non-Gaussian diffusion, computational reversal of postmortem biomolecule redistribution is likely a very challenging problem. It would require mapping multiple biomolecules and triangulating their predicted diffusion patterns, while accounting for fluid shifts, biomolecular degradation, and other factors. Decomposed biomolecules that have diffused about and partially degraded may be among the last remnants of an *in vivo* structure before the information about it is totally lost, thereby defining classical physical limits to the potential for reconstructive brain mapping.

Further studies of postmortem changes

A time series study in which the PMI is experimentally manipulated yields the most precise measurements of postmortem changes. However, when time series studies are used as a proxy for what happens in postmortem human brains, they often lack ecological validity. For example, studies on isolated surgical biopsy tissue introduce a dramatically different metabolic and biophysical state than that of the postmortem brain, which may limit the validity of these studies in predicting how decomposition occurs in an intact human brain postmortem. To address this, time series studies could measure and/or manipulate modifying variables, such as the location (*in situ* or *ex situ*), temperature, metabolic state, and tissue humidity. It would also be beneficial to perform time series studies that can help to account for variability across the existing studies, as reviewed here. One of the least widely studied areas is variability across brain regions. As we approach the ability to achieve brain-wide cellular mapping in the coming decades, there is a clear need to know whether some brain regions are more susceptible to postmortem decomposition than others, but this knowledge is currently limited.

Regarding correlational studies, scaling the sample size is likely to be helpful. Larger studies will be helpful to account for measured and unmeasured confounders, in addition to including these variables as covariates where available. With larger sample sizes also comes the possibility of unsupervised machine learning studies. Most of our existing knowledge of postmortem changes is based on subjective semi-quantitative scoring, but this is biased towards pre-existing knowledge. Unsupervised machine learning studies, as have recently begun to be performed in studying the neurobiology of disease, may also help to uncover biomarkers of postmortem decomposition (McKenzie et al., 2022). Developing an objective measure of histologic decomposition, analogous to the RNA Integrity Number (RIN) for RNA preservation quality, would be valuable as a quality metric in brain banking. The status quo involves investigators judgments subject to reporting bias. For example, the same cell could look “distorted” to one person but “largely preserved” to another, partially reflecting their prior expectations. This may be one reason for the heterogeneity in the decomposition outcomes we observed between studies. More quantitative histologic metrics, for example using morphology comparison algorithms, would help to mitigate reporting biases and make comparisons across studies more precise (Costa et al., 2016).

Among the most reliable histologic findings available today to measure the extent of postmortem decomposition are perivascular rarefaction, pericellular rarefaction, and vacuolization on morphologically stained tissue, such as H&E. Several studies describe these as common postmortem changes that become more prominent with increasing PMI (De Groot et al., 1995; Hilbig et al., 2004; Shepherd et al., 2009; Monroy-Gómez et al., 2020). However, the appearance and enlargement of these postmortem artifacts appears to have a non-linear relationship with PMI. Moreover, the kinetics of their appearance and the variables modifying them are poorly mapped out. Therefore, there is a need for additional research and validation prior to the routine use of these findings as measures of postmortem decomposition.

Comparison to other reviews

To our knowledge, there has not been a previous comprehensive review focused solely on the topic of brain cell morphology changes in the PMI, although several publications have touched on it as a part of a broader discussion. Oehmichen reviewed the extant literature on postmortem alterations in the histochemistry of CNS tissue (Oehmichen, 1980). They concluded that cell structures seen under the light microscope were effectively unchanged up to 6-8 h PMI and that after this, autolytic processes commence. Lewis, in a broader review of human brain research, included a discussion of PMI (Lewis, 2002). They noted that any PMI threshold for inclusion in a study, such as less than 24 h, would be arbitrary, and that tissue quality is highly dependent on antemortem factors. They also pointed out that postmortem effects can vary based on the feature measured and the brain region. Finally, this review noted that it can be difficult to distinguish differences between brains due to disease as opposed to postmortem artifact. Ravid and colleagues noted that the distribution of receptors tends to be stable in the postmortem period (Ravid et al., 1992). They also discussed the importance of developing profiling techniques for longer PMIs. Wohlsein and colleagues described common postmortem artifacts in animal brains, such as vacuolization, shrinkage of glial cells, hemolysis, and putrefactive decomposition in advanced stages (Wohlsein et al., 2013). Hostiuc and colleagues performed a systematic review on ultrastructural changes as a marker of the PMI in various organs; however, they used different search and selection criteria than our review and identified just two studies from the brain (Hostiuc et al., 2018). A forensic neuropathology textbook by Oehmichen and colleagues discusses histologic changes in the PMI (Oehmichen et al., 2006, p. 74). In their assessment, neuronal swelling is the most fundamental postmortem change, causing cells to lose their contours and become spherical. They note that oligodendrocytes and astrocytes can also have postmortem swelling, but that these changes are slight compared to neuronal changes and less specific. Ramirez and colleagues reported that there is no correlation between the PMI and tissue quality in brain banking samples (Ramirez et al., 2018). They note that many investigators are rigid about the PMI, despite this number not accurately reflecting the degree of metabolic changes that have occurred in the pre- and post-mortem tissue. There have also been reviews on cell morphology changes in brain death, which results from the same underlying process as in the PMI, namely a global lack of blood flow to the brain (Oehmichen, 1994; Folkerth et al., 2022). Notably, the kinetics of decomposition are faster in brain death because a relatively higher body temperature is maintained.

Strengths and limitations of this review

A strength of this review is that, to the best of our knowledge, this is the largest collection of studies yet assembled on this topic. Another strength is that a semi-quantitative grading system was developed and implemented on the time series studies. Finally, we have attempted to integrate the literature from studies using both light and electron microscopy to share insights between these two interrelated fields. In addition, this review has several limitations. First, the decomposition grades in the time series studies may give a false sense of precision. Instead, the purpose of these grades is to aid in conceptualization and visualization. Second, we largely did not consider disease state among the correlational studies which may have contributed to variations in the effects of PMI. Finally, there is no doubt that we missed a substantial set of the literature. This includes the non-English literature, especially the relatively large German and Russian language literatures. Also, we did not systematically evaluate references or citing articles of all included articles, which further limited the literature identified. Nevertheless, we expect that the studies included are a representative sample.

Conclusions

A reductionist focus on the numerical PMI, while convenient, does not account for variability based on the visualization method used, feature analyzed, region or cell type, and variables that modify the decomposition speed. Indeed, there is no obvious single PMI threshold at which cell morphometry is clearly lost. Instead, research is likely to be more

fruitful in understanding how the actual amount of decomposition in each brain can be measured, which structural features are likely to be altered sooner than others, and which visualization methods are most robust to postmortem changes. In biorepository contexts, it may make the most sense to cast a wider net on the inclusion of brain tissue, as opposed to having strict PMI inclusion requirements. On the other hand, it is essential to recognize that decomposition starts in the first minutes and is clearly occurring throughout the PMI. Therefore, there is a need to minimize postmortem decomposition by expediting processing procedures to the extent possible. More research into knowledge gaps regarding the postmortem decomposition of brain cells will help to further elucidate this critical barrier to studying human neurobiology using donated brains.

Abbreviations

ATPase - Adenosine triphosphatase, **CSF** - Cerebrospinal fluid, **d** - Day, **EM** - Electron microscopy, **ER** - Endoplasmic reticulum, **GFAP** - Glial fibrillary acidic protein, **GFRalpha** - Glial cell line-derived neurotrophic factor family receptor alpha, **h** - Hour, **H&E** - Hematoxylin and eosin, **ICC** - Intraclass correlation, **IHC** - Immunohistochemistry, **LFB** - Luxol fast blue, **MAP2** - Microtubule associated protein 2, **min** - Minute, **NF-H** - Neurofilament heavy chain, **NF-L** - Neurofilament light chain, **NF-M** - Neurofilament medium chain, **NeuN** - Neuronal nuclear protein, **PMI** - Postmortem Interval, **RAMESES** - Realist and meta-narrative evidence syntheses evolving standards, **RIN** - RNA integrity number, **rRNA** - Ribosomal RNA, **ssDNA** - Single-stranded DNA.

Author contributions

M.K., K.F., J.C., and A.M. conceptualized the study. S.W. advised on the search strategy and performed the database searches. A.M. performed abstract and article screening. M.K. and A.M. performed data extraction and review from the individual studies. M.K., J.K., and A.M. performed grading of the studies. A.S. and K.C. performed electron microscopy studies. A.M. wrote the initial draft of the manuscript. All authors reviewed the manuscript and approved the final manuscript.

Acknowledgements

We would like to thank Rebecca Folkerth, Etty Cortes, and Thomas Beach for helpful personal communications regarding this topic. The Icahn School of Medicine at Mount Sinai provided access to library resources. Electron Microscopy tissue preparation and imaging were performed at The Microscopy and Advanced Bioimaging CoRE at the Icahn School of Medicine at Mount Sinai.

Funding

The study was supported by NIH grants P30AG066514, RF1MH128969, R01AG054008, RF1NS095252, RF1AG060961, R01NS086736, R01AG062348, and the Rainwater Charitable Foundation. The funders had no role in the design of the study or in the collection or interpretation of the data.

Data availability

The generated database of studies studying postmortem changes in brain cell morphometry is freely available at https://github.com/andymckenzie/Postmortem_Interval. This repository also contains the code required to reproduce the figures created in R.

Supplementary Files

Supplementary File 1. RAMESES checklist for the review (PDF).

Supplementary File 2. Supplementary methods including database search methods (PDF).

Supplementary File 3. Export of Covidence files containing study screening results (zip file).

Supplementary File 4. Table with information about the included studies (PDF).

Supplementary File 5. Table with extracted data from the time series studies (PDF).

Supplementary File 6. Table with extracted data from the correlational studies (PDF).

Supplementary File 7. Table with extracted data from the case report studies (PDF).

References

Abbas, F., Becker, S., Jones, B.W., Mure, L.S., Panda, S., Hanneken, A., Vinberg, F., 2022. Revival of light signalling in the postmortem mouse and human retina. Nature 606, 351–357. https://doi.org/10.1038/s41586-022-04709-x

Acs, G., Paragh, G., Rakosy, Z., Laronga, C., Zhang, P.J., 2012. The extent of retraction clefts correlates with lymphatic vessel density and VEGF-C expression and predicts nodal metastasis and poor prognosis in early-stage breast carcinoma. Mod. Pathol. Off. J. U. S. Can. Acad. Pathol. Inc 25, 163–177. https://doi.org/10.1038/modpathol.2011.138

Adrian, M., Kusters, R., Wierenga, C.J., Storm, C., Hoogenraad, C.C., Kapitein, L.C., 2014. Barriers in the brain: resolving dendritic spine morphology and compartmentalization. Front. Neuroanat. 8, 142. https://doi.org/10.3389/fnana.2014.00142

Airaksinen, M.S., Paetau, A., Paljärvi, L., Reinikainen, K., Riekkinen, P., Suomalainen, R., Panula, P., 1991. Histamine neurons in human hypothalamus: anatomy in normal and Alzheimer diseased brains. Neuroscience 44, 465–481. https://doi.org/10.1016/0306-4522(91)90070-5

Albrechtsen, R., 1977a. Naphthylamidase used as a lysosome marker in the study of acute selective necrosis of the internal granular layer of cerebellum. Acta Pathol. Microbiol. Scand. [A] 85, 875–888. https://doi.org/10.1111/j.1699-0463.1977.tb03904.x

Albrechtsen, R., 1977b. The incidence of the so-called acute selective necrosis of the granular layer of cerebellum in 1000 autopsied patients. Acta Pathol. Microbiol. Scand. [A] 85A, 193–202. https://doi.org/10.1111/j.1699-0463.1977.tb00417.x

Ananthakrishnan, R., Guck, J., Wottawah, F., Schinkinger, S., Lincoln, B., Romeyke, M., Moon, T., Käs, J., 2006. Quantifying the contribution of actin networks to the elastic strength of fibroblasts. J. Theor. Biol. 242, 502–516. https://doi.org/10.1016/j.jtbi.2006.03.021

Anders, V.N., 1977. [Human brain synapses during postmortem autolysis (electron-microscopic and electron-cytochemical studies)]. Zhurnal Nevropatol. Psikhiatrii Im. SS Korsakova Mosc. Russ. 1952 77, 1080–1084.

Ansari, K.A., Hendrickson, H., Rand, A., 1976a. Electrophoretic and morphologic studies on normal human white matter obtained at surgery with special reference to its basic protein component. J. Neuropathol. Exp. Neurol. 35, 606–612. https://doi.org/10.1097/00005072-197611000-00002

Ansari, K.A., Hendrickson, H., Sinha, A.A., Rand, A., 1975. Myelin basic protein in frozen and unfrozen bovine brain: a study of autolytic changes in situ. J. Neurochem. 25, 193–195. https://doi.org/10.1111/j.1471-4159.1975.tb06952.x

Ansari, K.A., Rand, A., Hendrickson, H., Bentley, M.D., 1976b. Qualitative and quantitative studies on human myelin basic protein in situ with respect to time interval between death and autopsy. J. Neuropathol. Exp. Neurol. 35, 180–90. https://doi.org/10.1097/00005072-197603000-00005

Arsénio-Nunes, M.L., Hossmann, K.A., Farkas-Bargeton, E., 1973. Ultrastructural and histochemical investigation of the cerebral cortex of cat during and after complete ischaemia. Acta Neuropathol. (Berl.) 26, 329–344. https://doi.org/10.1007/BF00688080

Averback, P., 1980. A study of the rate of cell depletion in solid tissue. J. Pathol. 130, 173–178. https://doi.org/10.1002/path.1711300306

Badonic, T., Frumkina, L.J., Jakovleva, N.I., Hornáková, A., 1992. Ultrastructural changes of neurons in dependence on the death cause in human brain. Funct. Dev. Morphol. 2, 231–234.

Bailey, D.M., 2019. Oxygen and brain death; back from the brink. Exp. Physiol. 104, 1769–1779. https://doi.org/10.1113/EP088005

Beach, T.G., Adler, C.H., Sue, L.I., Serrano, G., Shill, H.A., Walker, D.G., Lue, L., Roher, A.E., Dugger, B.N., Maarouf, C., Birdsill, A.C., Intorcia, A., Saxon-Labelle, M., Pullen, J., Scroggins, A., Filon, J., Scott, S., Hoffman, B., Garcia, A., Caviness, J.N., Hentz, J.G., Driver-Dunckley, E., Jacobson, S.A., Davis, K.J., Belden, C.M., Long, K.E., Malek-Ahmadi, M., Powell, J.J., Gale, L.D., Nicholson, L.R., Caselli, R.J., Woodruff, B.K., Rapscak, S.Z., Ahern, G.L., Shi, J., Burke, A.D., Reiman, E.M., Sabbagh, M.N., 2015. Arizona study of aging and neurodegenerative disorders and brain and body donation program. Neuropathology 35, 354–389. https://doi.org/10.1111/neup.12189

Beach, T.G., Sue, L.I., Walker, D.G., Roher, A.E., Lue, L., Vedders, L., Connor, D.J., Sabbagh, M.N., Rogers, J., 2008. The Sun Health Research Institute Brain Donation Program: Description and Eexperience, 1987–2007. Cell Tissue Bank. 9, 229–245. https://doi.org/10.1007/s10561-008-9067-2

Benes, F.M., Todtenkopf, M.S., Kostoulakos, P., 2001. GluR5,6,7 subunit immunoreactivity on apical pyramidal cell dendrites in hippocampus of schizophrenics and manic depressives. Hippocampus 11, 482–491. https://doi.org/10.1002/hipo.1065

Berdenis van Berlekom, A., Muflihah, C.H., Snijders, G.J.L.J., MacGillavry, H.D., Middeldorp, J., Hol, E.M., Kahn, R.S., de Witte, L.D., 2020. Synapse Pathology in Schizophrenia: A Meta-analysis of Postsynaptic Elements in Postmortem Brain Studies. Schizophr. Bull. 46, 374–386. https://doi.org/10.1093/schbul/sbz060

Blair, J.A., Wang, C., Hernandez, D., Siedlak, S.L., Rodgers, M.S., Achar, R.K., Fahmy, L.M., Torres, S.L., Petersen, R.B., Zhu, X., Casadesus, G., Lee, H.G., 2016. Individual Case Analysis of Postmortem Interval Time on Brain Tissue Preservation. PloS One 11, e0151615. https://doi.org/10.1371/journal.pone.0151615

Boekhoorn, K., Joels, M., Lucassen, P.J., 2006. Increased proliferation reflects glial and vascular-associated changes, but not neurogenesis in the presenile Alzheimer hippocampus. Neurobiol. Dis. 24, 1–14. https://doi.org/10.1016/j.nbd.2006.04.017

Booze, R.M., Mactutus, C.F., Gutman, C.R., Davis, J.N., 1993. Frequency analysis of catecholamine axonal morphology in human brain. I. Effects of postmortem delay interval. J. Neurol. Sci. 119, 99–109. https://doi.org/10.1016/0022-510x(93)90197-7

Boros, B.D., Greathouse, K.M., Gentry, E.G., Curtis, K.A., Birchall, E.L., Gearing, M., Herskowitz, J.H., 2017. Dendritic spines provide cognitive resilience against Alzheimer's disease. Ann. Neurol. 82, 602–614. https://doi.org/10.1002/ana.25049

Bruce, A., Dawson, J.W., 1911. On the relations of the lymphatics of the spinal cord. J. Pathol. Bacteriol. 15, 169–178.

Brück, Y., Brück, W., Kretzschmar, H.A., Lassmann, H., 1996. Evidence for neuronal apoptosis in pontosubicular neuron necrosis. Neuropathol. Appl. Neurobiol. 22. https://doi.org/10.1111/j.1365-2990.1996.tb00842.x

Budday, S., Nay, R., de Rooij, R., Steinmann, P., Wyrobek, T., Ovaert, T.C., Kuhl, E., 2015. Mechanical properties of gray and white matter brain tissue by indentation. J. Mech. Behav. Biomed. Mater. 46, 318–330. https://doi.org/10.1016/j.jmbbm.2015.02.024

Buell, S.J., 1982. Golgi-Cox and rapid golgi methods as applied to autopsied human brain tissue: widely disparate results. J. Neuropathol. Exp. Neurol. 41, 500–507. https://doi.org/10.1097/00005072-198209000-00003

Buja, L.M., Barth, R.F., Krueger, G.R., Brodsky, S.V., Hunter, R.L., 2019. The Importance of the Autopsy in Medicine: Perspectives of Pathology Colleagues. Acad. Pathol. 6, 2374289519834041. https://doi.org/10.1177/2374289519834041

Bywater, J.E., Glees, P., Hauffe, H., 1962. The variability of neuron structure caused by the type of fixation or by the autolytic changes. II. Silver method. J. Hirnforsch. 5, 147–161. https://doi.org/10.1515/9783112519806-003

Cammermeyer, J., 1979. Argentophil neuronal perikarya and neurofibrils induced by postmortem trauma and hypertonic perfusates. Acta Anat. (Basel) 105, 9–24. https://doi.org/10.1159/000145102

Cammermeyer, J., 1978. Is the solitary dark neuron a manifestation of postmortem trauma to the brain inadequately fixed by perfusion? Histochemistry 56, 97–115. https://doi.org/10.1007/BF00508437

Cammermeyer, J., 1960. The post-mortem origin and mechanism of neuronal hyperchromatosis and nuclear pyknosis. Exp. Neurol. 2, 379–405. https://doi.org/10.1016/0014-4886(60)90022-4

Chan, J.K.C., 2014. The wonderful colors of the hematoxylin-eosin stain in diagnostic surgical pathology. Int. J. Surg. Pathol. 22, 12–32. https://doi.org/10.1177/1066896913517939

Charpak, S., Audinat, E., 1998. Cardiac arrest in rodents: Maximal duration compatible with a recovery of neuronal activity. Proc. Natl. Acad. Sci. U. S. A. 95, 4748–4753. https://doi.org/10.1073/pnas.95.8.4748

Choe, B.Y., Gil, H.J., Suh, T.S., Shinn, K.S., 1995. Postmortem metabolic and morphologic alterations of the dog brain thalamus with use of in vivo 1H magnetic resonance spectroscopy and electron microscopy. Invest. Radiol. 30, 269–274. https://doi.org/10.1097/00004424-199505000-00001

Chugh, P., Paluch, E.K., 2018. The actin cortex at a glance. J. Cell Sci. 131, jcs186254. https://doi.org/10.1242/jcs.186254

Cockle, D.L., Bell, L.S., 2015. Human decomposition and the reliability of a "Universal" model for post mortem interval estimations. Forensic Sci. Int. 253, 136.e1–9. https://doi.org/10.1016/j.forsciint.2015.05.018

Coleman, M., 2005. Axon degeneration mechanisms: commonality amid diversity. Nat. Rev. Neurosci. 6, 889–898. https://doi.org/10.1038/nrn1788

Compaine, A., Schein, J.D., Tabb, J.S., Mohan, P.S., Nixon, R.A., 1995. Limited proteolytic processing of the mature form of cathepsin D in human and mouse brain: Postmortem stability of enzyme structure and activity. Neurochem. Int. 27, 385–396. https://doi.org/10.1016/0197-0186(95)00020-9

Costa, M., Manton, J.D., Ostrovsky, A.D., Prohaska, S., Jefferis, G.S.X.E., 2016. NBLAST: Rapid, Sensitive Comparison of Neuronal Structure and Construction of Neuron Family Databases. Neuron 91, 293–311. https://doi.org/10.1016/j.neuron.2016.06.012

Dachet, F., Brown, J.B., Valyi-Nagy, T., Narayan, K.D., Serafini, A., Boley, N., Gingeras, T.R., Celniker, S.E., Mohapatra, G., Loeb, J.A., 2021. Selective time-dependent changes in activity and cell-specific gene expression in human postmortem brain. Sci. Rep. 11, 6078. https://doi.org/10.1038/s41598-021-85801-6

D'Andrea, M.R., Howanski, R.J., Saller, C.F., 2017. MAP2 IHC detection: a marker of antigenicity in CNS tissues. Biotech. Histochem. Off. Publ. Biol. Stain Comm. 92, 363–373. https://doi.org/10.1080/10520295.2017.1295169

D'Arcy, M.S., 2019. Cell death: a review of the major forms of apoptosis, necrosis and autophagy. Cell Biol. Int. 43, 582–592. https://doi.org/10.1002/cbin.11137

Das, S.C., Chen, D., Callor, W.B., Christensen, E., Coon, H., Williams, M.E., 2019. DiI-mediated analysis of presynaptic and postsynaptic structures in human postmortem brain tissue. J. Comp. Neurol. 527, 3087–3098. https://doi.org/10.1002/cne.24722

De Groot, C.J., Theeuwes, J.W., Dijkstra, C.D., van der Valk, P., 1995. Postmortem delay effects on neuroglial cells and brain macrophages from Lewis rats with acute experimental allergic encephalomyelitis: an immunohistochemical and cytochemical study. J. Neuroimmunol. 59, 123–134. https://doi.org/10.1016/0165-5728(95)00034-y

de la Torre, J.C., Fortin, T., Saunders, J.K., Butler, K., Richard, M.T., 1992. The no-reflow phenomenon is a post-mortem artifact. Acta Neurochir. (Wien) 115, 37–42. https://doi.org/10.1007/BF01400588

de Ruiter, J.P., Uylings, H.B., 1987. Morphometric and dendritic analysis of fascia dentata granule cells in human aging and senile dementia. Brain Res. 402, 217–229. https://doi.org/10.1016/0006-8993(87)90028-X

de Wolf, A., Phaedra, C., Perry, R.M., Maire, M., 2020. Ultrastructural Characterization of Prolonged Normothermic and Cold Cerebral Ischemia in the Adult Rat. Rejuvenation Res. 23, 193–206. https://doi.org/10.1089/rej.2019.2225

Dehghani, A., Karatas, H., Can, A., Erdemli, E., Yemisci, M., Eren-Kocak, E., Dalkara, T., 2018. Nuclear expansion and pore opening are instant signs of neuronal hypoxia and can identify poorly fixed brains. Sci. Rep. 8, 14770. https://doi.org/10.1038/s41598-018-32878-1

Del Bigio, M.R., Deck, J.H., Davidson, G.S., 2000. Glial swelling with eosinophilia in human post-mortem brains: a change indicative of plasma extravasation. Acta Neuropathol. (Berl.) 100, 688–694. https://doi.org/10.1007/s004010000236

Demetrius, L., 2005. Of mice and men. When it comes to studying ageing and the means to slow it down, mice are not just small humans. EMBO Rep. 6 Spec No, S39-44. https://doi.org/10.1038/sj.embor.7400422

Douglas, J.F., 2018. Weak and Strong Gels and the Emergence of the Amorphous Solid State. Gels Basel Switz. 4, E19. https://doi.org/10.3390/gels4010019

Dreier, J.P., Victorov, I.V., Petzold, G.C., Major, S., Windmüller, O., Fernández-Klett, F., Kandasamy, M., Dirnagl, U., Priller, J., 2013. Electrochemical failure of the brain cortex is more deleterious when it is accompanied by low perfusion. Stroke 44, 490–496. https://doi.org/10.1161/STROKEAHA.112.660589

Eberhardt, F., Bushong, E.A., Phan, S., Peltier, S., Monteagudo, P., Weinkauf, T., Herz, A.V.M., Stemmler, M., Ellisman, M., 2022. A uniform and isotropic cytoskeletal tiling fills dendritic spines. eNeuro ENEURO.0342-22.2022. https://doi.org/10.1523/ENEURO.0342-22.2022

Eggan, S.M., Lewis, D.A., 2007. Immunocytochemical distribution of the cannabinoid CB1 receptor in the primate neocortex: a regional and laminar analysis. Cereb. Cortex 17. https://doi.org/Immunocytochemical distribution of the cannabinoid CB1 receptor in the primate neocortex: a regional and laminar analysis

Faitg, J., Lacefield, C., Davey, T., White, K., Laws, R., Kosmidis, S., Reeve, A.K., Kandel, E.R., Vincent, A.E., Picard, M., 2021. 3D neuronal mitochondrial morphology in axons, dendrites, and somata of the aging mouse hippocampus. Cell Rep. 36, 109509. https://doi.org/10.1016/j.celrep.2021.109509

Ferrer, I., Santpere, G., Arzberger, T., Bell, J., Blanco, R., Boluda, S., Budka, H., Carmona, M., Giaccone, G., Krebs, B., Limido, L., Parchi, P., Puig, B., Strammiello, R., Ströbel, T., Kretzschmar, H., 2007. Brain protein preservation largely depends on the postmortem storage temperature: implications for study of proteins in human neurologic diseases and management of brain banks: a BrainNet Europe Study. J. Neuropathol. Exp. Neurol. 66, 35–46. https://doi.org/10.1097/nen.0b013e31802c3e7d

Fink, S.L., Cookson, B.T., 2005. Apoptosis, pyroptosis, and necrosis: mechanistic description of dead and dying eukaryotic cells. Infect. Immun. 73, 1907–1916. https://doi.org/10.1128/IAI.73.4.1907-1916.2005

Finnie, J.W., Blumbergs, P.C., Manavis, J., 2016. Temporal Sequence of Autolysis in the Cerebellar Cortex of the Mouse. J. Comp. Pathol. 154, 323–328. https://doi.org/10.1016/j.jcpa.2016.03.005

Finnie, J.W., Jerrett, I.V., Manavis, J., 2022. Red neurons in ovine polioencephalomalacia (cerebrocortical necrosis) are strongly amyloid precursor protein immunopositive. Vet. Res. Commun. 46, 289–293. https://doi.org/10.1007/s11259-022-09888-6

Fix, A.S., Garman, R.H., 2000. Practical aspects of neuropathology: a technical guide for working with the nervous system. Toxicol. Pathol. 28, 122–131. https://doi.org/10.1177/019262330002800115

Fodor, M., van Leeuwen, F.W., Swaab, D.F., 2002. Differences in postmortem stability of sex steroid receptor immunoreactivity in rat brain. J. Histochem. Cytochem. Off. J. Histochem. Soc. 50, 641–650. https://doi.org/10.1177/002215540205000505

Folkerth, R.D., Crary, J.F., Shewmon, D.A., 2022. Neuropathologic findings in a young woman 4 years following declaration of brain death: case analysis and literature review. J. Neuropathol. Exp. Neurol. nlac090. https://doi.org/10.1093/jnen/nlac090

Fountoulakis, M., Hardmeier, R., Höger, H., Lubec, G., 2001. Postmortem changes in the level of brain proteins. Exp. Neurol. 167, 86–94. https://doi.org/10.1006/exnr.2000.7529

Fricker, M., Tolkovsky, A.M., Borutaite, V., Coleman, M., Brown, G.C., 2018. Neuronal Cell Death. Physiol. Rev. 98, 813–880. https://doi.org/10.1152/physrev.00011.2017

Furukawa, S., Nishi, K., Morita, S., Hitosugi, M., Wingenfeld, L., 2015. The damaging in the granular cells and expression patterns of CIRBP, RBM3, HSP70, HIF-1, AIF1, SIRT1, Ngb, cFos, p53 and CCC9 in the postmortem human cerebellums obtained from individuals who died due to hanging, strangulation, drowning, or asphyxia by anaphylaxis or food aspiration may be closely linking with agonal duration. Anil Aggrawals Internet J. Forensic Med. Toxicol. 16.

Galluzzi, L., Vitale, I., Aaronson, S.A., Abrams, J.M., Adam, D., Agostinis, P., Alnemri, E.S., Altucci, L., Amelio, I., Andrews, D.W., Annicchiarico-Petruzzelli, M., Antonov, A.V., Arama, E., Baehrecke, E.H., Barlev, N.A., Bazan, N.G., Bernassola, F., Bertrand, M.J.M., Bianchi, K., Blagosklonny, M.V., Blomgren, K., Borner, C., Boya, P., Brenner, C., Campanella, M., Candi, E., Carmona-Gutierrez, D., Cecconi, F., Chan, F.K.-M., Chandel, N.S., Cheng, E.H., Chipuk, J.E., Cidlowski, J.A., Ciechanover, A., Cohen, G.M., Conrad, M., Cubillos-Ruiz, J.R., Czabotar, P.E., D'Angiolella, V., Dawson, T.M., Dawson, V.L., De Laurenzi, V., De Maria, R., Debatin, K.-M., DeBerardinis, R.J., Deshmukh, M., Di Daniele, N., Di Virgilio, F., Dixit, V.M., Dixon, S.J., Duckett, C.S., Dynlacht, B.D., El-Deiry, W.S., Elrod, J.W., Fimia, G.M., Fulda, S., García-Sáez, A.J., Garg, A.D., Garrido, C., Gavathiotis, E., Golstein, P., Gottlieb, E., Green, D.R., Greene, L.A., Gronemeyer, H., Gross, A., Hajnoczky, G., Hardwick, J.M., Harris, I.S., Hengartner, M.O., Hetz, C., Ichijo, H., Jäättelä, M., Joseph, B., Jost, P.J., Juin, P.P., Kaiser, W.J., Karin, M., Kaufmann, T., Kepp, O., Kimchi, A., Kitsis, R.N., Klionsky, D.J., Knight, R.A., Kumar, S., Lee, S.W., Lemasters, J.J., Levine, B., Linkermann, A., Lipton, S.A., Lockshin, R.A., López-Otín, C., Lowe, S.W., Luedde, T., Lugli, E., MacFarlane, M., Madeo, F., Malewicz, M., Malorni, W., Manic, G., Marine, J.-C., Martin, S.J., Martinou, J.-C., Medema, J.P., Mehlen, P., Meier, P., Melino, S., Miao, E.A., Molkentin, J.D., Moll, U.M., Muñoz-Pinedo, C., Nagata, S., Nuñez, G., Oberst, A., Oren, M., Overholtzer, M., Pagano, M., Panaretakis, T., Pasparakis, M., Penninger, J.M., Pereira, D.M., Pervaiz, S., Peter, M.E., Piacentini, M., Pinton, P., Prehn, J.H.M., Puthalakath, H., Rabinovich, G.A., Rehm, M., Rizzuto, R., Rodrigues, C.M.P., Rubinsztein, D.C., Rudel, T., Ryan, K.M., Sayan, E., Scorrano, L., Shao, F., Shi, Y., Silke, J., Simon, H.-U., Sistigu, A., Stockwell, B.R., Strasser, A., Szabadkai, G., Tait, S.W.G., Tang, D., Tavernarakis, N., Thorburn, A., Tsujimoto, Y., Turk, B., Vanden Berghe, T., Vandenabeele, P., Vander Heiden, M.G., Villunger, A., Virgin, H.W., Vousden, K.H., Vucic, D., Wagner, E.F., Walczak, H., Wallach, D., Wang, Y., Wells, J.A., Wood, W., Yuan, J., Zakeri, Z., Zhivotovsky, B., Zitvogel, L., Melino, G., Kroemer, G., 2018. Molecular mechanisms of cell death: recommendations of the Nomenclature Committee on Cell Death 2018. Cell Death Differ. 25, 486–541. https://doi.org/10.1038/s41418-017-0012-4

Garcia, J.H., Liu, K.F., Ho, K.L., 1995. Neuronal necrosis after middle cerebral artery occlusion in Wistar rats progresses at different time intervals in the caudoputamen and the cortex. Stroke 26, 636–642; discussion 643. https://doi.org/10.1161/01.str.26.4.636

Garcia, J.H., Liu, K.F., Yoshida, Y., Chen, S., Lian, J., 1994a. Brain microvessels: factors altering their patency after the occlusion of a middle cerebral artery (Wistar rat). Am. J. Pathol. 145, 728–740.

Garcia, J.H., Liu, K.F., Yoshida, Y., Lian, J., Chen, S., del Zoppo, G.J., 1994b. Influx of leukocytes and platelets in an evolving brain infarct (Wistar rat). Am. J. Pathol. 144, 188–199.

Garcia, J.H., Lossinsky, A.S., Kauffman, F.C., Conger, K.A., 1978. Neuronal ischemic injury: light microscopy, ultrastructure and biochemistry. Acta Neuropathol. (Berl.) 43, 85–95. https://doi.org/10.1007/BF00685002

Garey, L.J., Ong, W.Y., Patel, T.S., Kanani, M., Davis, A., Mortimer, A.M., Barnes, T.R., Hirsch, S.R., 1998. Reduced dendritic spine density on cerebral cortical pyramidal neurons in schizophrenia. J. Neurol. Neurosurg. Psychiatry 65, 446–453. https://doi.org/10.1136/jnnp.65.4.446

Garman, R.H., 2011. Common Histological Artifacts in Nervous System Tissues, in: Fundamental Neuropathology for Pathologists and Toxicologists. John Wiley & Sons, Ltd, pp. 191–201. https://doi.org/10.1002/9780470939956.ch13

Garman, R.H., 1990. Artifacts in routinely immersion fixed nervous tissue. Toxicol. Pathol. 18, 149–153. https://doi.org/10.1177/019262339001800120

Gärtner, U., Janke, C., Holzer, M., Vanmechelen, E., Arendt, T., 1998. Postmortem changes in the phosphorylation state of tau-protein in the rat brain. Neurobiol. Aging 19, 535–543. https://doi.org/10.1016/s0197-4580(98)00094-3

Geddes, J.W., Bondada, V., Tekirian, T.L., Pang, Z., Siman, R.G., 1995. Perikaryal accumulation and proteolysis of neurofilament proteins in the post-mortem rat brain. Neurobiol. Aging 16, 651–660. https://doi.org/10.1016/0197-4580(95)00062-j

Geiger, K.D., Stoldt, P., Schlote, W., Derouiche, A., 2006. Ezrin immunoreactivity reveals specific astrocyte activation in cerebral HIV. J. Neuropathol. Exp. Neurol. 65, 87–96. https://doi.org/10.1097/01.jnen.0000195943.32786.39

Gelpi, E., Preusser, M., Bauer, G., Budka, H., 2007. Autopsy at 2 months after death: brain is satisfactorily preserved for neuropathology. Forensic Sci. Int. 168, 177–182. https://doi.org/10.1016/j.forsciint.2006.07.017

George, J., Van Wettere, A.J., Michaels, B.B., Crain, D., Lewbart, G.A., 2016. Histopathologic evaluation of postmortem autolytic changes in bluegill (Lepomis macrohirus) and crappie (Pomoxis anularis) at varied time intervals and storage temperatures. PeerJ 4, e1943. https://doi.org/10.7717/peerj.1943

Gibson, P.H., Tomlinson, B.E., 1979. Vacuolation in the human cerebral cortex and its relationship to the interval between death and autopsy and to synapse numbers: an electron microscopic study. Neuropathol. Appl. Neurobiol. 5, 1–7. https://doi.org/10.1111/j.1365-2990.1979.tb00608.x

Glausier, J.R., Konanur, A., Lewis, D.A., 2019. Factors Affecting Ultrastructural Quality in the Prefrontal Cortex of the Postmortem Human Brain. J. Histochem. Cytochem. Off. J. Histochem. Soc. 67, 185–202. https://doi.org/10.1369/0022155418819481

Gonzalez-Riano, C., Tapia-González, S., García, A., Muñoz, A., DeFelipe, J., Barbas, C., 2017. Metabolomics and neuroanatomical evaluation of post-mortem changes in the hippocampus. Brain Struct. Funct. 222, 2831–2853. https://doi.org/10.1007/s00429-017-1375-5

Haider, L., Hametner, S., Endmayr, V., Mangesius, S., Eppensteiner, A., Frischer, J.M., Iglesias, J.E., Barkhof, F., Kasprian, G., 2022. Post-mortem correlates of Virchow-Robin spaces detected on in vivo MRI. J. Cereb. Blood Flow Metab. Off. J. Int. Soc. Cereb. Blood Flow Metab. 42, 1224–1235. https://doi.org/10.1177/0271678X211067455

Haines, D.E., Jenkins, T.W., 1968. Studies on the epithalamus. I. Morphology of post-mortem degeneration: the habenular nucleus in dog. J. Comp. Neurol. 132, 405–417. https://doi.org/10.1002/cne.901320304

Halim, N.D., Weickert, C.S., McClintock, B.W., Hyde, T.M., Weinberger, D.R., Kleinman, J.E., Lipska, B.K., 2003. Presynaptic proteins in the prefrontal cortex of patients with schizophrenia and rats with abnormal prefrontal development. Mol. Psychiatry 8, 797–810. https://doi.org/10.1038/sj.mp.4001319

Hansma, P., Powers, S., Diaz, F., Li, W., 2015. Agonal thrombi at autopsy. Am. J. Forensic Med. Pathol. 36, 141–144. https://doi.org/10.1097/PAF.0000000000000162

Harada, K., Sorimachi, Y., Yoshida, K., 1997. Proteolysis of ankyrin and Na+/K(+)-ATPase in postmortem rat brain: is calpain involved? Forensic Sci. Int. 86, 77–85. https://doi.org/10.1016/s0379-0738(97)02120-8

Hardy, J.A., Wester, P., Winblad, B., Gezelius, C., Bring, G., Eriksson, A., 1985. The patients dying after long terminal phase have acidotic brains; implications for biochemical measurements on autopsy tissue. J. Neural Transm. 61, 253–264. https://doi.org/10.1007/BF01251916

Harris, K.M., Spacek, J., 2016. Dendrite structure, in: Stuart, G., Spruston, N., Häusser, M. (Eds.), Dendrites. Oxford University Press, p. 0. https://doi.org/10.1093/acprof:oso/9780198745273.003.0001

Hau, T.C., Hamzah, N.H., Lian, H.H., Hamzah, S., 2014. Decomposition process and post mortem changes. Sains Malays. 43, 1873–1882.

Hausmann, R., Seidl, S., Betz, P., 2007. Hypoxic changes in Purkinje cells of the human cerebellum. Int. J. Legal Med. 121, 175–183. https://doi.org/10.1007/s00414-006-0122-x

Hayes, T.L., Cameron, J.L., Fernstrom, J.D., Lewis, D.A., 1991. A comparative analysis of the distribution of prosomatostatin-derived peptides in human and monkey neocortex. J. Comp. Neurol. 303, 584–599. https://doi.org/10.1002/cne.903030406

Hayman, J., Oxenham, M., 2017. Estimation of the time since death in decomposed bodies found in Australian conditions. Aust. J. Forensic Sci. 49, 31–44. https://doi.org/10.1080/00450618.2015.1128972

Henics, T., Wheatley, D.N., 1999. Cytoplasmic vacuolation, adaptation and cell death: a view on new perspectives and features. Biol. Cell 91, 485–498. https://doi.org/10.1016/s0248-4900(00)88205-2

Henstridge, C.M., Jackson, R.J., Kim, J.M., Herrmann, A.G., Wright, A.K., Harris, S.E., Bastin, M.E., Starr, J.M., Wardlaw, J., Gillingwater, T.H., Smith, C., McKenzie, C.-A., Cox, S.R., Deary, I.J., Spires-Jones, T.L., 2015. Post-mortem brain analyses of the Lothian Birth Cohort 1936: extending lifetime cognitive and brain phenotyping to the level of the synapse. Acta Neuropathol. Commun. 3, 53. https://doi.org/10.1186/s40478-015-0232-0

Hetzel, W., 1980. Post-mortem modifications of the ependyma of the lateral ventricular wall. Acta Neuropathol. (Berl.) 51, 15–22. https://doi.org/10.1007/BF00688845

Hilbig, H., Bidmon, H.-J., Oppermann, O.T., Remmerbach, T., 2004. Influence of post-mortem delay and storage temperature on the immunohistochemical detection of antigens in the CNS of mice. Exp. Toxicol. Pathol. Off. J. Ges. Toxikol. Pathol. 56, 159–171. https://doi.org/10.1016/j.etp.2004.08.002

Hostiuc, S., Rusu, M.C., Mănoiu, V.S., Vrapciu, A.D., Negoi, I., Popescu, M.V., 2018. Usefulness of ultrastructure studies for the estimation of the postmortem interval. A systematic review. Romanian J. Morphol. Embryol. Rev. Roum. Morphol. Embryol.

Hua, Y., Laserstein, P., Helmstaedter, M., 2015. Large-volume en-bloc staining for electron microscopy-based connectomics. Nat. Commun. 6, 7923. https://doi.org/10.1038/ncomms8923

Hukkanen, V., Röyttä, M., 1987. Autolytic changes of human white matter: an electron microscopic and electrophoretic study. Exp. Mol. Pathol. 46, 31–9. https://doi.org/10.1016/0014-4800(87)90028-1

Hunziker O., Schweizer A., 1977. Postmortem changes in stereological parameters of cerebral capillaries. Beitr Pathol. 161, 244-255. https://doi.org/10.1016/s0005-8165(77)80080-2

Huttenlocher, P.R., 1979. Synaptic density in human frontal cortex - developmental changes and effects of aging. Brain Res. 163, 195–205. https://doi.org/10.1016/0006-8993(79)90349-4

Ikuta, F., Hirano, A., Zimmerman, H.M., 1963. An Experimental Study of Post-Mortem Alterations in the Granular Layer of the Cerebellar Cortex. J. Neuropathol. Exp. Neurol. 22, 581–593. https://doi.org/10.1097/00005072-196310000-00002

Ilse, G., Kovacs, K., Ryan, N., Horvath, E., Ilse, D., 1979. Autolytic changes in the rat adenohypophysis. A histologic, immunocytologic and electron microscopic study. Exp. Pathol. (Jena) 17, 185–95. https://doi.org/10.1016/s0014-4908(79)80011-3

Irving, E.A., McCulloch, J., Dewar, D., 1997. The effect of postmortem delay on the distribution of microtubule-associated proteins tau, MAP2, and MAP5 in the rat. Mol. Chem. Neuropathol. 30, 253–271. https://doi.org/10.1007/BF02815102

Ith, M., Scheurer, E., Kreis, R., Thali, M., Dirnhofer, R., Boesch, C., 2011. Estimation of the postmortem interval by means of ^{1}H MRS of decomposing brain tissue: influence of ambient temperature. NMR Biomed. 24, 791–798. https://doi.org/10.1002/nbm.1623

Itoyama, Y., Sternberger, N.H., Kies, M.W., Cohen, S.R., Richardson, E.P., Webster, H., 1980. Immunocytochemical method to identify myelin basic protein in oligodendroglia and myelin sheaths of the human nervous system. Ann. Neurol. 7, 157–166. https://doi.org/10.1002/ana.410070211

Jacobs, B., Scheibel, A.B., 1993. A quantitative dendritic analysis of Wernicke's area in humans. I. Lifespan changes. J. Comp. Neurol. 327, 83–96. https://doi.org/10.1002/cne.903270107

Jamal, A., Mongelli, M.T., Vidotto, M., Madekurozwa, M., Bernardini, A., Overby, D.R., De Momi, E., Rodriguez Y Baena, F., Sherwood, J.M., Dini, D., 2021. Infusion Mechanisms in Brain White Matter and Their Dependence on Microstructure: An Experimental Study of Hydraulic Permeability. IEEE Trans. Biomed. Eng. 68, 1229–1237. https://doi.org/10.1109/TBME.2020.3024117

Jenkins, L.W., Povlishock, J.T., Becker, D.P., Miller, J.D., Sullivan, H.G., 1979. Complete cerebral ischemia. An ultrastructural study. Acta Neuropathol. (Berl.) 48, 113–125. https://doi.org/10.1007/BF00691152

Jernerén, F., Söderquist, M., Karlsson, O., 2015. Post-sampling release of free fatty acids - effects of heat stabilization and methods of euthanasia. J. Pharmacol. Toxicol. Methods 71, 13–20. https://doi.org/10.1016/j.vascn.2014.11.001

Johnston, N.L., Cervenak, J., Shore, A.D., Torrey, E.F., Yolken, R.H., Cerevnak, J., 1997. Multivariate analysis of RNA levels from postmortem human brains as measured by three different methods of RT-PCR. Stanley Neuropathology Consortium. J. Neurosci. Methods 77, 83–92. https://doi.org/10.1016/s0165-0270(97)00115-5

Kádár, A., Wittmann, G., Liposits, Z., Fekete, C., 2009. Improved method for combination of immunocytochemistry and Nissl staining. J. Neurosci. Methods 184, 115–118. https://doi.org/10.1016/j.jneumeth.2009.07.010

Kang, H.W., Kim, H.K., Moon, B.H., Lee, Seo Jun, Lee, Se Jung, Rhyu, I.J., 2017. Comprehensive review of Golgi staining methods for nervous tissue. Appl. Microsc. 47, 63–69. https://doi.org/10.9729/AM.2017.47.2.63

Karlsson, U., Schultz, R.L., 1966. Fixation of the central nervous system for electron microscopy by aldehyde perfusion: III. Structural changes after exsanguination and delayed perfusion. J. Ultrastruct. Res. 14, 47–63. https://doi.org/10.1016/S0022-5320(66)80034-5

Kay, K.R., Smith, C., Wright, A.K., Serrano-Pozo, A., Pooler, A.M., Koffie, R., Bastin, M.E., Bak, T.H., Abrahams, S., Kopeikina, K.J., McGuone, D., Frosch, M.P., Gillingwater, T.H., Hyman, B.T., Spires-Jones, T.L., 2013. Studying synapses in human brain with array tomography and electron microscopy. Nat. Protoc. 8, 1366–1380. https://doi.org/10.1038/nprot.2013.078

Kekenes-Huskey, P., Scott, C., Atalay, S., 2016. Quantifying the Influence of the Crowded Cytoplasm on Small Molecule Diffusion. J. Phys. Chem. B 120, 8696–8706. https://doi.org/10.1021/acs.jpcb.6b03887

Kherani, Z.S., Auer, R.N., 2008. Pharmacologic analysis of the mechanism of dark neuron production in cerebral cortex. Acta Neuropathol. (Berl.) 116, 447–452. https://doi.org/10.1007/s00401-008-0386-y

Kies, M.W., Schwimmer, S., 1942. OBSERVATIONS ON PROTEINASE IN BRAIN. J. Biol. Chem. 145, 685–691. https://doi.org/10.1016/S0021-9258(18)51311-9

Kinney, J.P., Spacek, J., Bartol, T.M., Bajaj, C.L., Harris, K.M., Sejnowski, T.J., 2013. Extracellular Sheets and Tunnels Modulate Glutamate Diffusion in Hippocampal Neuropil. J. Comp. Neurol. 521, 448–464. https://doi.org/10.1002/cne.23181

Kitamura, O., Gotohda, T., Ishigami, A., Tokunaga, I., Kubo, S., Nakasono, I., 2005. Effect of hypothermia on postmortem alterations in MAP2 immunostaining in the human hippocampus. Leg. Med. 7, 340–344. https://doi.org/10.1016/j.legalmed.2005.08.006

Kloner, R.A., King, K.S., Harrington, M.G., 2018. No-reflow phenomenon in the heart and brain. Am. J. Physiol. Heart Circ. Physiol. 315, H550–H562. https://doi.org/10.1152/ajpheart.00183.2018

Knudsen, L.M., Pallesen, G., 1986. The preservation and loss of various non-haematopoietic antigens in human post-mortem tissues as demonstrated by monoclonal antibody immunohistological staining. Histopathology 10, 1007–1014. https://doi.org/10.1111/j.1365-2559.1986.tb02537.x

Koenig, R.S., Koenig, H., 1952. An experimental study of post mortem alterations in neurons of the central nervous system. J. Neuropathol. Exp. Neurol. 11, 69–78. https://doi.org/10.1097/00005072-195201000-00008

Kolomeets, N.S., Orlovskaya, D.D., Rachmanova, V.I., Uranova, N.A., 2005. Ultrastructural alterations in hippocampal mossy fiber synapses in schizophrenia: a postmortem morphometric study. Synap. N. Y. N 57. https://doi.org/10.1002/syn.20153

Kolomeets, N.S., Orlovskaya, D.D., Uranova, N.A., 2007. Decreased numerical density of CA3 hippocampal mossy fiber synapses in schizophrenia. Synap. N. Y. N 61, 615–621. https://doi.org/10.1002/syn.20405

Koo, T.K., Li, M.Y., 2016. A Guideline of Selecting and Reporting Intraclass Correlation Coefficients for Reliability Research. J. Chiropr. Med. 15, 155–163. https://doi.org/10.1016/j.jcm.2016.02.012

Kovács, B., Bukovics, P., Gallyas, F., 2007. Morphological effects of transcardially perfused SDS on the rat brain. Biol. Cell 99, 425–432. https://doi.org/10.1042/BC20060128

Kramer, E.M., Myers, D.R., 2013. Osmosis is not driven by water dilution. Trends Plant Sci. 18, 195–197. https://doi.org/10.1016/j.tplants.2012.12.001

Kretzschmar, H., 2009. Brain banking: opportunities, challenges and meaning for the future. Nat. Rev. Neurosci. 10, 70–78. https://doi.org/10.1038/nrn2535

Kulkarni, V.A., Firestein, B.L., 2012. The dendritic tree and brain disorders. Mol. Cell. Neurosci. 50, 10–20. https://doi.org/10.1016/j.mcn.2012.03.005

Kuroiwa, T., Nagaoka, T., Ueki, M., Yamada, I., Miyasaka, N., Akimoto, H., 1998. Different apparent diffusion coefficient: water content correlations of gray and white matter during early ischemia. Stroke 29, 859–865. https://doi.org/10.1161/01.str.29.4.859

Kwee, R.M., Kwee, T.C., 2007. Virchow-Robin spaces at MR imaging. Radiogr. Rev. Publ. Radiol. Soc. N. Am. Inc 27, 1071–1086. https://doi.org/10.1148/rg.274065722

Lafontaine, D.L.J., Riback, J.A., Bascetin, R., Brangwynne, C.P., 2021. The nucleolus as a multiphase liquid condensate. Nat. Rev. Mol. Cell Biol. 22, 165–182. https://doi.org/10.1038/s41580-020-0272-6

Lafrenaye, A.D., Simard, J.M., 2019. Bursting at the Seams: Molecular Mechanisms Mediating Astrocyte Swelling. Int. J. Mol. Sci. 20, 330. https://doi.org/10.3390/ijms20020330

Lavenex, P., Lavenex, P.B., Bennett, J.L., Amaral, D.G., 2009. Postmortem changes in the neuroanatomical characteristics of the primate brain: hippocampal formation. J. Comp. Neurol. 512, 27–51. https://doi.org/10.1002/cne.21906

Lee, T.-K., Kim, Hyunjung, Song, M., Lee, J.-C., Park, J.H., Ahn, J.H., Yang, G.E., Kim, Hyeyoung, Ohk, T.G., Shin, M.C., Cho, J.H., Won, M.-H., 2019. Time-course pattern of neuronal loss and gliosis in gerbil hippocampi following mild, severe, or lethal transient global cerebral ischemia. Neural Regen. Res. 14, 1394–1403. https://doi.org/10.4103/1673-5374.253524

Leonard, A., Vink, R., Byard, R.W., 2016. Brain Fluid Content Related to Body Position and Postmortem Interval - An Animal Model. J. Forensic Sci. 61, 671–673. https://doi.org/10.1111/1556-4029.13038

Lesnikova, I., Schreckenbach, M.N., Kristensen, M.P., Papanikolaou, L.L., Hamilton-Dutoit, S., 2018. Usability of Immunohistochemistry in Forensic Samples With Varying Decomposition. Am. J. Forensic Med. Pathol. 39, 185–191. https://doi.org/10.1097/PAF.0000000000000408

Levin, S., Bucci, T.J., Cohen, S.M., Fix, A.S., Hardisty, J.F., LeGrand, E.K., Maronpot, R.R., Trump, B.F., 1999. The nomenclature of cell death: recommendations of an ad hoc Committee of the Society of Toxicologic Pathologists. Toxicol. Pathol. 27, 484–490. https://doi.org/10.1177/019262339902700419

Lewis, D.A., 2002. The human brain revisited: opportunities and challenges in postmortem studies of psychiatric disorders. Neuropsychopharmacol. Off. Publ. Am. Coll. Neuropsychopharmacol. 26, 143–154. https://doi.org/10.1016/S0893-133X(01)00393-1

Li, J.Z., Vawter, M.P., Walsh, D.M., Tomita, H., Evans, S.J., Choudary, P.V., Lopez, J.F., Avelar, A., Shokoohi, V., Chung, T., Mesarwi, O., Jones, E.G., Watson, S.J., Akil, H., Bunney, W.E., Jr, Myers, R.M., 2004. Systematic changes in gene expression in postmortem human brains associated with tissue pH and terminal medical conditions. Hum. Mol. Genet. 13, 609–616. https://doi.org/10.1093/hmg/ddh065

Li, Y., Zhou, Y., Danbolt, N.C., 2012. The rates of postmortem proteolysis of glutamate transporters differ dramatically between cells and between transporter subtypes. J. Histochem. Cytochem. Off. J. Histochem. Soc. 60, 811–821. https://doi.org/10.1369/0022155412458589

Lindenberg, R., 1956. Morphotropic and morphostatic necrobiosis; investigations on nerve cells of the brain. Am. J. Pathol. 32, 1147–1177.

Lingwood, B.E., Healy, G.N., Sullivan, S.M., Pow, D.V., Colditz, P.B., 2008. MAP2 provides reliable early assessment of neural injury in the newborn piglet model of birth asphyxia. J. Neurosci. Methods 171, 140–146. https://doi.org/10.1016/j.jneumeth.2008.02.011

Link, C.D., 2021. Is There a Brain Microbiome? Neurosci. Insights 16, 26331055211018708. https://doi.org/10.1177/26331055211018709

Lipton, P., 1999. Ischemic Cell Death in Brain Neurons. Physiol. Rev. 79, 1431–1568. https://doi.org/10.1152/physrev.1999.79.4.1431

Liu, C.N., Windle, W.F., 1950. Effects of inanition on the central nervous system; an experimental study on the guinea pig. Arch. Neurol. Psychiatry 63, 918–927. https://doi.org/10.1001/archneurpsyc.1950.02310240077004

Liu, X., Brun, A., 1995. Synaptophysin immunoreactivity is stable 36 h postmortem. Dement. Basel Switz. 6, 211–217. https://doi.org/10.1159/000106949

Lodish, H.F., Rothman, J.E., 1979. The assembly of cell membranes. Sci. Am. 240, 48–63. https://doi.org/10.1038/scientificamerican0179-48

Loh, K.Y., Wang, Z., Liao, P., 2019. Oncotic Cell Death in Stroke. Rev. Physiol. Biochem. Pharmacol. 176, 37–64. https://doi.org/10.1007/112_2018_13

Lossi, L., 2022. The concept of intrinsic versus extrinsic apoptosis. Biochem. J. 479, 357–384. https://doi.org/10.1042/BCJ20210854

Lucassen, P.J., Chung, W.C., Kamphorst, W., Swaab, D.F., 1997. DNA damage distribution in the human brain as shown by in situ end labeling; area-specific differences in aging and Alzheimer disease in the absence of apoptotic morphology. J. Neuropathol. Exp. Neurol. https://doi.org/10.1097/00005072-199708000-00007

Lucassen, P.J., Chung, W.C., Vermeulen, J.P., Van Lookeren Campagne, M., Van Dierendonck, J.H., Swaab, D.F., 1995. Microwave-enhanced in situ end-labeling of fragmented DNA: parametric studies in relation to postmortem delay and fixation of rat and human brain. J. Histochem. Cytochem. Off. J. Histochem. Soc. 43, 1163–1171. https://doi.org/10.1177/43.11.7560899

MacKenzie, J.M., 2014. Examining the decomposed brain. Am. J. Forensic Med. Pathol. 35, 265–270. https://doi.org/10.1097/PAF.0000000000000111

Madea, B., 1994. Importance of supravitality in forensic medicine. Forensic Sci. Int. 69, 221–241. https://doi.org/10.1016/0379-0738(94)90386-7

Mahesh, S., Tang, K.-C., Raj, M., 2018. Amide Bond Activation of Biological Molecules. Mol. Basel Switz. 23, E2615. https://doi.org/10.3390/molecules23102615

Majno, G., Joris, I., 1995. Apoptosis, oncosis, and necrosis. An overview of cell death. Am. J. Pathol. 146, 3–15.

Manzo, C., Garcia-Parajo, M.F., 2015. A review of progress in single particle tracking: from methods to biophysical insights. Rep. Prog. Phys. Phys. Soc. G. B. 78, 124601. https://doi.org/10.1088/0034-4885/78/12/124601

Martin, M. da G.M., Paes, V.R., Cardoso, E.F., Neto, C.E.B.P., Kanamura, C.T., Leite, C. da C., Otaduy, M.C.G., Monteiro, R.A. de A., Mauad, T., da Silva, L.F.F., Castro, L.H.M., Saldiva, P.H.N., Dolhnikoff, M., Duarte-Neto, A.N., 2022. Postmortem brain 7T MRI with minimally invasive pathological correlation in deceased COVID-19 subjects. Insights Imaging 13, 7. https://doi.org/10.1186/s13244-021-01144-w

Martin, S.B., Waniewski, R.A., Battaglioli, G., Martin, D.L., 2003. Post-mortem degradation of brain glutamate decarboxylase. Neurochem. Int. 42, 549–554. https://doi.org/10.1016/s0197-0186(02)00189-4

Maynard, E.A., Schultz, R.L., Pease, D.C., 1957. Electron microscopy of the vascular bed of rat cerebral cortex. Am. J. Anat. 100, 409–433. https://doi.org/10.1002/aja.1001000306

McCullumsmith, R.E., Hammond, J.H., Shan, D., Meador-Woodruff, J.H., 2014. Postmortem Brain: An Underutilized Substrate for Studying Severe Mental Illness. Neuropsychopharmacology 39, 65–87. https://doi.org/10.1038/npp.2013.239

McFadden, W.C., Walsh, H., Richter, F., Soudant, C., Bryce, C.H., Hof, P.R., Fowkes, M., Crary, J.F., McKenzie, A.T., 2019. Perfusion fixation in brain banking: a systematic review. Acta Neuropathol. Commun. 7, 146. https://doi.org/10.1186/s40478-019-0799-y

McKenzie, A.T., Marx, G.A., Koenigsberg, D., Sawyer, M., Iida, M.A., Walker, J.M., Richardson, T.E., Campanella, G., Attems, J., McKee, A.C., Stein, T.D., Fuchs, T.J., White, C.L., PART working group, Farrell, K., Crary, J.F., 2022. Interpretable deep learning of myelin histopathology in age-related cognitive impairment. Acta Neuropathol. Commun. 10, 131. https://doi.org/10.1186/s40478-022-01425-5

Mena, H., Cadavid, D., Rushing, E.J., 2004. Human cerebral infarct: a proposed histopathologic classification based on 137 cases. Acta Neuropathol. (Berl.) 108. https://doi.org/10.1007/s00401-004-0918-z

Michiue, T., Quan, L., Ishikawa, T., Zhu, B.-L., Maeda, H., 2009. Quantitative analysis of single-stranded DNA immunoreactivity as a marker of neuronal apoptosis in hippocampus with regard to the causes of death in medicolegal autopsy. Leg. Med. Tokyo Jpn. 11 Suppl 1, S168-170. https://doi.org/10.1016/j.legalmed.2009.01.105

Miller, M.A., Zachary, J.F., 2017. Mechanisms and Morphology of Cellular Injury, Adaptation, and Death. Pathol. Basis Vet. Dis. 2-43.e19. https://doi.org/10.1016/B978-0-323-35775-3.00001-1

Mogilner, A., Manhart, A., 2018. Intracellular Fluid Mechanics: Coupling Cytoplasmic Flow with Active Cytoskeletal Gel. Annu. Rev. Fluid Mech. 50, 347–370. https://doi.org/10.1146/annurev-fluid-010816-060238

Monroy-Gómez, J., Santamaría, G., Sarmiento, L., Torres-Fernández, O., 2020. Effect of Postmortem Degradation on the Preservation of Viral Particles and Rabies Antigens in Mice Brains. Light and Electron Microscopic Study. Viruses 12, E938. https://doi.org/10.3390/v12090938

Montero-Crespo, M., Domínguez-Álvaro, M., Alonso-Nanclares, L., DeFelipe, J., Blazquez-Llorca, L., 2021. Three-dimensional analysis of synaptic organization in the hippocampal CA1 field in Alzheimer's disease. Brain 144, 553–573. https://doi.org/10.1093/brain/awaa406

Mori, S., Sternberger, N.H., Herman, M.M., Sternberger, L.A., 1992. Variability of laminin immunoreactivity in human autopsy brain. Histochemistry 97, 237–241. https://doi.org/10.1007/BF00267633

Mori, S., Sternberger, N.H., Herman, M.M., Sternberger, L.A., 1991. Leakage and neuronal uptake of serum protein in aged and Alzheimer brains. A postmortem phenomenon with antemortem etiology. Lab. Investig. J. Tech. Methods Pathol. 64, 345–351.

Morton-Hayward, A.L., Thompson, T., Thomas-Oates, J.E., Buckley, S., Petzold, A., Ramsøe, A., O'Connor, S., Collins, M.J., 2020. A conscious rethink: Why is brain tissue commonly preserved in the archaeological record? Commentary on: Petrone P, Pucci P, Niola M, et al. Heat-induced brain vitrification from the Vesuvius eruption in C.E. 79. N Engl J Med 2020;382:383-4. DOI: 10.1056/NEJMc1909867. STAR Sci. Technol. Archaeol. Res. 6, 87–95. https://doi.org/10.1080/20548923.2020.1815398

Moscardini, A., Di Pietro, S., Signore, G., Parlanti, P., Santi, M., Gemmi, M., Cappello, V., 2020. Uranium-free X solution: a new generation contrast agent for biological samples ultrastructure. Sci. Rep. 10, 11540. https://doi.org/10.1038/s41598-020-68405-4

Müller, M.B., Lucassen, P.J., Yassouridis, A., Hoogendijk, W.J., Holsboer, F., Swaab, D.F., 2001. Neither major depression nor glucocorticoid treatment affects the cellular integrity of the human hippocampus. Eur. J. Neurosci. 14, 1603–1612. https://doi.org/10.1046/j.0953-816x.2001.01784.x

Nagy, C., Maheu, M., Lopez, J.P., Vaillancourt, K., Cruceanu, C., Gross, J.A., Arnovitz, M., Mechawar, N., Turecki, G., 2015. Effects of postmortem interval on biomolecule integrity in the brain. J. Neuropathol. Exp. Neurol. 74, 459–469. https://doi.org/10.1097/NEN.0000000000000190

Nahirney, P.C., Tremblay, M.-E., 2021. Brain Ultrastructure: Putting the Pieces Together. Front. Cell Dev. Biol. 9, 629503. https://doi.org/10.3389/fcell.2021.629503

Nakabayashi, Y., Nabeka, H., Kuwahara, N., Matsuda, S., Asano, M., 2021. Postmortem Interval Estimation by Evaluating Saposin D Levels and Morphological Alterations in Hippocampal Neurons. Albanian J. Med. Health Sci. 55.

Nunley, W.C., Schuit, K.E., Dickie, M.W., Kinlaw, J.B., 1972. Delayed, in vivo hepatic post-mortem autolysis. Virchows Arch. B Cell Pathol. 11, 289–302. https://doi.org/10.1007/BF02889410

Oehmichen, M., 1994. Brain death: neuropathological findings and forensic implications. Forensic Sci. Int. 69, 205–219. https://doi.org/10.1016/0379-0738(94)90385-9

Oehmichen, M., 1980. Enzyme alterations in brain tissue during the early postmortal interval with reference to the histomorphology: review of the literature. Z. Rechtsmed. 85, 81–95. https://doi.org/10.1007/BF02092198

Oehmichen, M., Auer, R.N., König, H.G., 2006. Forensic Neuropathology and Associated Neurology. Springer, Berlin, Heidelberg. https://doi.org/10.1007/3-540-28995-X

Ohm, T.G., Diekmann, S., 1994. The use of Lucifer Yellow and Mini-Ruby for intracellular staining in fixed brain tissue: methodological considerations evaluated in rat and human autopsy brains. J. Neurosci. Methods 55, 105–110. https://doi.org/10.1016/0165-0270(94)90046-9

Palkovits, M., Harvey-White, J., Liu, J., Kovacs, Z.S., Bobest, M., Lovas, G., Bagó, A.G., Kunos, G., 2008. Regional distribution and effects of postmortal delay on endocannabinoid content of the human brain. Neuroscience 152, 1032–1039. https://doi.org/10.1016/j.neuroscience.2008.01.034

Palmer, A.M., Lowe, S.L., Francis, P.T., Bowen, D.M., 1988. Are post-mortem biochemical studies of human brain worthwhile? Biochem. Soc. Trans. 16, 472–475. https://doi.org/10.1042/bst0160472

Pantoni, L., Garcia, J.H., Gutierrez, J.A., 1996. Cerebral white matter is highly vulnerable to ischemia. Stroke 27, 1641–1646; discussion 1647. https://doi.org/10.1161/01.str.27.9.1641

Pearce, J.M., Komoroski, R.A., 2000. Analysis of phospholipid molecular species in brain by (31)P NMR spectroscopy. Magn. Reson. Med. 44, 215–223. https://doi.org/10.1002/1522-2594(200008)44:2<215::aid-mrm8>3.0.co;2-n

Pélissier-Alicot, A.-L., Gaulier, J.-M., Champsaur, P., Marquet, P., 2003. Mechanisms underlying postmortem redistribution of drugs: a review. J. Anal. Toxicol. 27, 533–544. https://doi.org/10.1093/jat/27.8.533

Pelucchi, S., Stringhi, R., Marcello, E., 2020. Dendritic Spines in Alzheimer's Disease: How the Actin Cytoskeleton Contributes to Synaptic Failure. Int. J. Mol. Sci. 21, 908. https://doi.org/10.3390/ijms21030908

Peroski, M., Proudan, N., Grignol, G., Merchenthaler, I., Dudas, B., 2016. Corticotropin-releasing hormone (CRH)-immunoreactive (IR) axon varicosities target a subset of growth hormone-releasing hormone (GHRH)-IR neurons in the human hypothalamus. J. Chem.

Neuroanat. 78, 119–124. https://doi.org/10.1016/j.jchemneu.2016.09.005

Perry, R.H., Tomlinson, B.E., Taylor, M.J., Perry, E.K., 1977. Human brain temperature at necropsy: a guide in post-mortem biochemistry. Lancet Lond. Engl. 1, 38. https://doi.org/10.1016/s0140-6736(77)91669-5

Petit, T.L., LeBoutillier, J.C., 1990. Quantifying synaptic number and structure: effects of stain and post-mortem delay. Brain Res. 517, 269–275. https://doi.org/10.1016/0006-8993(90)91037-h

Petzold, A., Lu, C.-H., Groves, M., Gobom, J., Zetterberg, H., Shaw, G., O'Connor, S., 2020. Protein aggregate formation permits millennium-old brain preservation. J. R. Soc. Interface 17, 20190775. https://doi.org/10.1098/rsif.2019.0775

Powers, R.H., 2005. The Decomposition of Human Remains, in: Rich, J., Dean, D.E., Powers, R.H. (Eds.), Forensic Medicine of the Lower Extremity: Human Identification and Trauma Analysis of the Thigh, Leg, and Foot, Forensic Science and Medicine. Humana Press, Totowa, NJ, pp. 3–15. https://doi.org/10.1385/1-59259-897-8:003

Pozhitkov, A.E., Neme, R., Domazet-Lošo, T., Leroux, B.G., Soni, S., Tautz, D., Noble, P.A., 2017. Tracing the dynamics of gene transcripts after organismal death. Open Biol. 7, 160267. https://doi.org/10.1098/rsob.160267

Quartu, M., Serra, M.P., Manca, A., Mascia, F., Follesa, P., Del Fiacco, M., 2005. Neurturin, persephin, and artemin in the human pre- and full-term newborn and adult hippocampus and fascia dentata. Brain Res. 1041, 157–166. https://doi.org/10.1016/j.brainres.2005.02.007

Radzicka, A., Wolfenden, R., 1996. Rates of Uncatalyzed Peptide Bond Hydrolysis in Neutral Solution and the Transition State Affinities of Proteases. J. Am. Chem. Soc. 118, 6105–6109. https://doi.org/10.1021/ja954077c

Ramirez, E.P.C., Keller, C.E., Vonsattel, J.P., 2018. The New York Brain Bank of Columbia University: practical highlights of 35 years of experience. Handb. Clin. Neurol. 150, 105–118. https://doi.org/10.1016/B978-0-444-63639-3.00008-6

Ravid, R., Van Zwieten, E.J., Swaab, D.F., 1992. Brain banking and the human hypothalamus--factors to match for, pitfalls and potentials. Prog. Brain Res. 93, 83–95. https://doi.org/10.1016/s0079-6123(08)64565-3

Rees, S., 1977. The incidence of ultrastructural abnormalities in the cortex of two retarded human brains (Down's syndrome). Acta Neuropathol. (Berl.) 37, 65–68. https://doi.org/10.1007/BF00684542

Rees, S., 1976. A quantitative electron microscopic study of the ageing human cerebral cortex. Acta Neuropathol. (Berl.) 36, 347–362. https://doi.org/10.1007/BF00699640

Riback, J.A., Eeftens, J.M., Lee, D.S.W., Quinodoz, S.A., Beckers, L., Becker, L.A., Brangwynne, C.P., 2022. Viscoelastic RNA entanglement and advective flow underlie nucleolar form and function. https://doi.org/10.1101/2021.12.31.474660

Roberts, R.C., Gaither, L.A., Peretti, F.J., Lapidus, B., Chute, D.J., 1996. Synaptic organization of the human striatum: a postmortem ultrastructural study. J. Comp. Neurol. 374, 523–534. https://doi.org/10.1002/(SICI)1096-9861(19961028)374:4<523::AID-CNE4>3.0.CO;2-3

Roberts, R.C., Roche, J.K., Conley, R.R., 2005. Synaptic differences in the postmortem striatum of subjects with schizophrenia: a stereological ultrastructural analysis. Synap. N. Y. N 56, 185–197. https://doi.org/10.1002/syn.20144

Roberts, R.C., Roche, J.K., McCullumsmith, R.E., 2014. Localization of excitatory amino acid transporters EAAT1 and EAAT2 in human postmortem cortex: a light and electron microscopic study. Neuroscience 277, 522–540. https://doi.org/10.1016/j.neuroscience.2014.07.019

Routtenberg, A., Tarrant, S., 1974. Synaptic morphology and cytoplasmic densities: rapid post-mortem effects. Tissue Cell 6, 777–788. https://doi.org/10.1016/0040-8166(74)90015-9

Samarasekera, N., Al-Shahi Salman, R., Huitinga, I., Kliioueva, N., McLean, C.A., Kretzschmar, H., Smith, C., Ironside, J.W., 2013. Brain banking for neurological disorders. Lancet Neurol. 12, 1096–1105. https://doi.org/10.1016/S1474-4422(13)70202-3

Sarnat, H.B., Flores-Sarnat, L., Trevenen, C.L., 2010. Synaptophysin immunoreactivity in the human hippocampus and neocortex from 6 to 41 weeks of gestation. J. Neuropathol. Exp. Neurol. 69, 234–245. https://doi.org/10.1097/NEN.0b013e3181d0151f

Schallock, K., Schulz-Schaeffer, W.J., Giese, A., Kretzschmar, H.A., 1997. Postmortem delay and temperature conditions affect the in situ end-labeling (ISEL) assay in brain tissue of mice. Clin. Neuropathol. 16, 133–136.

Schavemaker, P.E., Boersma, A.J., Poolman, B., 2018. How Important Is Protein Diffusion in Prokaryotes? Front. Mol. Biosci. 5, 93. https://doi.org/10.3389/fmolb.2018.00093

Scheff, S.W., DeKosky, S.T., Price, D.A., 1990. Quantitative assessment of cortical synaptic density in Alzheimer's disease. Neurobiol. Aging 11, 29–37. https://doi.org/10.1016/0197-4580(90)90059-9

Scheff, S.W., Price, D.A., 1993. Synapse loss in the temporal lobe in Alzheimer's disease. Ann. Neurol. 33, 190–199. https://doi.org/10.1002/ana.410330209

Schultz, R.L., Maynard, E.A., Pease, D.C., 1957. Electron microscopy of neurons and neuroglia of cerebral cortex and corpus callosum. Am. J. Anat. 100, 369–407. https://doi.org/10.1002/aja.1001000305

Schulz, U., Hunziker, O., Frey, H., Schweizer, A., 1980. Postmortem changes in stereological parameters of cerebral neurons. Pathol. Res. Pract. 166, 260–270. https://doi.org/10.1016/S0344-0338(80)80134-8

Schwab, C., Bondada, V., Sparks, D.L., Cahan, L.D., Geddes, J.W., 1994. Postmortem changes in the levels and localization of microtubule-associated proteins (tau, MAP2 and MAP1B) in the rat and human hippocampus. Hippocampus 4, 210–225. https://doi.org/10.1002/hipo.450040212

Schwarzmaier, S.M., Knarr, M.R.O., Hu, S., Ertürk, A., Hellal, F., Plesnila, N., 2022. Perfusion pressure determines vascular integrity and histomorphological quality following perfusion fixation of the brain. J. Neurosci. Methods 372, 109493. https://doi.org/10.1016/j.jneumeth.2022.109493

Scudamore, C.L., Hodgson, H.K., Patterson, L., Macdonald, A., Brown, F., Smith, K.C., 2011. The effect of post-mortem delay on immunohistochemical labelling—a short review. Comp. Clin. Pathol. 20, 95–101. https://doi.org/10.1007/s00580-010-1149-4

Sele, M., Wernitznig, S., Lipovšek, S., Radulović, S., Haybaeck, J., Birkl-Toeglhofer, A.M., Wodlej, C., Kleinegger, F., Sygulla, S., Leoni, M., Ropele, S., Leitinger, G., 2019. Optimization of ultrastructural preservation of human brain for transmission electron microscopy after long post-mortem intervals. Acta Neuropathol. Commun. 7, 144. https://doi.org/10.1186/s40478-019-0794-3

Serra, M.P., Quartu, M., Mascia, F., Manca, A., Boi, M., Pisu, M.G., Lai, M.L., Del Fiacco, M., 2005. Ret, GFRalpha-1, GFRalpha-2 and GFRalpha-3 receptors in the human hippocampus and fascia dentata. Int. J. Dev.

Neurosci. Off. J. Int. Soc. Dev. Neurosci. 23, 425–438. https://doi.org/10.1016/j.ijdevneu.2005.05.003

Sheleg, S.V., Lobello, J.R., Hixon, H., Coons, S.W., Lowry, D., Nedzved, M.K., 2008. Stability and autolysis of cortical neurons in post-mortem adult rat brains. Int. J. Clin. Exp. Pathol. 1, 291–299.

Shepherd, T.M., Flint, J.J., Thelwall, P.E., Stanisz, G.J., Mareci, T.H., Yachnis, A.T., Blackband, S.J., 2009. Postmortem interval alters the water relaxation and diffusion properties of rat nervous tissue--implications for MRI studies of human autopsy samples. NeuroImage 44, 820–826. https://doi.org/10.1016/j.neuroimage.2008.09.054

Shibayama, H., Kitoh, J., 1976. The postmortem changes of pyramidal neurons in the hippocampus of rats. Folia Psychiatr. Neurol. Jpn. 30, 73–91. https://doi.org/10.1111/j.1440-1819.1976.tb00113.x

Shubin, A.V., Demidyuk, I.V., Komissarov, A.A., Rafieva, L.M., Kostrov, S.V., 2016. Cytoplasmic vacuolization in cell death and survival. Oncotarget 7, 55863–55889. https://doi.org/10.18632/oncotarget.10150

Siew, L.K., Love, S., Dawbarn, D., Wilcock, G.K., Allen, S.J., 2004. Measurement of pre- and post-synaptic proteins in cerebral cortex: effects of post-mortem delay. J. Neurosci. Methods 139, 153–159. https://doi.org/10.1016/j.jneumeth.2004.04.020

Sillevis Smitt, P.A., van der Loos, C., Vianney de Jong, J.M., Troost, D., 1993. Tissue fixation methods alter the immunohistochemical demonstrability of neurofilament proteins, synaptophysin, and glial fibrillary acidic protein in human cerebellum. Acta Histochem. 95, 13–21. https://doi.org/10.1016/s0065-1281(11)80381-8

Silva, I., Silva, J., Ferreira, R., Trigo, D., 2021. Glymphatic system, AQP4, and their implications in Alzheimer's disease. Neurol. Res. Pract. 3, 5. https://doi.org/10.1186/s42466-021-00102-7

Ślęzak, J., Burov, S., 2021. From diffusion in compartmentalized media to non-Gaussian random walks. Sci. Rep. 11, 5101. https://doi.org/10.1038/s41598-021-83364-0

Snyder, J.M., Gibson-Corley, K.N., Radaelli, E., 2021. Nervous System, in: Pathology of Genetically Engineered and Other Mutant Mice. John Wiley & Sons, Ltd, pp. 462–492. https://doi.org/10.1002/9781119624608.ch21

Solenski, N.J., diPierro, C.G., Trimmer, P.A., Kwan, A.-L., Helm, G.A., Helms, G.A., 2002. Ultrastructural changes of neuronal mitochondria after transient and permanent cerebral ischemia. Stroke 33, 816–824. https://doi.org/10.1161/hs0302.104541

Sorimachi, Y., Harada, K., Yoshida, K., 1996. Involvement of calpain in postmortem proteolysis in the rat brain. Forensic Sci. Int. 81, 165–174. https://doi.org/10.1016/s0379-0738(96)01981-0

Spector, R.G., 1963. Selective changes in dehydrogenase enzymes and pyridine nucleotides in rat brain in anoxic-ischaemic encephalopathy. Br. J. Exp. Pathol. 44, 312–316.

Stadelmann, C., Timmler, S., Barrantes-Freer, A., Simons, M., 2019. Myelin in the Central Nervous System: Structure, Function, and Pathology. Physiol. Rev. 99, 1381–1431. https://doi.org/10.1152/physrev.00031.2018

Stan, A.D., Ghose, S., Gao, X.-M., Roberts, R.C., Lewis-Amezcua, K., Hatanpaa, K.J., Tamminga, C.A., 2006. Human Postmortem Tissue: What Quality Markers Matter? Brain Res. 1123, 1–11. https://doi.org/10.1016/j.brainres.2006.09.025

Suárez-Pinilla, M., Fernández-Vega, I., 2015. An acute metabolic insult highly increased postmortem cerebellar autolysis: an autopsy case. Clin. Neuropathol. 34, 166–168. https://doi.org/10.5414/NP300809

Sullivan, S.M., Björkman, S.T., Miller, S.M., Colditz, P.B., Pow, D.V., 2010. Morphological changes in white matter astrocytes in response to hypoxia/ischemia in the neonatal pig. Brain Res. 1319, 164–174. https://doi.org/10.1016/j.brainres.2010.01.010

Susaki, E.A., Shimizu, C., Kuno, A., Tainaka, K., Li, X., Nishi, K., Morishima, K., Ono, H., Ode, K.L., Saeki, Y., Miyamichi, K., Isa, K., Yokoyama, C., Kitaura, H., Ikemura, M., Ushiku, T., Shimizu, Y., Saito, T., Saido, T.C., Fukayama, M., Onoe, H., Touhara, K., Isa, T., Kakita, A., Shibayama, M., Ueda, H.R., 2020. Versatile whole-organ/body staining and imaging based on electrolyte-gel properties of biological tissues. Nat. Commun. 11, 1982. https://doi.org/10.1038/s41467-020-15906-5

Suzuki, J., 1987. Histological Study, in: Suzuki, J. (Ed.), Treatment of Cerebral Infarction: Experimental and Clinical Study. Springer, Vienna, pp. 23–53. https://doi.org/10.1007/978-3-7091-8861-3_3

Svitkina, T.M., 2020. Actin Cell Cortex: Structure and Molecular Organization. Trends Cell Biol. 30, 556–565. https://doi.org/10.1016/j.tcb.2020.03.005

Swaab, D.F., Bao, A.-M., 2021. Matching of the postmortem hypothalamus from patients and controls. Handb. Clin. Neurol. 179, 141–156. https://doi.org/10.1016/B978-0-12-819975-6.00007-8

Switzer, R.C., 2000. Application of silver degeneration stains for neurotoxicity testing. Toxicol. Pathol. 28, 70–83. https://doi.org/10.1177/019262330002800109

Szöllősi, D., Tóth, L., Kálmán, M., 2018. Postmortem immunohistochemical alterations following cerebral lesions: A possible pathohistological importance of the β-dystroglycan immunoreactivity. Neuropathol. Off. J. Jpn. Soc. Neuropathol. 38. https://doi.org/10.1111/neup.12447

Tafrali, D., 2019. Post-mortem changes and autolysis in frontal lobe cells of Sus scrofa. Medical University of Graz, Graz, Austria. https://doi.org/10.13140/RG.2.2.31901.87520

Takahashi, N., Satou, C., Higuchi, T., Shiotani, M., Maeda, H., Hirose, Y., 2010. Quantitative analysis of intracranial hypostasis: comparison of early postmortem and antemortem CT findings. AJR Am. J. Roentgenol. 195, W388-393. https://doi.org/10.2214/AJR.10.4442

Tang, Y., Nyengaard, J.R., De Groot, D.M., Gundersen, H.J., 2001. Total regional and global number of synapses in the human brain neocortex. Synap. N. Y. N 41, 258–273. https://doi.org/10.1002/syn.1083

Tao-Cheng, J.-H., Gallant, P.E., Brightman, M.W., Dosemeci, A., Reese, T.S., 2007. Structural changes at synapses after delayed perfusion fixation in different regions of the mouse brain. J. Comp. Neurol. 501, 731–740. https://doi.org/10.1002/cne.21276

Tapia, J.C., Kasthuri, N., Hayworth, K.J., Schalek, R., Lichtman, J.W., Smith, S.J., Buchanan, J., 2012. High-contrast en bloc staining of neuronal tissue for field emission scanning electron microscopy. Nat. Protoc. 7, 193–206. https://doi.org/10.1038/nprot.2011.439

Terstege, D.J., Addo-Osafo, K., Campbell Teskey, G., Epp, J.R., 2022. New neurons in old brains: implications of age in the analysis of neurogenesis in post-mortem tissue. Mol. Brain 15, 38. https://doi.org/10.1186/s13041-022-00926-7

Torres-Platas, S.G., Comeau, S., Rachalski, A., Bo, G.D., Cruceanu, C., Turecki, G., Giros, B., Mechawar, N., 2014. Morphometric characterization of microglial phenotypes in human cerebral cortex. J. Neuroinflammation 11. https://doi.org/10.1186/1742-2094-11-12

Tóth, K., Eross, L., Vajda, J., Halász, P., Freund, T.F., Maglóczky, Z., 2010. Loss and reorganization of calretinin-containing interneurons in the epileptic human hippocampus. Brain J. Neurol. 133, 2763–2777. https://doi.org/10.1093/brain/awq149

Trump, B.F., Berezesky, I.K., Chang, S.H., Phelps, P.C., 1997. The pathways of cell death: oncosis, apoptosis, and necrosis. Toxicol. Pathol. 25, 82–88. https://doi.org/10.1177/019262339702500116

Trump, B.F., Berezesky, I.K., Sato, T., Laiho, K.U., Phelps, P.C., DeClaris, N., 1984. Cell calcium, cell injury and cell death. Environ. Health Perspect. 57, 281–287. https://doi.org/10.1289/ehp.8457281

Van Nimwegen, D., Sheldon, H., 1966. Early postmortem changes in cerebellar neurons of the rat. J. Ultrasructure Res. 14, 36–46. https://doi.org/10.1016/S0022-5320(66)80033-3

Vass, A.A., 2011. The elusive universal post-mortem interval formula. Forensic Sci. Int. 204, 34–40. https://doi.org/10.1016/j.forsciint.2010.04.052

Vonsattel, J.P.G., Amaya, M. del P., Cortes, E.P., Mancevska, K., Keller, C.E., 2008. 21st century brain banking practical prerequisites and lessons from the past: the experience of New York Brain Bank – Taub Institute - Columbia University. Cell Tissue Bank. 9, 247–258. https://doi.org/10.1007/s10561-008-9079-y

Vrselja, Z., Daniele, S.G., Silbereis, J., Talpo, F., Morozov, Y.M., Sousa, A.M.M., Tanaka, B.S., Skarica, M., Pletikos, M., Kaur, N., Zhuang, Z.W., Liu, Z., Alkawadri, R., Sinusas, A.J., Latham, S.R., Waxman, S.G., Sestan, N., 2019. Restoration of brain circulation and cellular functions hours post-mortem. Nature 568, 336–343. https://doi.org/10.1038/s41586-019-1099-1

Wagensveld, I.M., Blokker, B.M., Wielopolski, P.A., Renken, N.S., Krestin, G.P., Hunink, M.G., Oosterhuis, J.W., Weustink, A.C., 2017. Total-body CT and MR features of postmortem change in in-hospital deaths. PLoS ONE 12, e0185115. https://doi.org/10.1371/journal.pone.0185115

Waldvogel, H.J., Curtis, M.A., Baer, K., Rees, M.I., Faull, R.L.M., 2006. Immunohistochemical staining of post-mortem adult human brain sections. Nat. Protoc. 1, 2719–2732. https://doi.org/10.1038/nprot.2006.354

Wang, N.S., Minassian, H., 1987. The formaldehyde-fixed and paraffin-embedded tissues for diagnostic transmission electron microscopy: a retrospective and prospective study. Hum. Pathol. 18, 715–727. https://doi.org/10.1016/s0046-8177(87)80243-5

Weerasinghe, P., Buja, L.M., 2012. Oncosis: an important non-apoptotic mode of cell death. Exp. Mol. Pathol. 93, 302–308. https://doi.org/10.1016/j.yexmp.2012.09.018

Weller, R.O., Sharp, M.M., Christodoulides, M., Carare, R.O., Møllgård, K., 2018. The meninges as barriers and facilitators for the movement of fluid, cells and pathogens related to the rodent and human CNS. Acta Neuropathol. (Berl.) 135, 363–385. https://doi.org/10.1007/s00401-018-1809-z

Wenzlow, N., Neal, D., Stern, A.W., Prakoso, D., Liu, J.J., Delcambre, G.H., Beachboard, S., Long, M.T., 2021. Feasibility of using tissue autolysis to estimate the postmortem interval in horses. J. Vet. Diagn. Investig. Off. Publ. Am. Assoc. Vet. Lab. Diagn. Inc 33, 825–833. https://doi.org/10.1177/10406387211021865

Whitney, E.R., Kemper, T.L., Rosene, D.L., Bauman, M.L., Blatt, G.J., 2008. Calbindin-D28k is a more reliable marker of human Purkinje cells than standard Nissl stains: a stereological experiment. J. Neurosci. Methods 168, 42–47. https://doi.org/10.1016/j.jneumeth.2007.09.009

Williams, R.S., Ferrante, R.J., Caviness, V.S., 1978. The Golgi rapid method in clinical neuropathology: the morphologic consequences of suboptimal fixation. J. Neuropathol. Exp. Neurol. 37, 13–33. https://doi.org/10.1097/00005072-197801000-00002

Wohlsein, P., Deschl, U., Baumgärtner, W., 2013. Nonlesions, unusual cell types, and postmortem artifacts in the central nervous system of domestic animals. Vet. Pathol. 50, 122–143. https://doi.org/10.1177/0300985812450719

Wong, G., Greenhalgh, T., Westhorp, G., Buckingham, J., Pawson, R., 2013. RAMESES publication standards: realist syntheses. BMC Med. 11, 21. https://doi.org/10.1186/1741-7015-11-21

Yarema, M.C., Becker, C.E., 2005. Key concepts in postmortem drug redistribution. Clin. Toxicol. Phila. Pa 43, 235–241. https://doi.org/10.1081/CLT-58950

Yeung, L.Y., Wai, M.S.M., Yew, D.T., 2010. Silver impregnation of the prefrontal cortices in the brains with long postmortem delay. Int. J. Neurosci. 120, 314–317. https://doi.org/10.3109/00207450903243507

Zhang, S., Boyd, J., Delaney, K., Murphy, T.H., 2005. Rapid reversible changes in dendritic spine structure in vivo gated by the degree of ischemia. J. Neurosci. Off. J. Soc. Neurosci. 25, 5333–5338. https://doi.org/10.1523/JNEUROSCI.1085-05.2005

Zhou, C., Byard, R.W., 2011. Factors and processes causing accelerated decomposition in human cadavers - An overview. J. Forensic Leg. Med. 18, 6–9. https://doi.org/10.1016/j.jflm.2010.10.003

Zissler, A., Stoiber, W., Steinbacher, P., Geissenberger, J., Monticelli, F.C., Pittner, S., 2020. Postmortem Protein Degradation as a Tool to Estimate the PMI: A Systematic Review. Diagn. Basel Switz. 10, E1014. https://doi.org/10.3390/diagnostics10121014